STRENGTH OF CEMENT BONDED STEEL CONNECTIONS IN GLUE LAMINATED TIMBER

by

Sabine Eistetter

Supervised by

Dr. Andrew H. Buchanan (Christchurch, New Zealand)

and

Professor Franz A. Zahn (Konstanz, Germany)

Civil Engineering Research Report 99/1

February 1999

This report was presented as a thesis in partial fulfillment of the requirements for the German Degree of Diplom Ingenieur (FH)

University of Canterbury
Department of Civil Engineering
Private Bag 4800
Christchurch, New Zealand

Fachhochschule Konstanz
Fachbereich Bauingenieurwesen
Brauneggerstrasse 55
78462 Konstanz, Germany

ABSTRACT

The use of epoxy bonded steel connections is gaining increasing acceptance not only in New Zealand but worldwide, due to ongoing research and development. Of concern is the fire resistance, as it has been observed that heat affects the strength of epoxy and consequently the pull out strength of the connection.

This report presents an investigation of the use of cement grout for bonded steel connections in glue laminated timber. It is intended to make cement grout a possible adhesive alternative to epoxy for bonded steel connections, with regard to better fire resistance. Small sized tests of wood and cement were carried out.

In the study, ten various designs of the connection with variables of embedment length, hole geometry and reinforcement were tested in tension to find out their effect on the pull out strength of the connection.

The results show that the bond between timber and cement is the main problem due to the fact that cement does not bond to timber. To prevent the steel-cement block from pulling out, tests were carried out using additional screws and bolts, which increased the strength significantly, compared to connections with straight holes. A minor increase of load capacity was achieved in connections with a distinct key between the cement and the wood. An equation was developed to predict the strength of connections using screws or bolts as reinforcement.

ACKNOWLEDGEMENT

This investigation was carried out in the Department of Civil Engineering at the University of Canterbury in Christchurch, New Zealand.

I would like to thank my supervisor Dr. Andrew H. Buchanan for his encouraging assistance and enthusiasm throughout this project.
My thanks also go to my German supervisor Professor Franz A. Zahn (PhD from University of Canterbury). His initial contact to the University of Canterbury made it possible for me to do this research in New Zealand.

Special thanks to Norrie Hickey for his technical support and assistance in preparing the test specimens and test facilities for the experiments.

I would also like to thank Mark Stuart-Jones for his time and his assistance in setting-up and testing the test specimens. Thanks to Ray Allen, for his technical support and assistance in the workshop and Kevin Stobbs (Mechanical Engineering) for his assistance in testing material.

TABLE OF CONTENTS

CHAPTER FOUR: MATERIAL PROPERTIES

CHAPTER FIVE: TENSION TESTS

APPENDICES

LIST OF TABLES AND FIGURES

NOTATION

β = ratio of cement strength and timber strength [MPa]

d = pilot hole diameter [mm]

D = pilot hole diameter plus key size [mm]

d_b = diameter of cement block around bolt [mm]

d_{rod} = diameter of threaded steel rod [mm]

d_s = effective screw diameter [mm]

F = pull-out strength [N]

f_{h1d} = characteristic timber strength [MPa]

f_{h2d} = characteristic cement strength [MPa]

l = embedment length of steel rod [mm]

$l_{s,b}$ = length of screws and bolts [mm]

l' = span [mm]

l_b = length of bolts [mm]

M_{pl} = plastic moment [MPa]

n = number of bolts

n_{ef} = effective number of bolts

P_{max} = ultimate load [N]

S = plastic modulus [mm^3]

$\sigma_{friction}$ = coefficient of friction [MPa]

σ_y = yield strength [MPa]

t_l = embedment length of screw in timber

x = key size [mm]

$\varnothing$ = diameter [mm]

$\varnothing_{th}$ = thread diameter [mm]

CHAPTER ONE: INTRODUCTION

Timber is a very popular building material in many countries of the world. It is not only used for smaller buildings, like residential houses, but also for large industrial buildings and commercial buildings. Especially when aesthetics is of importance, timber is a favourite material.

There are many types of joints used in timber construction. That makes it sometimes difficult to decide which type of connection to choose. The selection of fasteners is not only controlled by the load bearing capacities of the structure and the direction of load, but also aesthetics, the cost-efficiency and the fabrication process which has to be considered when planning and designing a building.

Glued-in bolted connections have been used in Europe for over twenty years and are becoming more and more accepted throughout the world. On-going investigations of epoxy bonded steel connections are providing more knowledge and experience about their performance.

Only very little research on performance of timber connections exposed to fire has been done. Studies have shown which connections have a high fire resistance and which are not suitable for being exposed to fires. An extensive review of the fire performance of connections in timber structure has been summarised by Carling (1989). One advantage of using glued laminated timber instead of other materials like steel is its better fire performance. This is because large timber members have a low charring rate which gives good fire resistance with no extra expense (Buchanan, 1999). The problem of a glulam structure with epoxy bonded steel connections is that the connection may fail prematurely, when exposed to fire. Investigations by Barber (1994) on fire resistance of epoxied bonded steel connections have shown that epoxy loses nearly its strength when heated above 50°C, causing the connection to fail. This has been the motivation for the investigation of alternatives to glued-in bolted connections. Gaunt (1998) has experimentally studied connections with large screw fixings where no adhesive such as epoxy had to be used. This research will investigate

a steel connection bonded by cement grout. Cement has been chosen as it is a building material that is easy to handle, inexpensive and fire resistant.

The cement bonded steel connection is a connection of timber members formed by placing a threaded steel rod into predrilled holes and bonding with cement grout. The holes are 10mm to 20mm larger than the steel rod. Different designs of the connection have been proposed with embedment length, hole geometry and reinforcement as variables. The cement grout must have a fluid consistency to ensure the cement can flow through the cavities when injected with air-pressure.

The major problem is the bond between the cement grout and the timber. Contrary to epoxy, cement does not bond to timber. Therefore, a mechanical bond has to be designed.

The objectives of this study are:

1. To experimentally study the mechanical properties of cement bonded steel connections subjected to short duration tensile load.

2. To experimentally study the properties of the material used for the tension tests.

3. To develop a method of predicting the strength of the connections with regard to the cement grout and the various hole geometries and reinforcement used.

This thesis is organised in six chapters. Chapter one gives the background and objectives of this study. Chapter two is a review of literature and chapter three gives an overview of cementitious grouts. Chapter four describes the investigation of some material properties. Chapter five describes the experimental study of cement bonded steel connections and Chapter six gives a summary and conclusions.

CHAPTER TWO: LITERATURE REVIEW

2.1 STRUCTURAL JOINTS IN TIMBER CONSTRUCTIONS

2.1.1 Various Connections in Glulam Timber Structures

The decision, which type of fastener to select, is often the most important one but not the easiest. It is of prime importance that the correct choice of joint type is made early in the development of a project so as to meet the client's requirements with regard to aesthetics, appearance and cost. At the same time, a sound technical solution needs to be provided.

Glue laminated timber is often used for multi-storey buildings with long span floor systems and for large span single-storey buildings. Moment resisting connections are the most difficult joints to design in such timber and glulam structures. Several common joint types can be used for designing moment resisting connections as nailed connections (and in combination with nail gusset plates made from steel or plywood), bolted connections (and in combination with split-rings, shear plates and tooth plates), dowel connections, glued connections, connections using drift pins and adhesive bonded steel connections.

Nails

Nails are the most common type of fastener in timber structures and can effectively be used for moment resisting joints, as there is no initial slip since a nail always fits the hole into which it is driven. Figure 2.1 (Buchanan & Fairweather, 1993) shows some possible applications of predrilled steel plates or plywood plates for moment resisting connections in large glulam frames. Plywood and steel plate nailed joints are used successfully for large span frames but due to their poor visual appearance, often unacceptable for buildings of high aesthetic demands. These connections also have a minimal fire resistance if not protected with a non-combustible overlayer such as solid wood or gypsum plaster board (Buchanan and King, 1991). Another method to

provide better fire resistance would be to apply an intumescent paint, but only a small increase in fire resistance has been achieved by this method. The cost of nailed joints for portal frame structures varies from 20% to 30% of the total frame cost (Batchelar, McIntosh, 1998).

Experiments of nailed connections showed poor ductile behaviour when high strength was obtained. Figure 2.1(d) shows a method of providing ductility by using necked steel plates.

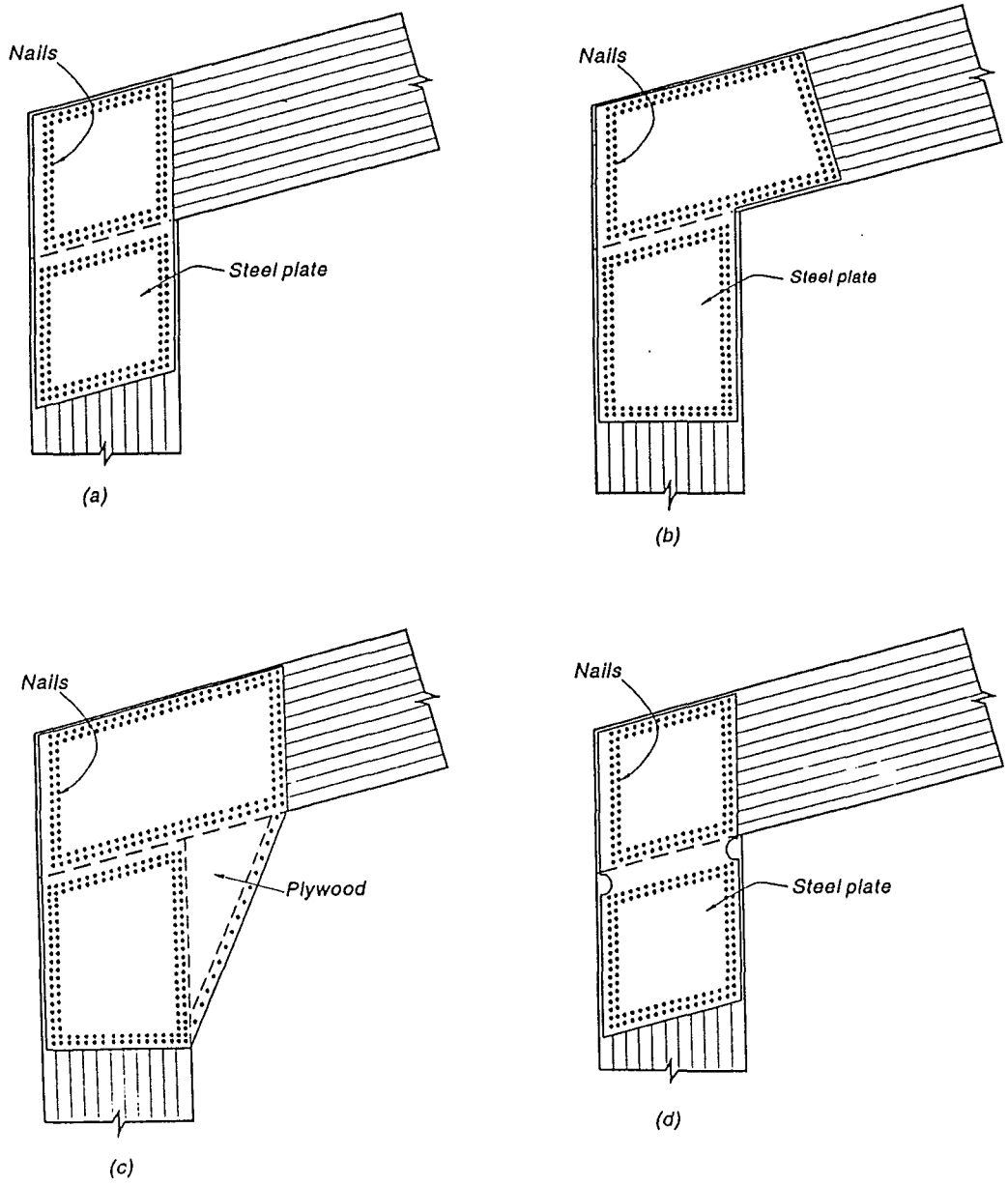

Figure 2.1 Nailed portal frame knee joint connections

Bolts

Bolts are the most popular method of connecting timber to timber or timber to steel. Significant variation was found in the timber design codes of different countries on the performance data for bolts. For example using the New Zealand code, values for designing a joint requires a lesser number of fastener compared to the requirements of the British Standard (Batchelar and McIntosh, 1998).

Compared to other dowel type fasteners, bolts have the advantage of being able to carry axial load in addition to shear load. Good durability in extreme exposure environments can be achieved by using stainless steel or bolts with corrosion protection. Bolts should not be used for structures, which are sensitive to displacement (Batchelar, McIntosh, 1998).

Carling (1989) reports tests by Aarnio and Kallioniemi (1979, 1983), who successfully used boxes made with glulam timber or particle board and mineral wool as a protection for gusset joints to achieve good fire resistance. The method of covering bolts for fire protection is not always acceptable, due to aesthetic aspects, therefore, an intumescent paint system was developed, which can provide a small increase in fire resistance. But still there is a lack of design information on fire resistance of bolted connections.

The cost of bolted joints is approximately 20% of the total frame cost. Compared to nailed connections, the cost per unit of load is higher for bolted connections (Batchelar and McIntosh, 1998). Figure 2.2 shows examples for a multi-member bolted joint.

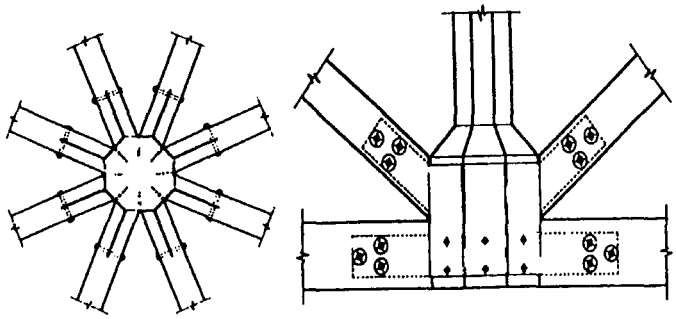

Figure 2.2 Multi-member bolted joint (Batchelar, McIntosh, 1998)

Glued Connections

A simple method of developing a full strength rigid moment resisting connection is by gluing and cross-lapping or interleaving the timber members. Because the joints are manufactured in a factory, they are difficult to transport, but easy to assemble on the construction site. The glued cross-lapped joints are commonly referred to in New Zealand as the McIntosh joint. The advantages of this connection are a very good fire resistance and a visually attractive joint as no fasteners are visible, although, the production requires a high quality control. Due to the lack of ductility, glued joints are not suitable for seismic design and can show a sudden brittle behaviour when loaded to failure.

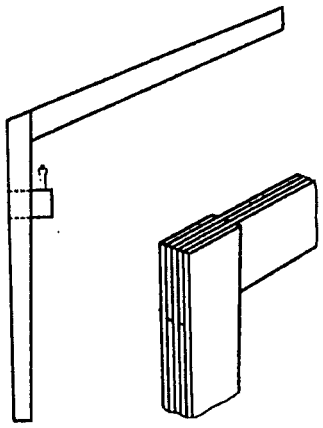

Figure 2.3 Glued cross-lapped joint (Batchelar, McIntosh, 1998)

Drift Pins

Although drift pin joints are a common connection system in the Northern Hemisphere, they have received limited use in New Zealand due to a lack of code guidance. Drift pins are similar to bolts but without any bolt head or nut and washer thus without the end moment restraint. The advantage of this connection is the aesthetic appearance of a joint without any visible fasteners. Though no fire research has yet been done, the fire resistance is likely to be better than bolted joints because of the smaller dowel surface exposed to the heat. The major disadvantage of this type of

connection is the high demand on supervision on site as the pins are driven into the timber members (Batchelar and McIntosh, 1998).

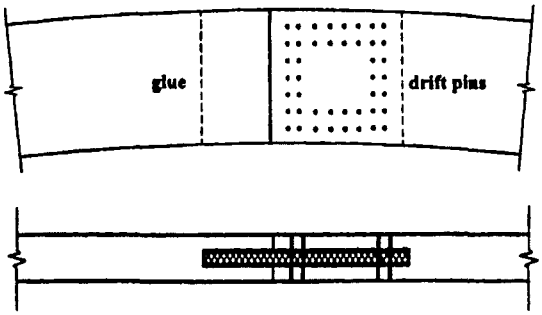

Figure 2.4 Timber and drift pin connection

Epoxied Connections

The use of epoxy bonded steel connections is becoming increasingly accepted in New Zealand and Europe. This type of joint has proven to be a very effective and useful method of joining large timber members. Applications showing the strength and fire resistance of glued in bolts is described in a following paragraph.

2.1.2 Development of Semi-rigid Joints

Pinned or rigid joints are the two classifications for structural connections, although in reality most joints show a semi-rigid behaviour. The structural performance and design principles of timber joints have been investigated and described by Haller (1998).

Dry timber is a brittle material. If no mechanical fastener is used in a connection, the joint shows the same brittle behaviour. The employment of mechanical fasteners such as bolts and nail-plate connectors provide ductility due to their ability to form plastic hinges prior to failure. But still, brittle failure may occur in the wood when using mechanical fasteners if the strength of the timber is reached before the yield strength of the fasteners.

The load deflection curve in Figure 2.5(a) shows the load bearing behaviour of various types of connections. The target in designing an efficient timber joint is to achieve a high loading capacity and a large deformation leading to high strength, stiffness and ductility.

When testing a connection subjected to a constant load, the load deflection curve can be divided into four stages of performance characterised by certain phenomena (Figure2.5(b) and (c)). The first phase describes a slip with a minor increase of load transfer because of the slightly loose fit of the fasteners. Phase two shows the linear elastic behaviour of the timber and the mechanical fastener. In phase three, the gradient of the curve slowly decreases and is characterised by irreversible action due to yielding, microcracking or damage. The last phase shows the further development of phase three until failure.

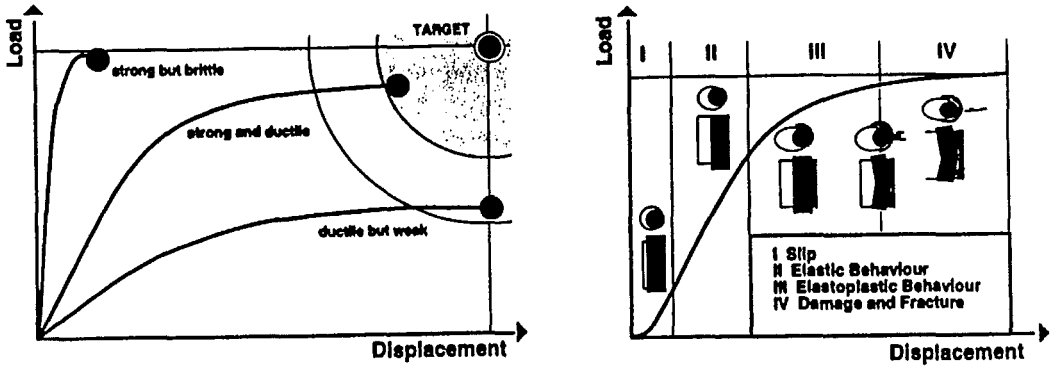

(a) Load carrying behaviour of brittle, ductile and weak joint with dowel type fastener

(b) Load displacement curve and related phenomena

Phase	Phenomenon	Related theory	Improvement
I	Lack of fit fasteners	Contact and friction	Precise manufacturing Tight fit *Resin injection* *Expanded fastener*
II	Elastic behaviour	Theory of elasticity	*Stiff foundation module* *High embed. strength* *Uniform load distrib.*
II	Elasto-plastic behaviour, Damage, Small cracks	Theory of plasticity, Damage and Fracture Mechanics	*Reinforcement* *Reduce brittleness*
IV	Stable and unstable Cracking with failure	Fracture Mechanics	*(Glassfibre)*

(c) Phases of load displacement curve, related phenomena and design principles for improvement

Figure 2.5 Ideal behaviour of ductile timber joints (Haller, 1998)

Some suggestions were made by Haller (1998) to improve the behaviour of timber joints. To avoid the initial slip and consequently a loss of stiffness due to the lack of fit of the fastener a technique developed by Rodd (1994) can be used. In this application the gap between the fastener and the timber is filled with resin. As an alternative, Leijten (1998) solved the problem by using mild steel expanded tubes. These tubes are inserted into the hole and the ends are formed to a flared collar by means of a special device loaded by a hydraulic jack. The axial compression causes a plastic expansion in circumference providing a tight fit of the fastener.

To improve the initial stiffness and elasticity, Haller suggests using timber with higher embedding module and stronger or less brittle material, respectively.

Due to the high number of available fasteners, various materials in timber construction and complex structures, it is difficult to develop a concept for designing semi-rigid joints. Four ways of modelling semi-rigid timber joints were suggested by Haller:

- testing
- mechanical modelling by means of spring-bar-models
- analytical determination of semi-rigidity
- finite element method

2.2 PREVIOUS STUDIES OF ADHESIVE BONDED CONNECTIONS

2.2.1 Application of Glued-in Bolts

Experimental research by Riberholt (1986) formed the basis for further studies and tests by Townsend (1990), Fairweather (1992), Barber (1994) and Deng (1997) supervised by Buchanan.

Epoxy bonded steel connections are mainly used for moment resisting joints in glued laminated timber structures or column-foundation joints. The bolts can be loaded either axially or laterally or by a combination of both. Glued-in bolts are also used to prevent cracks in the apex zone of curved beams and in end notched beams (Timber Engineering Step1, 1995). Figure 2.6 shows some examples.

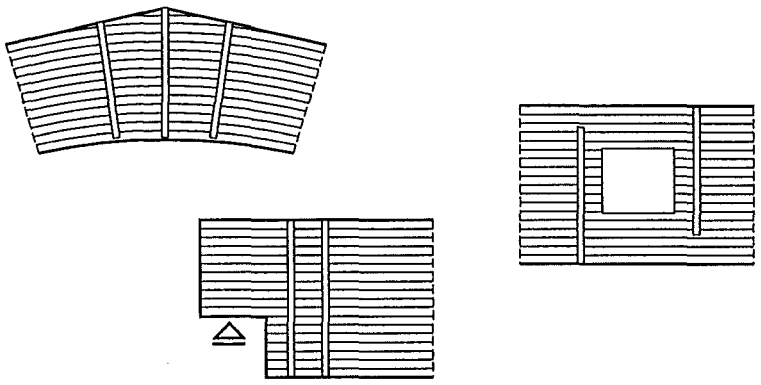

Glued in Bolts as a means of preventing cracks

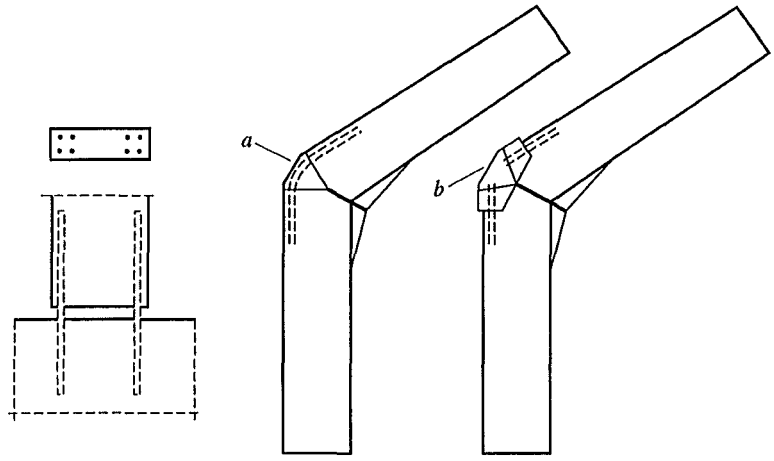

Glued-in Bolts in moment stiff column-foundation joint and moment stiff frame corner. (a) Space filled with mortar. (b) Steel fitting

Figure 2.6 Examples of the use of glued-in bolts (Timber Engineering Step 1, 1995).

According to Barber (1994) and Deng (1997), the major advantages of using epoxied bonded steel connections are:

- invisible fasteners meet high aesthetic appearance demands
- ductile behaviour for seismic design

- steel bolts are mostly protected from corrosion by surrounding timber
- high strength connection with good performance
- connections are glued in the factory

2.2.2 Strength of Epoxy Bonded Steel Connections

Extensive tests have been carried out by Deng (1997) to study the influence of variables such as embedment length, bar diameter, edge distance, hole diameter, moisture content, steel bar type and epoxy type on epoxied bonded steel connections loaded in tension.

Deng developed the following equation to predict the strength of epoxy bonded steel connections subjected to tensile load:

$$F = 10.94\ k_b\, k_e\, k_m \left(\frac{l}{d}\right)^{0.86} \left(\frac{d}{20}\right)^{1.62} \left(\frac{h}{d}\right)^{0.5} \left(\frac{e}{d}\right)^{0.5}$$

where F = ultimate tensile load of the connection [kN]

k_b = bar type factor

k_e = epoxy factor

k_m = moisture content factor

l = embedment length [mm]

d = steel bar diameter [mm]

h = hole diameter [mm]

e = edge distance from centre of steel bar [mm]

Deng found that all seven variables mentioned above influence the strength of the connections and are taken into account in the equation.

The European formula suggested by Riberholt is as follows (Timber Engineering Step1, 1995):

$F = f_{ws}\, \rho_k\, d\sqrt{l}$ for $l \geq 200$mm

$F = f_{wl}\, \rho_k\, d\sqrt{l}$ for $l < 200$mm

where F = characteristic axial capacity in tension and compression [N]

f_{ws} = strength parameter [MPa]. For brittle glues, such as phenol-resorcinol and epoxy, the value is 0.520 and for non-brittle glues, such as two-component polyurethane, the value is 0.650

f_{wl} = strength parameter [MPa]. For brittle glues, such as phenol-resorcinol and epoxy, the value is 0.037 and for non-brittle glues, such as two-component polyurethane the value is 0.046

ρ_k = characteristic density [kg/m^3]

d = hole diameter [mm]

l = glued-in length [mm]

A comparison has been made between the formula developed by Deng and the European formula suggested by Riberholt. For this comparison, results of experiments carried out by Deng (1997) have been used. It has been observed that Deng's equation gives a good agreement with the experimental results and the European formula seems to be too conservative as the strength of the experiments is approximately 11% above the predicted values.

Aicher and Herr (1998) carried out an experimental study of high strength glulam frame corners for a negative bending moment with glued-in steel connectors. For these tests the steel rods were screwed into a hole filled with two component polyurethane. The size of the hole was 1mm larger than the steel rod.

The load capacity of the glued-in rods was calculated according to EC 5, Part 2 Bridges as follows:

$$F_{ax,k} = \pi (d_{equ})^{0.8} l_a \, 1.2 \times 10^{-3} \, \rho_k^{1.5}$$

where $d_{equ} = d_{nom} + 1mm$ (hole diameter)

d_{nom} = steel rod diameter [mm]

A finite element model was designed to analyse the stress flow in the connection. The results obtained by strain and force measurements during the testing procedure and the finite element results were in good agreement. Aicher and Herr suggested this type of a high strength glulam frame corner to be an easily on site assembled connection with high efficiency.

2.2.3 Glued Bolt Joints Using Fibre Reinforced Plastic

The replacement of the traditional solid steel bar by fibre reinforced plastic bars was based on the idea of creating a more generic sound joint and efficient use of high tensile strength of fibre reinforced plastic (FRP). At this stage of the connection development, there is still a lack of knowledge about factors such as the influence of creep, changing environmental conditions and long term strength of the resin. First tests have shown promising test results.

Some of the advantages of using FRP are listed below (Guan, 1998):

- similar properties of timber and FRP and thus improved compatibility
- better resin bond to FRP than to steel, therefore higher performance
- improved fire resistance due to lower conductivity
- high corrosion resistance
- lower weight of FRP provides easier handling

Finite element analysis and experimental studies using glass fibre reinforced plastic (GFRP) and steel bars has been carried out by Guan. It has been observed that the load carrying capacity of the connections with GFRP bars are approximately 25% less than that of connections with steel bars. This can be explained by the better steel-epoxy bond than the GFRP-epoxy bond. All tests showed a brittle failure mode as can be seen in the load deflection curves of Figure 2.7 (Guan, 1998). The de-bonding, when using GFRP bars, happens between the bar and the glue, in contrast to steel bar connections where no de-bonding occurs due to the better bonding strength at the glue-timber interface. To improve the bonding strength of glue and FRP, the surface of the bars needs to be more structured.

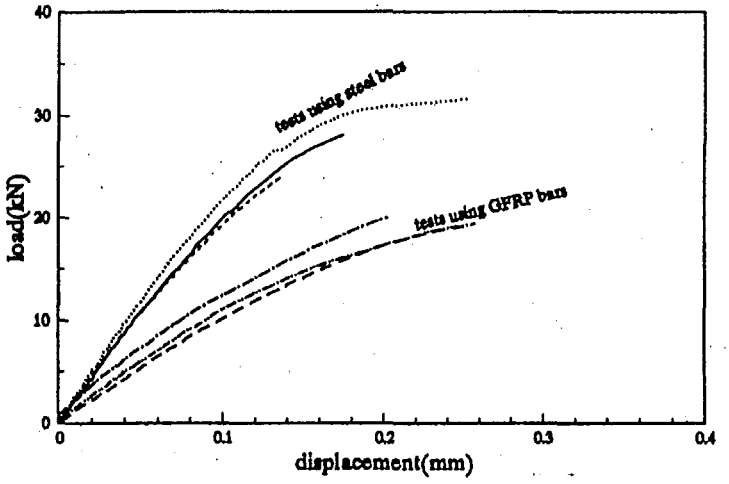

Figure 2.7 Load displacement curves of a resin bonded axially loaded bar in timber (14mm bar, 2mm clearance, 15mm embedment length)

The results of the simple finite element model for simulating the load-deflection relationship of the joint closely approximates the test results. Nevertheless, improvement of the model is suggested for better simulation (Guan, 1998).

2.3 FIRE RESISTANCE OF EPOXY BONDED STEEL CONNECTIONS

2.3.1 Previous Studies

In order to find out more about the performance and fire resistance of epoxy bonded steel connections, extensive research has been carried out by Barber (1994) at the University of Canterbury. Specimens have been investigated at elevated temperatures and a model to measure the heat transfer through the charring wood has been developed.

The first test specimens were heated up in an oven (between 40°-90°C) and loaded in tension parallel to the grain. The following test series was exposed to standard fire, tested in a furnace. The program TASEF (Temperature Analysis of Structures Exposed to Fire) was then used to model the heat flow through a section of timber.
Figure 2.8 (Barber, 1994) shows test results of the oven tension tests and the furnace tests, comparing ultimate load and temperature. The trend of strength loss at increasing temperature of the oven tension tests is obvious and depicted by the three straight lines. It can be seen that the critical point is reached at a temperature of about 50°C, which is followed by a rapid reduction of strength with increasing temperature. Compared to the oven tests, load bearing values are of lower value. This was explained by the rapid heating of the epoxy exposed to fire, while the oven test specimens were heated slowly over 24 hours.

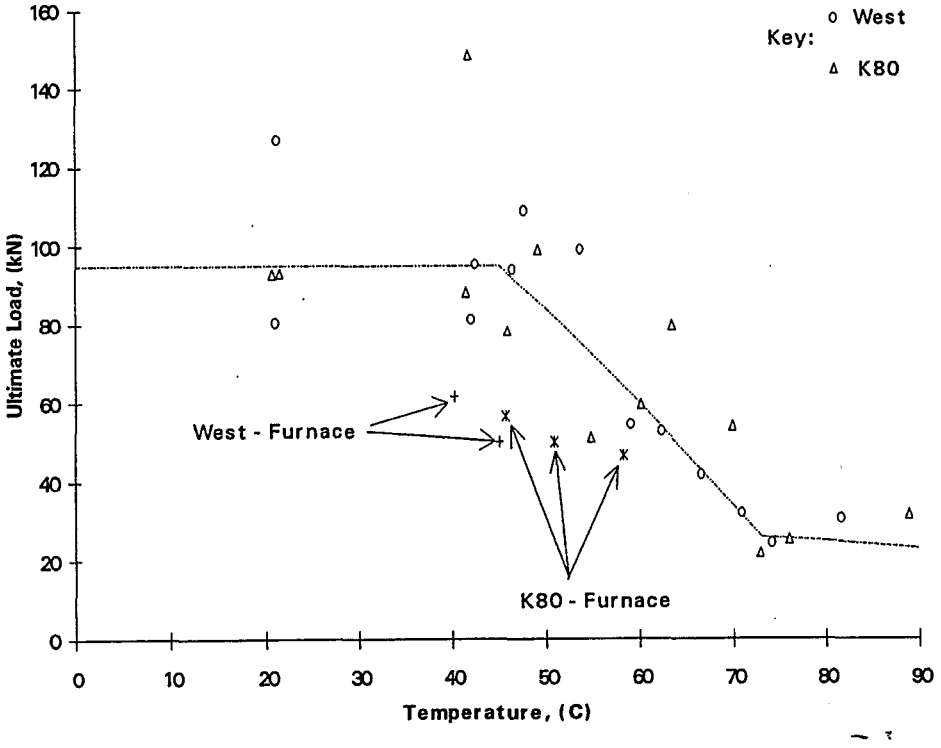

Figure 2.8 Oven tension test data and furnace test data

Failure was due to shear failure within the epoxy or loss of bond at the wood-epoxy interface, whereas the failure at ambient temperatures was either by tension failure of the wood or by loss of confinement.

The results of modelling the heat flow in wood with TASEF showed good agreement with the results of the furnace tests. Uncertain input data, such as information about the physical properties of wood, make it difficult to estimate the exactness of the output data obtained by computer modelling, though.

2.3.2 Alternative to Epoxy Bonding

An alternative to epoxy bonded steel connections was developed in order to achieve a joint with better fire resistance. A connection has been designed using large screw fixings where no adhesive such as epoxy has to be used (Gaunt, 1998). The different screws that were used in the experiments are shown in Figure 2.7. A pilot hole of a

16mm diameter was drilled to ensure that the thread would cut into the surrounding wood.

Initial tests were carried out using the top screw type in Figure 2.9 with varying embedment lengths. These connections showed a wood shear failure along the thread tips, leaving plugs of wood wrapped around the screw as they were pulled out. The design of the short thread of the other test screws shown in Figure 2.9 was based on the experience of the initial test. It was observed that during installation, the first 20 to 30mm of the embedment length failed partially in shear. This was explained by the fact that when the screw was forced into the pilot hole, it tried to gain more space to penetrate further in. This effect seemed to reduce the actual embedment depth.

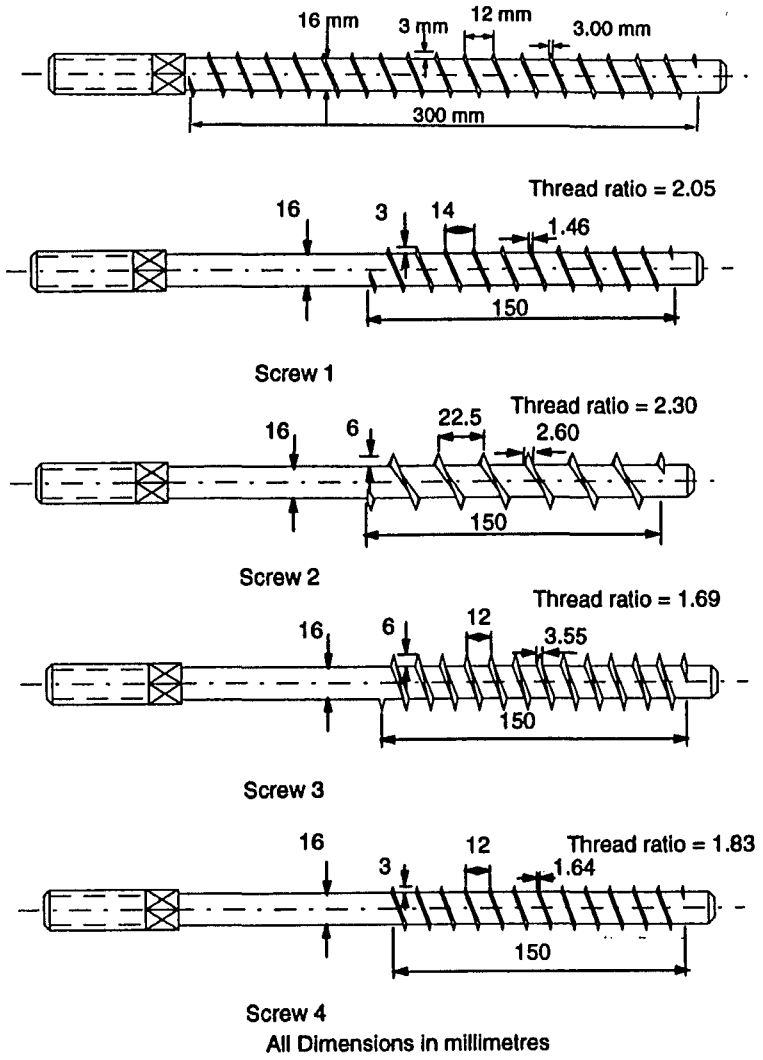

Figure 2.9 Various test screws

Results showed an increase of strength for the improved screws of approximately 25%. No direct relationship between wood density and pull out strength could be established but the trend of increasing pull out strength with increasing wood density was observed. Because of the 16mm diameter hole that had to be drilled for the screws in contrast to the larger hole of approximately 30mm diameter for the epoxied connections, there was a minor loss to the cross-section area. The larger cross-section seemed to provide a better stress distribution along and at the ends of the screw. The average load for a connection with a 300mm embedment length was 97 kN.

A comparison of the achievable strength of epoxied bonded steel connections, cement bonded steel connections and large screw fixings is given below.

Epoxy (300mm embedment length)	230 kN	(Deng, 1997)
Cement (300mm embedment length)	90 kN	(This study)
Screws (300mm embedment length)	97 kN	(Gaunt, 1998)

2.4 INJECTION GROUTING FOR TIMBER POLE REPAIR

Timber poles used for power transmission poles and pile support structures tend to be susceptible to deterioration because they are often exposed to an adverse environment. Since poles are usually loaded in compression, the decay starts in the centre of the pole developing hollow zones but leaving the outer appearance look sound. Replacement of the damaged poles can be very expensive and may require an interruption of the service. The alternative of mechanically repaired poles may not reach the full loading strength of the original pole. A different, but very promising method would be to repair the poles in-place by injecting a concrete or polymer-modified concrete grout into the hollow core.

An experimental and theoretical study was carried out to give more information about the grouting process and the performance of repaired poles (Alawady, Avent and Mukai, 1998).

Flexural load tests were carried out on pole specimens, repaired by pressure injecting cement grout. The selected grout was a cement based, nonmetallic, non-shrink fluid grout. To reduce shrinkage, micro-fibres were added to the grout.

The repaired poles reached between 42% and 70% of the design moment capacity. A reason for not achieving 100% could be that the shear strength was reached first. This is not expected to happen when repairing standard length poles where the bending moments are large and the shear forces are relatively small. For all grout injected poles, however the capacity was equal or above the capacity reached by retrofitting the poles with a c-truss, though.

This method for repairing timber poles has shown potential to be a very efficient and technical sound solution, but before an application, further investigations would be required.

CHAPTER THREE: CEMENTITIOUS GROUTS

3.1 CHEMISTRY OF CEMENT

The information in this chapter has been obtained from Bazant & Kaplan (1996) and Czernin (1962).

3.1.1 Chemical Composition

Materials that are used in the manufacture of Portland Cement consist mainly of lime (CaO), silica (SiO_2), alumina (Al_2O_3) and ferric oxide (Fe_2O_3). Portland Cement is made primarily from a combination of a calcareous material, such as limestone or chalk, and of silica and alumina containing materials found as clay or shale. In addition, there may be minor amounts of compounds, such as MgO, K_2O, and Na_2O.

After grinding and mixing, the materials are heated at a temperature of about 1400°C, they sinter and fuse partially into what is called clinker. To control the setting time of the cement paste, some gypsum is added to the clinker. Table 3.1 shows the main compound composition of Portland Cement.

Table 3.1 Main compound composition of Portland Cement

Compound	Formula	Abbreviation
Tricalcium silicate	$3CaO.SiO_2$	C_3S
Dicalcium silicate	$2CaO.SiO_2$	C_2S
Tricalcium aluminate	$3CaO.Al_2O_3$	C_3A
Tetracalcium alumineferite	$4CaO.Al_2O_3.Fe_3O_3$	C_4AF

where CaO is represented by C, SiO_2 is represented by S, Al_2O_3 is represented by A, Fe_2O_3 is represented by F, H_2O is represented by H

3.1.2 Hydration of Cement

The hydration of cement describes the chemical reaction of cement and water. When adding water to cement, the two silicates C_3S and C_2S produce calcium silicate hydrates, composed essentially of $3CaO.2SiO_2.3H_2O$ as well as $Ca(OH_2)$. The calcium silicate hydrate ($C_3S_2H_3$) is referred to as 'tobermorite gel'.

The hydration reactions are as follows:

$$\underset{[100]}{2\,C_3S} + \underset{[24]}{6H} \longrightarrow \underset{[75]}{C_3S_2H_3} + \underset{[49]}{3\,Ca(OH)_2}$$

$$\underset{[100]}{2\,C_2S} + \underset{[21]}{4H} \longrightarrow \underset{[99]}{C_3S_2H_3} + \underset{[22]}{Ca(OH)_2}$$

The numbers in brackets are the corresponding atomic masses. Both silicates require nearly the same amount of water. But C_3S produces about twice as much $Ca(OH)_2$ as C_2S.

Tricalcium aluminate (C_3A) reacts very rapidly when mixed with water producing heat. This reaction is called 'flash set' and can be prevented by adding gypsum to the cement.
The chemical reaction may be written as follows:

$$\underset{[100]}{C_3A} + \underset{[40]}{6H} \longrightarrow \underset{[140]}{C_3AH_6}$$

More water is required for this reaction than for the hydration of silicates.

The hydration of cement compounds is exothermic. The absolute volume of hydrated cement, referred to as cement gel, is less than the added volumes of cement and water, respectively.

3.1.3 Physical Structure of Hardened Cement Paste

Generally, cement paste consist mainly of gel, crystals of $Ca(OH)_2$, anhydrous cement, gel pores and capillary pores. The relative volumes at different stages of hydration are illustrated in Fig 3.1 (Bazant and Kaplan, 1996), respectively.

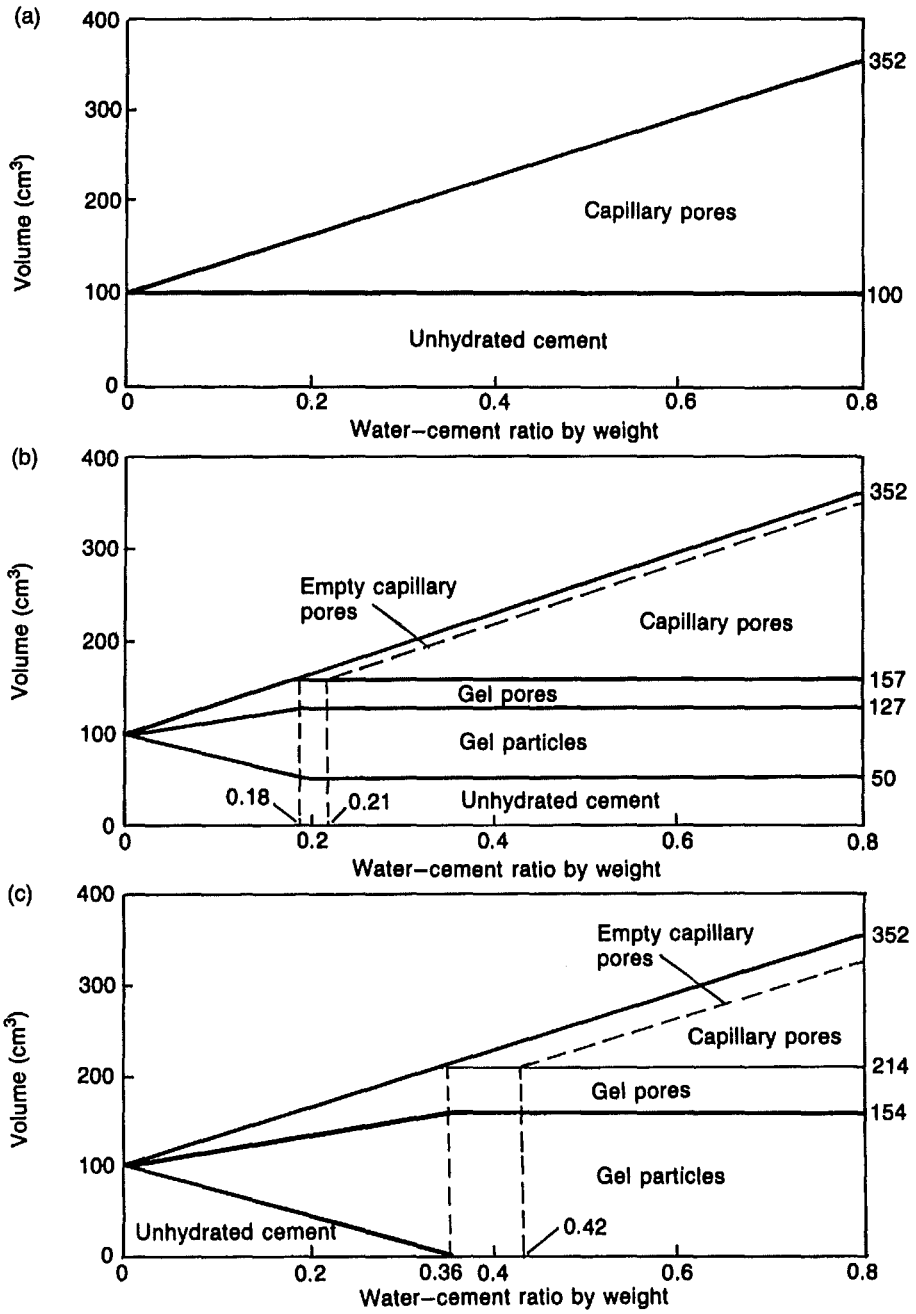

Figure 3.1 Relative Volumes of unhydrated cement, gel pores and capillary pores in hardened cement paste: (a) fresh paste – no hydration; (b) 50 per cent hydration; (c) 100 per cent hydration

The gel pores are very small spaces between the particles, whereas capillary pores are larger spaces that have not been occupied by hydration products.
Water in hydrated cement paste can be present as evaporable water in capillary pores and in gel pores, as well as chemically bound water. Increase of the water-cement ratio in the cement paste increases the amount of not chemically bound water, contained in the capillary pores. As hydration progresses, the previously continuous interconnected pore system becomes blocked by hydration products and thus becomes discontinuous. The initial water-cement ratio as well as the state of hydration thus effects the pore structure of the cement paste.

A grout mix with a high water/solids ratio is very fluid and has a low viscosity. It may also have sufficient water to counteract the effects of rapid water loss during placement within highly absorptive material. However, cement mixes with a high water content are prone to rapid segregation during injection and have less tension and compression strength.

3.2 CEMENT PROPERTIES AT ELEVATED TEMPERATURES

At temperatures of up to 105°C evaporable water, present in capillary and gel pores, is expelled from hardened cement paste. It is assumed that temperatures of up to 105°C do not affect chemically bound water. After a sufficient period of exposure time to these temperatures, all evaporable water is driven out of the cement gel.
Exceeding temperatures of 105°C, decomposition of the hydration products and destruction of the gel structure begins.

3.2.1 Dehydration

At temperatures greater than 105°C, a decomposition of the cement gel (CSH) and calcium hydroxide (CH) formed in the cement hydration commences. CSH decomposes mainly into dicalcium silicate (C_2S), wollastonite (CS) and water, whereas CH decomposes into calcium oxide (C) and water. The chemical reaction, where initially chemically bound water becomes evaporable water, is referred to as

dehydration of cement gel. The degree of conversion of cement gel and calcium hydroxide at various temperatures is shown in Fig 3.2 (Bazant and Kaplan, 1996). Differential thermal analysis (DTA) investigation by Lankard (1970) showed a broad endothermic reaction which commences at temperatures less than 100°C (Bazant and Kaplan, 1996).

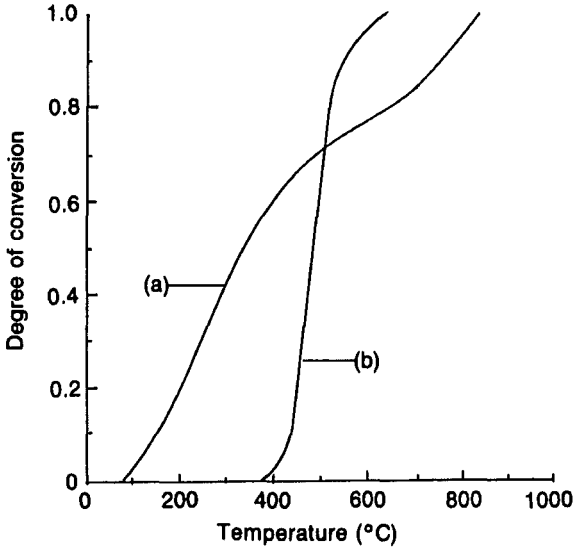

Figure 3.2 Degree of conversion of (a) tobermorite gel and (b) calcium hydroxide in idealised cement paste at various temperatures

3.2.2 Porosity

Elevated temperatures cause change in the pore structure of cement gel. These changes can affect the physical and mechanical properties of the hardened cement paste. Tests carried out by Bazant and Thonguthai (1978, 1979) showed a significant increase of porosity as temperature rises above 100°C. This can be explained by the fact that at temperatures greater than 105°C dehydration commences. Due to the progressive breakdown of the gel structure (CSH) as dehydration proceeds, average pore size and thus the specific internal pore surface area increase. When heating up to 600°C, expansion of the pores or formation of microcracks may occur.

3.2.3 Thermal expansion

Thermal expansion is not only affected by temperature, but by changes in moisture content, chemical reactions (dehydration, conversion), creep and microcracking. Lankard (1970) has investigated the dimensional stability of cement paste exposed to temperature of up to 260°C. The specimens were saturated and had a water-cement ratio of 0.6. Results are shown in Fig 3.3 (Bazant and Kaplan, 1996). The weight loss can be explained by expulsion of both evaporable and chemically bound water. The lower diagram illustrates that a maximum expansion of about 0.1 per cent occurs at approximately 80°C. Above a temperature of about 135°C, shrinkage counteracts expansion resulting in a net contraction of the cement paste. There is a change in physical and mechanical properties as well as the microstructure due to a simultaneous thermal expansion and contraction.

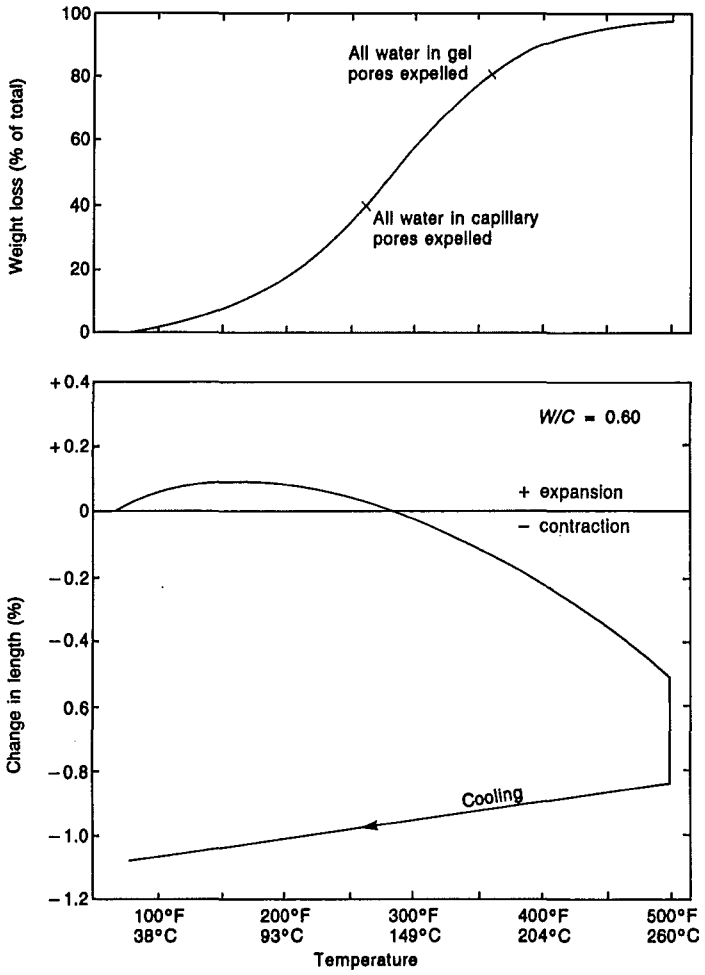

Figure 3.3 Typical relationship between weight loss, corresponding length change and temperature for Portland cement paste: + expansion, - contraction.

3.2.4 Strength Loss

Due to increasing porosity at increasing temperatures and the destruction of the cement gel at temperatures higher than 105°C, a loss of strength of the hardened cement paste has to be expected.

3.3 EVALUATION OF CEMENTITIOUS GROUTS FOR INJECTION PURPOSES

Injection of cementitious grout into cracks and voids has been used as a technique for repair or strengthening purposes, but only on masonry. Although this has been applied by contractors and engineers on an individual job basis, very little information is available on how to select the optimum grout mix or to judge the efficiency of the repair. An experimental program was conducted by Atkinson and Schuller (1992) to evaluate grouting procedures, the suitability of different types of cementitious grouts for injection, and the effect of grout injection on structural behaviour. Due to masonry being a porous material (similar to wood), the important parameters of the cement grout for masonry repair and cement bonded steel connections in glulam timber are the same.

3.3.1 Parameters

Injectability is one important parameter encompassing many different characteristics, including viscosity, particle size, fluidity, and cohesion, but basically implies the suitability of a given mix to flow without segregation within small cracks and voids. Atkinson and Schuller (1992) used several tests to provide a relative measure of injectability. The Marsh Funnel viscometer (Figure 3.4 (a)) was used to measure the viscosity. The minimum penetrable crack opening is calculated based on the observed grout penetration at the inclined plate test (Figure 3.4 (b)). The sand column test apparatus (Figure 3.4 (c)) provides a measure of the ability of a grout to penetrate small voids.

The mix stability indicates the ability of the mixture to remain homogeneous without continual mixing. 'Unstable' mixtures exhibit rapid settlement and segregation of the constituents during and after injection, leading to inferior penetration and incomplete filling of voids during grouting. When flow slows down, the cement particles in an unstable grout will sink to the bottom of the flow channel. This narrows the channel and finally blocks further injection. Stability also means that the grout is able to retain the water. When the grout passes through relatively dry material, some water will be absorbed from the grout. The more water is absorbed, the less fluid the grout will become, and hence injection will slow down and finally stop. These two blocking mechanisms show the importance of the stability of the grout. The bleeding and segregation test (Figure 3.4 (d)) measures the stability of a grout.

A more accurate test to determine the mix stability is the density test (Rickstahl and Gemert, 1996). Instability of the grout means that the heavy particles of the dispersion sink to the bottom of the recepticle due to gravity. This means that the density of the grout in the top region decreases because of this loss of heavy particles. Hence it is possible to measure the evolution of the density at any height in the recepticle.

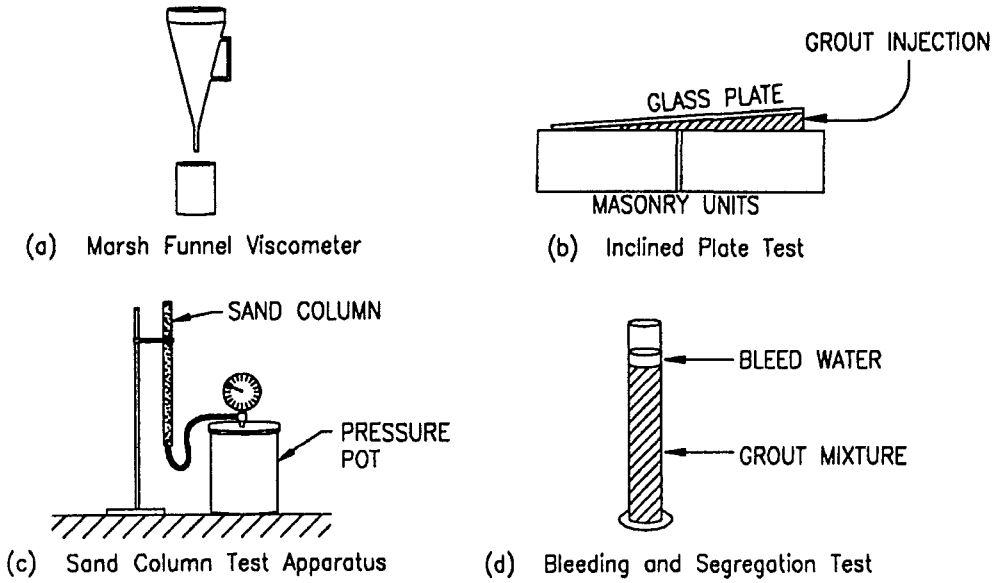

Figure 3.4 Apparatus used for evaluation of grout mix fluidity, injectability, and stability (Atkinson & Schuller, 1996)

3.3.2 Results of Grout Mix Evaluation

Over 30 separate combinations of cementitious materials, pozzolans, aggregates, and admixtures for varying water/cement ratios were evaluated by Atkinson and Schuller(1996). The following summary is given:

- Increasing the water/solids ratio enhances the capability of the grout to penetrate small cracks and voids, however mixtures with a high water/solids ratio exhibit excessive segregation and bleeding.

- Mix stability can be improved with addition of ultra-fines or water retaining agents: lime, fly ash, silica fume, and expansive admixture all work well to control bleeding and segregation.

- A water/cement ratio of 0.75 to 1.0 is optimal for a mix containing only Portland cement. Further evaluation is needed to determine the optimal w/c ratio for mixes containing other components.

- A more finely ground cement and microsilica increases stability and tensile strength of the grout.

- Addition of superplasticizer increases injectability of the mixture; a quantity of 2% by weight of cementitious materials is optimal.

- Addition of expansive admixtures have a beneficial effect on mix stability by reducing settlement and bleeding to nearly zero, with the added benefit that expansive action combats the high amount of plastic shrinkage encountered in mixes with a large water/cement ratio. It also provides an increase in tensile strength.

CHAPTER FOUR: MATERIAL PROPERTIES

4.1 OBJECTIVES AND SCOPE

An experimental study of some material properties has been undertaken. Experiments have been carried out to determine the shear strength of the cement grout, the shear strength of the timber and the crushing strength of the timber. The yield strength of screws and bolts, used as reinforcement for the cement bonded steel connections, has been obtained by three point bending tests. The test results have been used in order provide a better understanding of the different failure modes that are possible in the full-size tension tests. The values have also been employed in the calculations to predict the strength of the various experiments of cement bonded steel connections, described and discussed in Chapter five.

4.2 GROUT TESTS

4.2.1 Specimen Preparation

Two types of tests on cement grout were carried out. For grout test No.1, three test cylinders were made for each mixture and loaded in compression. The size of the test specimens was 50mm in diameter and 100mm long.

For grout test No.2, special timber moulds were made. They were designed to simulate the situation in the tension test connection (see Chapter five, Experiments No.2 and No.4) as can be seen in Figure 4.1. Therefore a 30mm diameter hole was drilled through a 90 x 90 x 150mm wooden block. The deformation inside the hole was drilled on the lathe, as for the tension test specimens. The key size was approximately 7mm deep and 70mm long. The two parts of the mould were screwed together, and the same cement grout was used as for the tension test with the

compression strength of 33MPa. Ingredients and mixing procedure of the grout are described in Chapter five. High strength steel rods were used for these tests.

The moulds were coated with mould release oil. This made it easier to take the specimens out of the mould. Before grouting, the specimens were filled with water to wet the wood. This was to prevent the dry wood sucking water out of the cement, causing a low strength grout.

The grout specimens were kept in water for 7 days. The surface where the load would be applied was levelled with plaster and a 1mm thick metal ring.

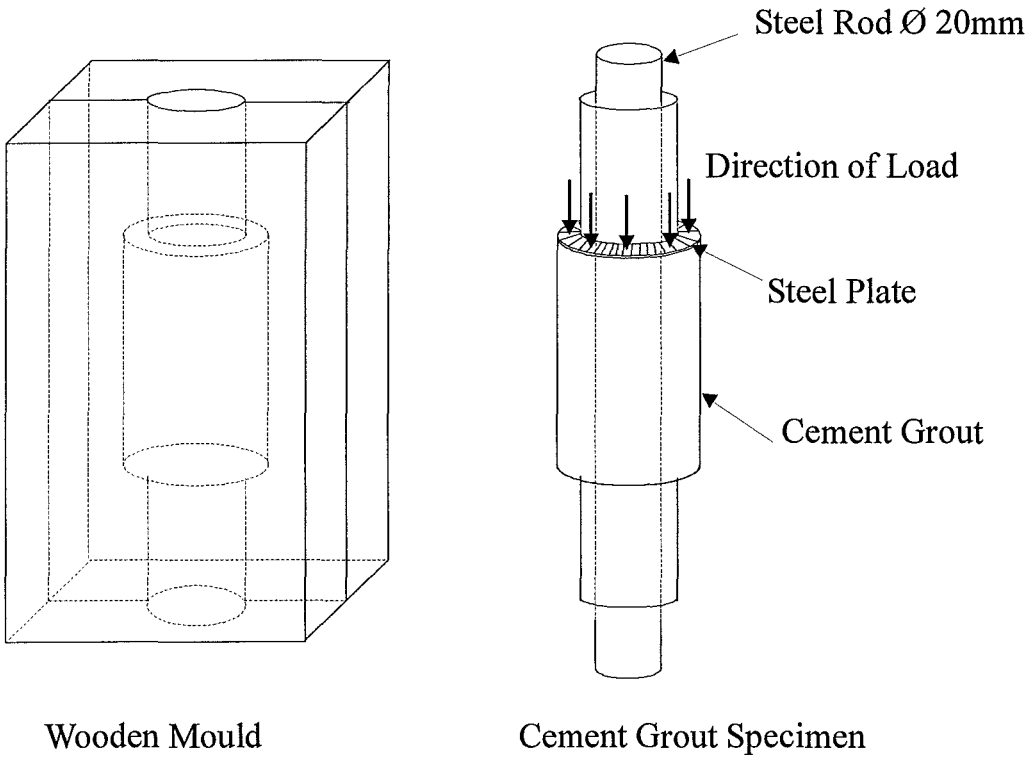

Figure 4.1 Cement grout specimen for grout test No.2

4.2.2 Testing Procedure

The loading system used is an Avery Testing Machine with 100kN capacity. The specimens were set up as shown in Figure 4.2. The loading rate was set to 18 kN per minute. The deflection was recorded by a potentiometer, measuring the movement of the upper head of the machine.

Each specimen was loaded until the maximum load was reached and the cement grout failed.

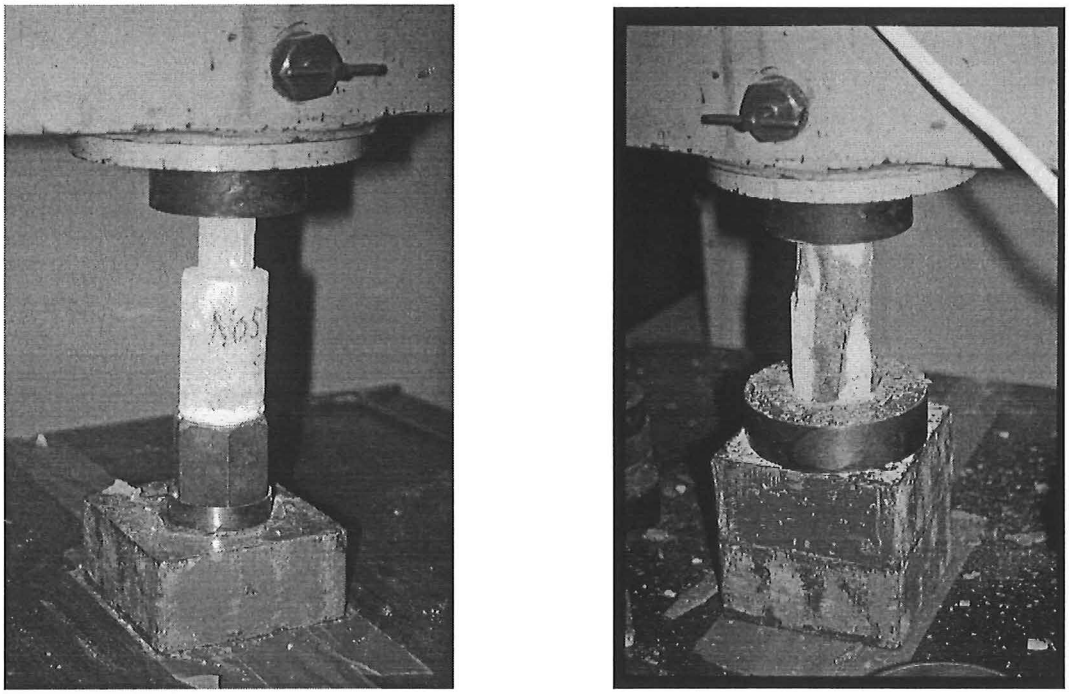

Figure 4.2 Test set-up for grout tests; left: test No.2, right: test No.1 (failed)

4.2.3 Results

The results of testing small cement grout cylinders in compression (grout test No.1) are shown in Table 4.1. Grout was mixed on four separate occasions, for making the specimens listed in column 2. The value for each mixture was obtained by taking the average of three test results. Figure 4.2 (left) shows the failure of a test specimen.

Table 4.1 Compression strength of cement grout (grout test No.1)

Mixture No.	Experiment No. (see Chapter Five)	Strength (MPa)
1	1	45.7
2	2 + 3	28.6
3	4 + 5 + Grout test No.2	33.3
4	6 + 7 + 8 + 9 + 10 + 11	46.2

Ten specimens were tested in grout test No.2. A typical load deflection curve is shown in Figure 4.3. The steep increase in load at the beginning turns into a fast, brittle failure as ultimate load is reached. The graph shows a lot of noise in the deflection measurement. The load deflection curves for all specimens are presented in Appendix 1. The average load of the tests was 18.3 kN.

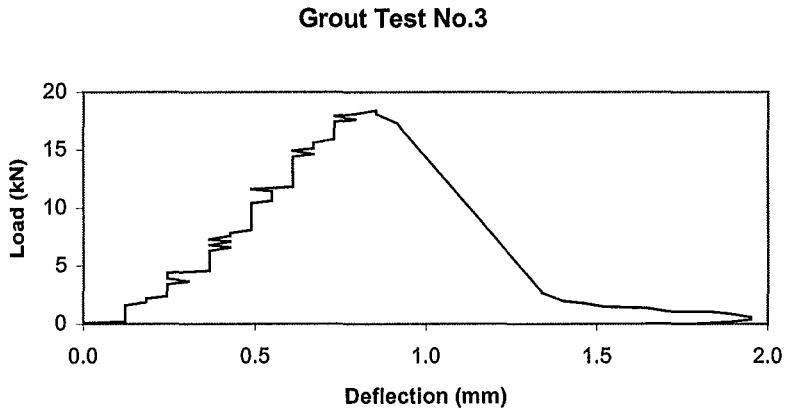

Figure 4.3 Typical load deflection curve of grout tests No.2

Neville (1997) recommends not undertaking strength tests on a neat cement paste because of difficulties of moulding and testing, with a consequently large variability of test results. For this reason, all results of grout testing might not be very reliable, but give a general direction.

Figure 4.4 shows the failure mode of the grout in grout test No.2. The cement failed in tension as can be seen in the 45°angle line of the remaining cone around the load bearing surface, and sheared along the threaded steel rod.

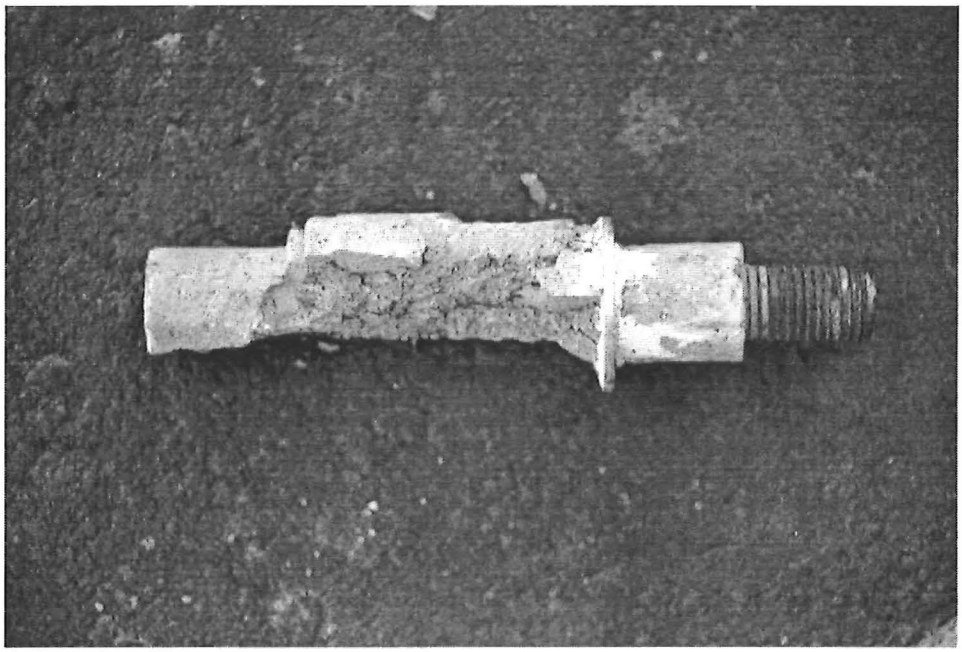

Figure 4.4 Grout failure of test No.2

4.3 TIMBER TESTS

Two material properties of timber were investigated, the crushing strength and the shear strength. The crushing strength was tested in two different ways. The first one was by pushing steel blocks into wood specimens and measuring the ultimate load. The second way was by testing small clear specimens of timber as described in the British Standard 373 (BS 373, 1957).

4.3.1 Specimen Preparation

To be consistent with the tension tests, Radiata Pine glue laminated timber from Auckland was used for the timber tests. The average density was 533 kg/m^3.

Beams of 90 x 90 mm were cut down to a length of 100mm. A 30mm diameter hole was drilled through the specimens using a drill-press. For the shear tests, the hole was widened to the diameter of 70mm, but only 70mm deep to leave a 30mm piece of wood to be pushed through. Figure 4.5 shows a sketch of the specimens.

Round steel blocks were made to simulate the load bearing surface of the tension test specimens. These blocks were of the shape shown in Figure 4.5, made in three different sizes, with a bearing surface of 542mm^2, 907mm^2 and 1280mm^2.

The 20 x 20 x 60mm test pieces for the compression test of small clear specimens were cut from the specimens used for the crushing test. The ends of the rectangular specimens had to be smooth and parallel and normal to the axis.

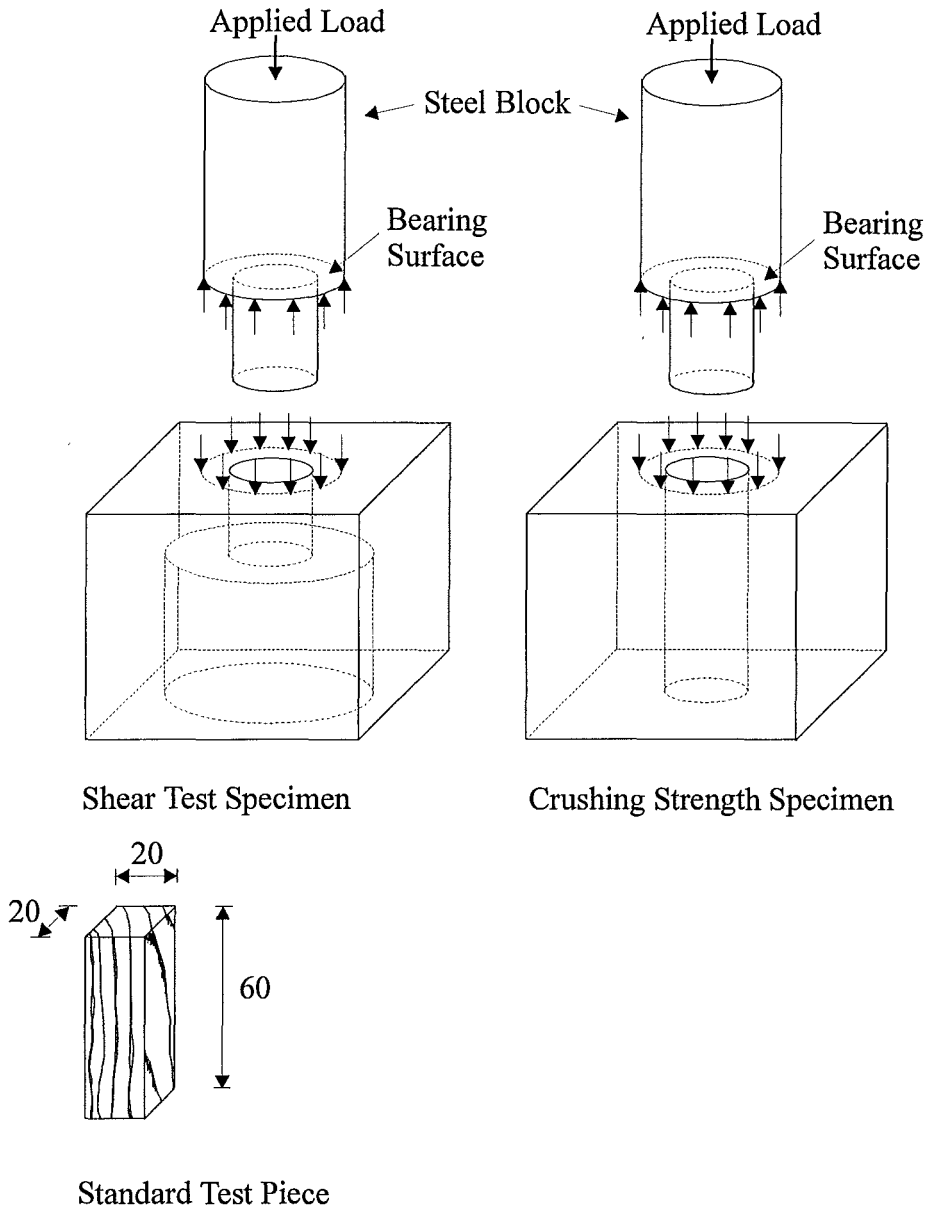

Figure 4.5 Design of timber test specimens

4.3.2 Testing Procedure

The loading system used was the Avery Testing Machine with 100kN capacity. The same software program was used as for the grout tests. The loading rate was set to 24kN per minute. Once the test machine was started, the program recorded the load and deflection. Each specimen was loaded until the maximum load was reached.

Crushing Test

The specimens were set up as shown in Figure 4.6. Each specimen of the crushing tests could be used twice. After pushing the steel block into one end, the specimen was turned around and the other end was tested using another steel block. This was to save material and to compare the strength obtained by two different bearing surfaces on the same specimen.

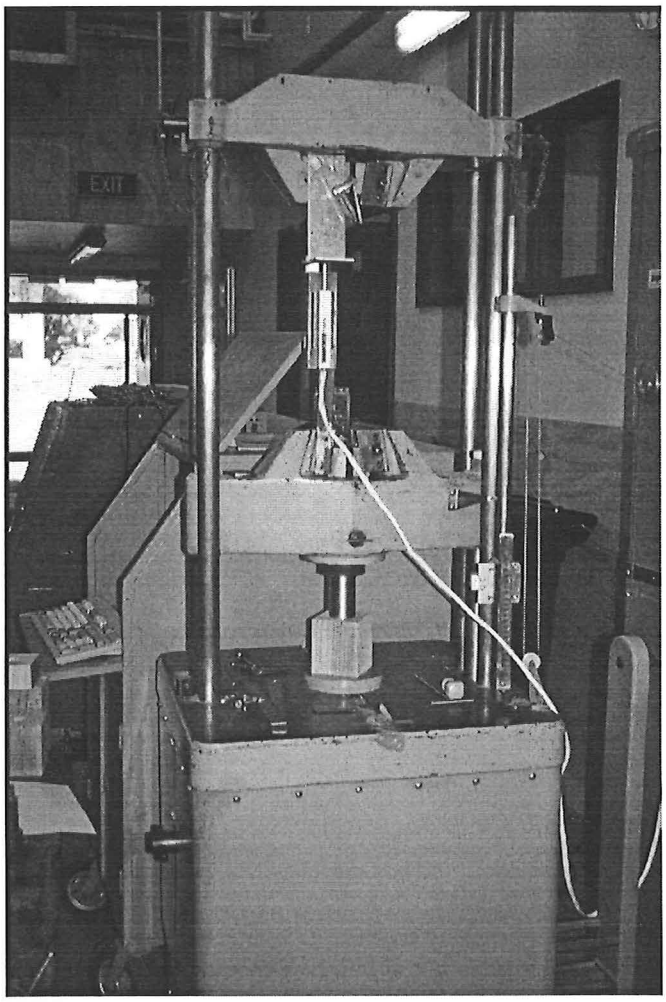

Figure 4.6 Test set-up for crushing test

Compression Test Parallel to the Grain (B.S.)

The compression strength of the small clear specimens was tested in accordance with the British Standard 373 (1957). The test set-up is shown in Figure 4.7, reproduced from this standard (Figure 6 in BS 373, 1957). The loading rate was set to 0.025in/min. It is important, that the plates, between which the specimen is placed, are parallel to each other and remain so during the whole period of test.

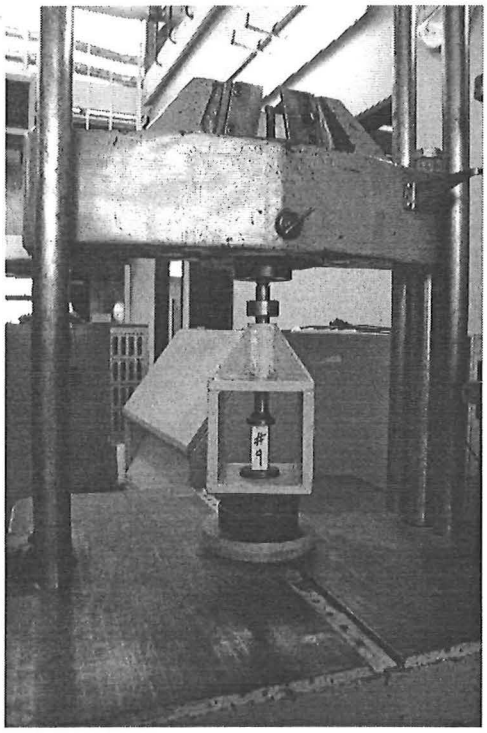

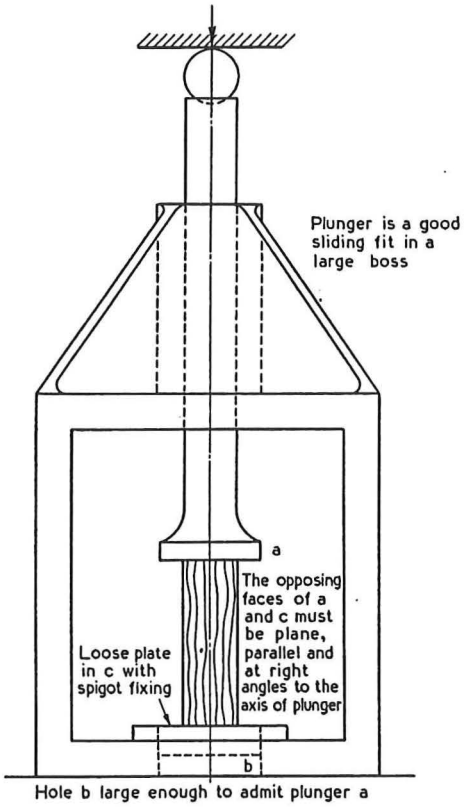

Figure 4.7 Test set-up for compression test parallel to grain

Shear Test

The specimens for the shear test were placed on top of a steel ring to enable the steel block to be pushed through the timber. The test procedure was stopped when the steel block was pushed through, forcing out a piece of timber. When trying to push through a larger piece of wood, the whole specimen split. The size of the steel ring the specimen was placed on, seemed to influence the failure mode. The medium sized steel block with a load bearing area of 907mm^2 was used.

4.3.3 Results

Crushing Strength

After reaching a maximum load, the steel block was just pushed further in, without increasing the load. The load deflection curves are plotted together and shown in Figure 4.8. Despite of the small size of the specimens and the varying quality of wood, the results of the tests show a consistency. The average crushing strength of the timber for 542mm^2, 907mm^2 and 1280mm^2 was 58 MPa, 54 MPa and 61 MPa, respectively.

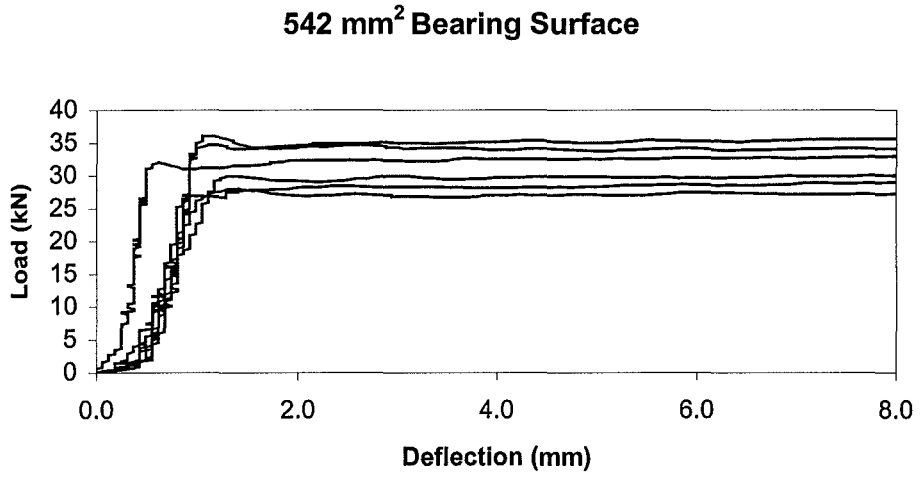

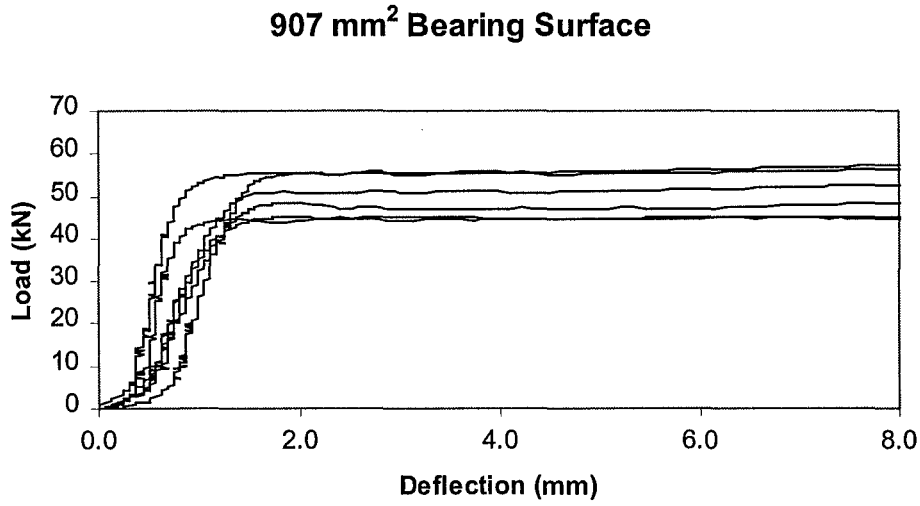

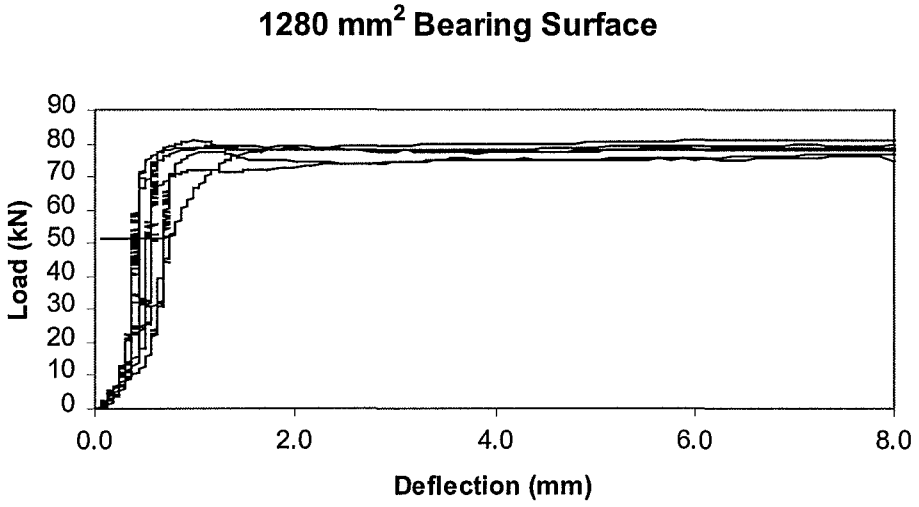

Figure 4.8 Load-deflection curves of timber crushing tests

The average compression strength of testing the small clear specimen was 46.7MPa. The difference between these two values for the compression strength can be explained by the fact that the strength, when pushing steel blocks through timber, is not only influenced by compression, but by shear.

The results of all timber compression tests are presented in table 4.2.

Shear Strength

Two specimens were tested for shear strength. Small wooden plugs, as can be seen in Figure 4.9, were forced through the timber by the steel block. The shear strength was 8.00 MPa and 9.02 MPa. However, this number is not very reliable, due to the very low number of tests. Shear strength of timber is very difficult to determine, as it varies a lot depending on the quality of the wood and the direction of the grain.

Table 4.2 Results of timber compression tests

Crushing Test		**Compression Test (BS 373)**		
Specimen No.	**Strength [Mpa]**	**Specimen No.**	**Strength [Mpa]**	**Density [kg/m^3]**
1a	51.9	1	37.5	501
2a	59.1	2	59.5	554
3a	66.4	3	42.3	554
4a	51.7	4	55.0	485
5a	55.2	5	56.3	490
6a	63.9	6	44.8	559
1b	47.4	-	-	501
2b	54.8	-	-	554
3b	59.7	-	-	554
4b	48.5	-	-	485
5b	52.1	-	-	490
6b	59.5	-	-	559
1c	63.1	7	39.5	554
2c	61.9	-	-	554
3c	61.2	8	36.3	554
4c	61.3	-	-	554
5c	60.5	9	49.3	552
6c	56.8	-	-	551
Average	**57.5**		**46.7**	**534**

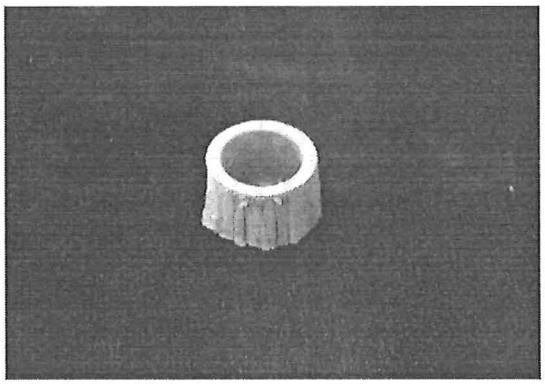

Figure 4.9 Wooden piece forced out by steel block

4.4 BENDING TESTS OF SCREWS AND BOLTS

Bolts and two different types of screws, used for the connections of the tension tests, were tested. A three point bending test was carried out to determine the yield strength and the plastic moment. The bolts were made out of high strength steel, the screws were mild steel. Type 1 screws were normal wood screws with a counter-sunk head. Type 2 screws had a raised hexagond head as shown in Figure 4.10

4.4.1 Test Procedure

Screws and bolts were tested in the MTS hydraulic testing machine with a 100kN capacity. The loading rate was set to 0.5mm/s and the level increment to 0.1mm. The screws and bolts were placed on the three point bending test apparatus and the span was adjusted to a maximum length possible (Table 4.3). They were then loaded until a deflection of 10mm was reached. The test set-up can be seen in Figure 4.10.

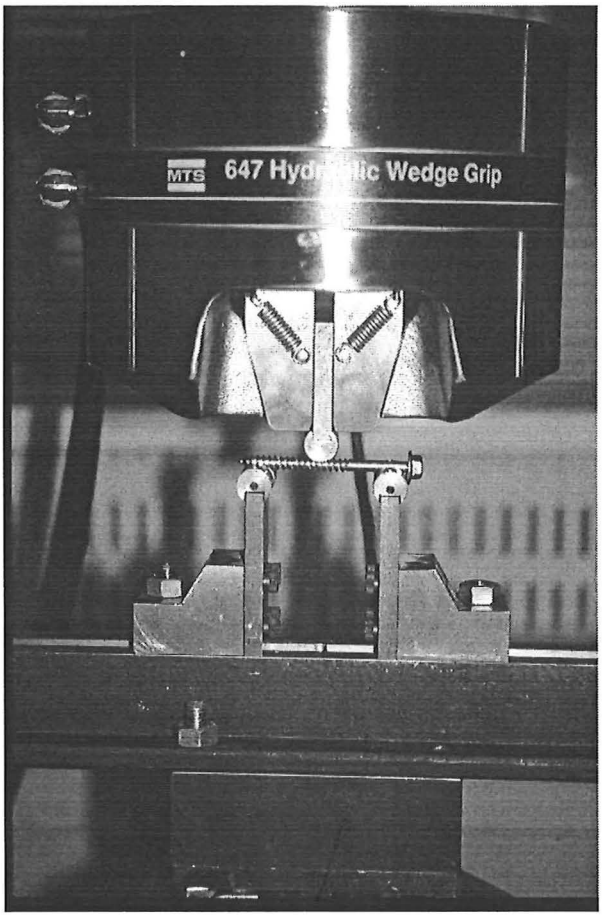

Figure 4.10 Test set-up for three point bending test of screw type 2

4.4.2 Results

Figure 4.11 shows a typical load-deflection curve of type 1 screw tests. The load increased steadily up to the ultimate load where it is held while deflection was increasing. This is a typical load-deflection curve of material with ductile behaviour. The average yield strength was 1080 MPa.

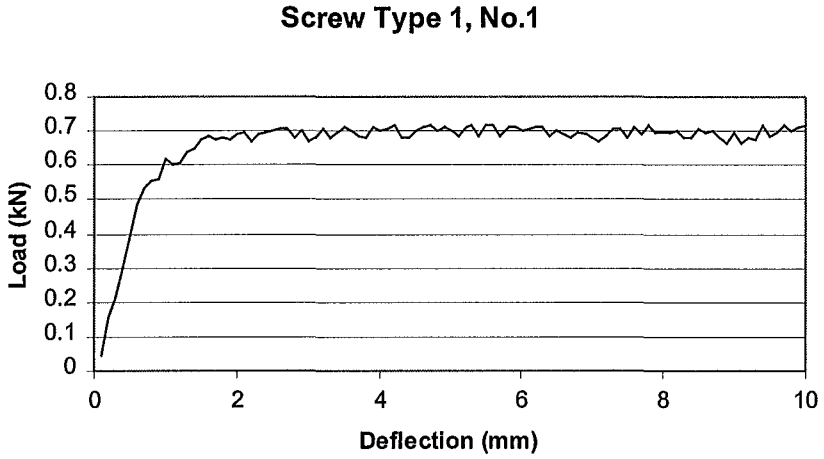

Figure 4.11 Typical load-deflection curve of type 1 screws

The type 2 screws showed a brittle failure mode after some yielding as can be seen in Figure 4.12. Some of the screws broke in the middle during the test. The average yield strength was 1390 MPa.

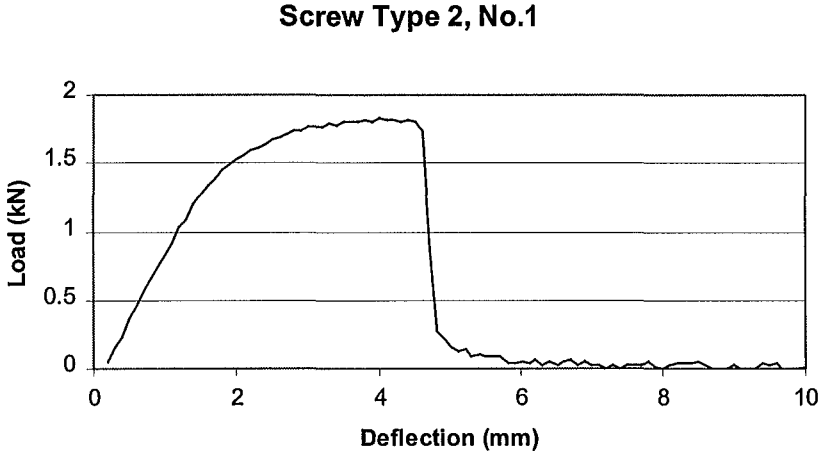

Figure 4.12 Typical load-deflection curve of the type 2 screws

Figure 4.13 shows a typical load-deflection curve of the bolt tests. The bolts show a very ductile behaviour as can be seen in large deformation at constant load. The average yield strength was 2075 MPa. The load-deflection curves of all tests are presented in Appendix 2.

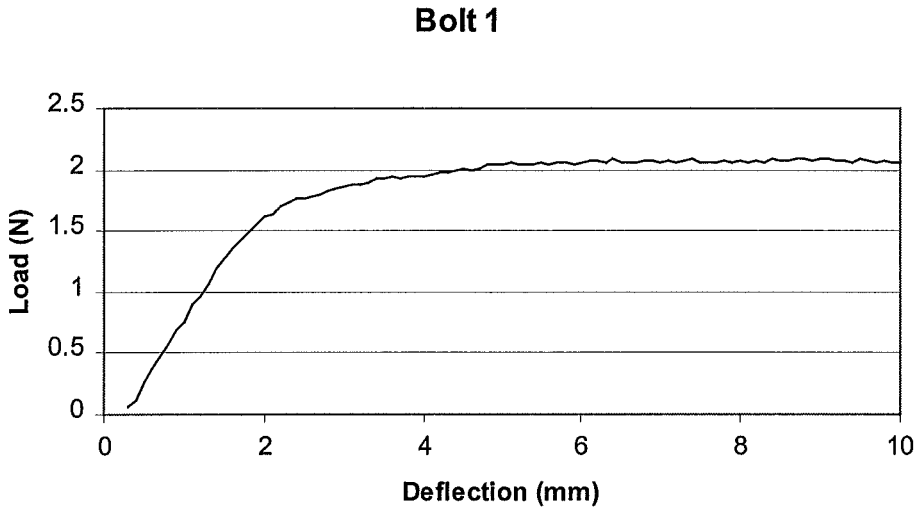

Figure 4.13 Typical load deflection curve of bolts

Table 4.3 gives an overview of the parameters of the test materials, the yield strength and the plastic moment.

The equation for the plastic moment is as follows:

$$Mpl = \frac{P \times l}{4}$$

where P= Load [N]

l = span [mm]

The equation for yield strength is as follows:

$$\sigma y = \frac{Mpl}{S}$$

where d = thread diameter(screws) or diameter (bolts)

S = plastic modulus

$$S = \frac{d^3}{6}$$

The thread diameter $\varnothing_{th}$ was measured between the thread with a digital caliper.

Table 4.3 Parameters, yield strength and plastic moment of screws and bolts

	$\varnothing$ [mm]	$\varnothing_{th}$ [mm]	L [mm]	l' [mm]	P_{max} [N]	S [mm^3]	σ_y [MPa]	Mpl [Nmm]
Screw Type 1	5.5	3.8	85	60	660	9.145	1080	9860
Screw Type 2	6	4.8	76	57	1800	18.432	1390	25650
Bolt	4.5	-	80	60	2100	15.188	2075	31500

where $\varnothing$ = diameter

$\varnothing_{th}$ = thread diameter

l = length

l' = span

P_{max} = ultimate load

S = plastic modulus

σ_y = yield strength

M_{pl} = plastic moment

CHAPTER FIVE: TENSION TESTS

5.1 OBJECTIVES

The objectives of these experiments are to investigate the tensile strength and the failure mode of the glued in steel rod connection, using cement grout as an adhesive. A wide range of various designs of the hole geometry has been tested, with the objective of achieving a reasonable strength compared to the epoxy bonded steel connections.

Investigations by Barber (1994) showed that as the epoxy bonded steel connection is heated or exposed to fire, it softens and loses its tension strength. The critical temperature, when loss of strength commences, is approximately 50°C. As an alternative to epoxy cement was chosen, due to its better properties at elevated temperatures.

In comparison to epoxy, cement does not bond to wood. Therefore, a mechanical bond between the wood and cement interface had to be created. Different geometries were drilled inside the holes to investigate their effect on the tensile strength of the connection.

To prevent water being sucked out of the cement grout by dry wood and weaken the cement, various possibilities are available. A review of the literature shows that water to wet the porous material is usually used and is sufficient.

With this in mind, it was expected that the cement bonded steel connection would not be as strong as the one using epoxy.

5.2 DESIGN OF EXPERIMENTS

Experiments were designed to be simple to set up and carry out. A variety of geometries of the connection were chosen, to investigate their influence on the strength of the connection. The geometry of the connection includes the shape and roughness of the inner hole surface and the hole diameter.

In addition, two different types of reinforcement were used. These may provide a method to prevent the cement grout from pulling out but also prevent the wood from splitting around the connection.

Eleven different designs were tested, as described below. An overview of all the designs is shown in Figure 5.1. Table 5.1 gives an overview of the design parameters for the tension tests.

Table 5.1 Overview of design parameters for tension tests

Experiment No.	Specimen No.	Rough (R)/ Smooth (S) Surface	Key	Number of Type1 Screws	Number of Type2 Screws	Number of Bolts
1	1003	R	-	-	-	-
1	1013	R	-	-	-	-
1	1023	R	-	-	-	-
1	1033	R	-	-	-	-
1	1043	R	-	-	-	-
1	1052	R	-	-	-	-
1	1062	R	-	-	-	-
1	1072	R	-	-	-	-
1	1082	R	-	-	-	-
1	1092	R	-	-	-	-
2	2013	S	K	-	-	-
2	2023	S	K	-	-	-
2	2033	S	K	-	-	-
3	3013	S	K	-	-	-

Experiment No.	Specimen No.	Rough (R)/ Smooth (S) Surface	Key	Number of Type1 Screws	Number of Type2 Screws	Number of Bolts
3	3023	S	K	-	-	-
3	3033	S	K	-	-	-
4	4013	S	K	-	-	-
4	4023	S	K	-	-	-
4	4033	S	K	-	-	-
5	5013	R	-	-	-	1
5	5023	R	-	-	-	1
5	5033	R	-	-	-	1
6	6013	R	-	-	-	1
6	6023	R	-	-	-	1
6	6033	R	-	-	-	1
7	7013	R	-	-	-	2
7	7023	R	-	-	-	2
7	7033	R	-	-	-	2
8	8013	R	-	-	-	3
8	8023	R	-	-	-	3
8	8033	R	-	-	-	3
9	9013	R	-	-	-	4
9	9023	R	-	-	-	4
9	9033	R	-	-	-	4
10	10013	S	-	-	8	-
10	10023	S	-	8	-	-
10	10033	S	-	8	-	-
11	11013	S	-	-	16	-
11	11023	S	-	16	-	-
11	11033	S	-	16	-	-

Experiment Number	Design
1	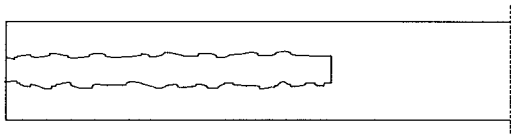
2+4	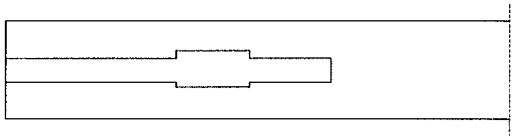
3	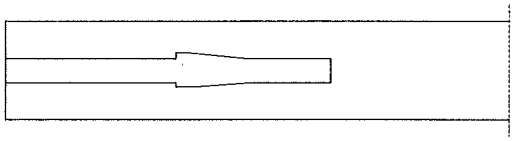
5	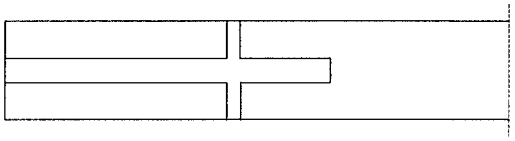
6	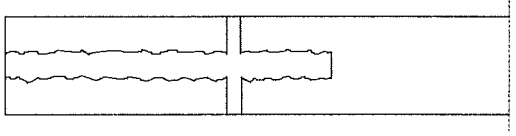
7	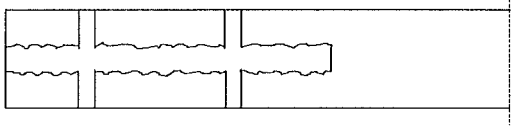
8	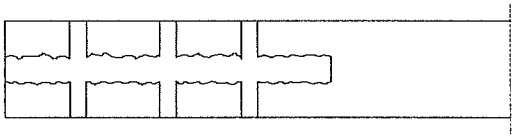
9	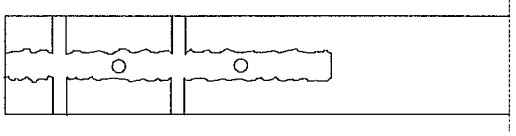
10	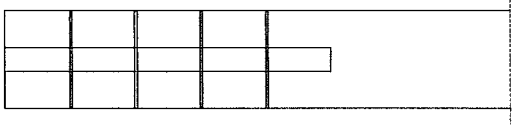
11	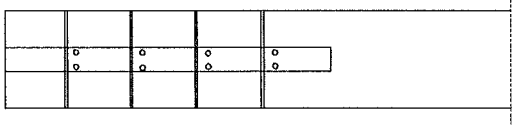

Figure 5.1 Overview of various designs

5.2.1 Design of Experiment No.1

Experiment No.1 was designed to be a very simple connection. Based on research of the epoxy bonded steel connections, embedment lengths of 200mm and 300mm were chosen. A smooth surface hole was drilled, using a drill press. Afterwards, the inner surface of the hole was roughed up with a special cutting tool, to provide a mechanical bonding between the cement and the timber. This cutting tool consists of a sharp knife attached to the top of a drill bit in a 90-degree angle to the length of the drill bit. The length of the knife was adjustable. Thus the depth of the key size was variable and was approximately 2mm. A sketch of the design of the experiment and the parameters are shown in Figure 5.2 and Table 5.2, respectively.

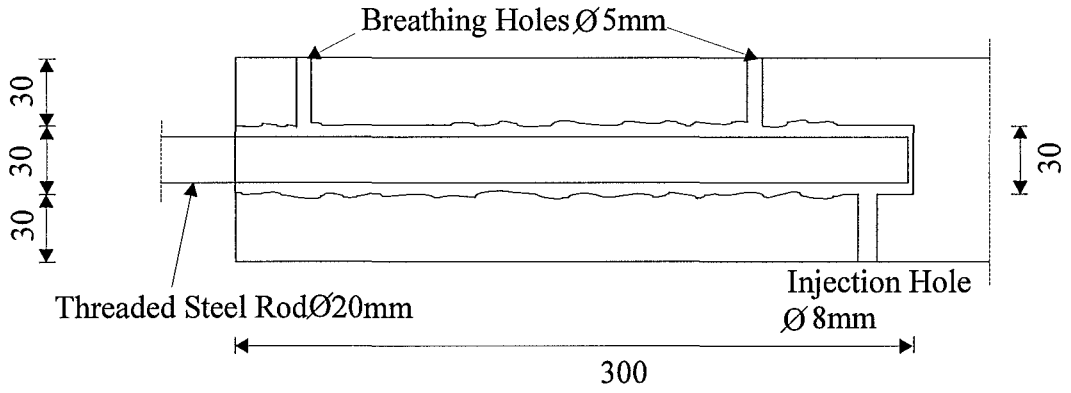

Figure 5.2 Design of Experiment No.1

Table 5.2 Design parameters of Experiment No.1

Number of Specimens	Threaded Rod Dim. [mm]		Embedment Length [mm]
	Length	Diameter	
5	400	20	200
5			300
Injecting Method (see 5.4.4)	Key Size [mm]		Embedment Hole Diameter [mm]
1	Rough Surface (approx. 2mm)		30

5.2.2 Design of Experiments No.2 and No.4

Experiments No.2 and No.4 were designed to have a distinct key in comparison to the indefinite key of Experiment No.1. The 30mm diameter hole was drilled, using a drill-press. The expansion inside the hole was drilled on the lathe. Problems occurred when drilling the expansion, because of the inability to visually control the actual key depth. Therefore, a test sample was drilled and cut open to check the key depth. In addition, the test specimens were cut open after tension testing to review the required depth.

The Design of Experiment No.4 as shown in Figure 5.4 was based on the material property results from Chapter Four. The design parameters are listed in Table 5.4.

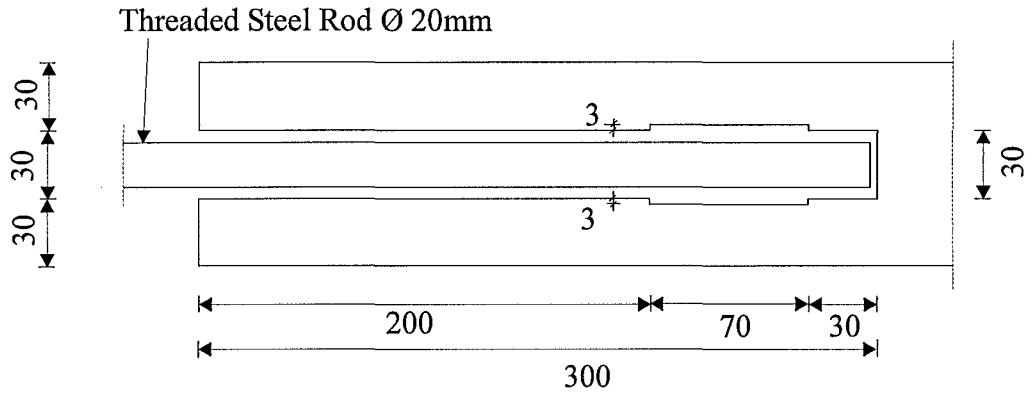

Figure 5.3 Design of Experiment No.2

Table 5.3 Design parameters of Experiment No.2

Number of Specimens	Threaded Rod Dim. [mm]		Embedment Length [mm]
	Length	Diameter	
3	400	20	300
Injecting Method (see 5.4.4)	Key Size [mm]		Embedment Hole Diameter [mm]
2	Approx. 3		30

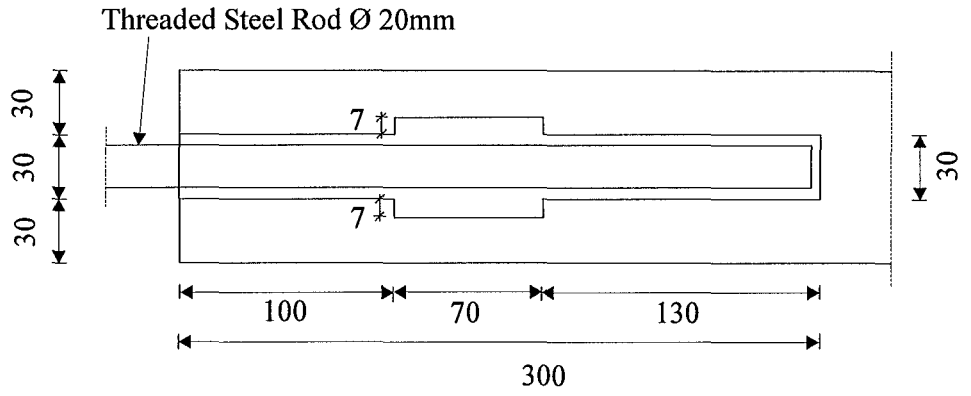

Figure 5.4 Design of Experiment No.4

Table 5.4 Design parameters of Experiment No.4

Number of Specimens	Threaded Rod Dim. [mm]		Embedment Length [mm]
	Length	Diameter	
3	400	20	300
Injecting Method (see 5.4.4)	Key Size [mm]		Embedment Hole Diameter [mm]
2	7		30

5.2.3 Design of Experiment No.3

A tapered shape of the expansion in the hole was used for Experiment No.3 in order to increase the timber surface near the stress concentration point, which is at the end of the hole (Figure 5.5). The 30mm diameter pilot hole was drilled first with a drill-press. The inner shape was drilled on the lathe, as was the hole of Experiment No.2. Drilling this tapered shape was even more difficult than the square shape, due to the lack of visual control. The design parameters are listed in Table 5.5.

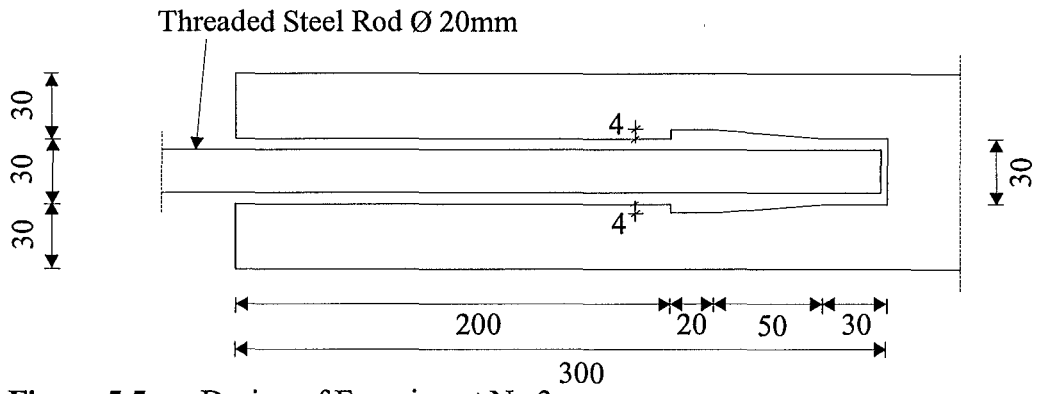

Figure 5.5 Design of Experiment No.3

Table 5.5 Design parameters of Experiment No.3

Number of Specimens	Threaded Rod Dim. [mm]		Embedment Length [mm]
	Length	Diameter	
3	400	20	300
Injecting Method (see 5.4.4)	Key Size [mm]		Embedment Hole Diameter [mm]
2	4		30

5.2.4 Design of Experiments No.5 to No.9

In these experiments, high strength steel pins were used to prevent the cement grout from slipping out. The required number of holes, with a diameter of 5mm, was drilled through the threaded steel rod. Perpendicular to the embedment hole, the 20mm sized holes were drilled into the timber using the drill press. The inner hole surfaces of the specimens of Experiments No.6 to No.9 were roughed up using the special cutting tool of Experiment No.2. The threaded steel rod was placed centrally inside the hole and the steel pins were pushed through the predrilled holes. The apertures were blocked by wooden plates, to prevent the cement grout from running out, as it was injected. The design parameters are listed in Table 5.6.

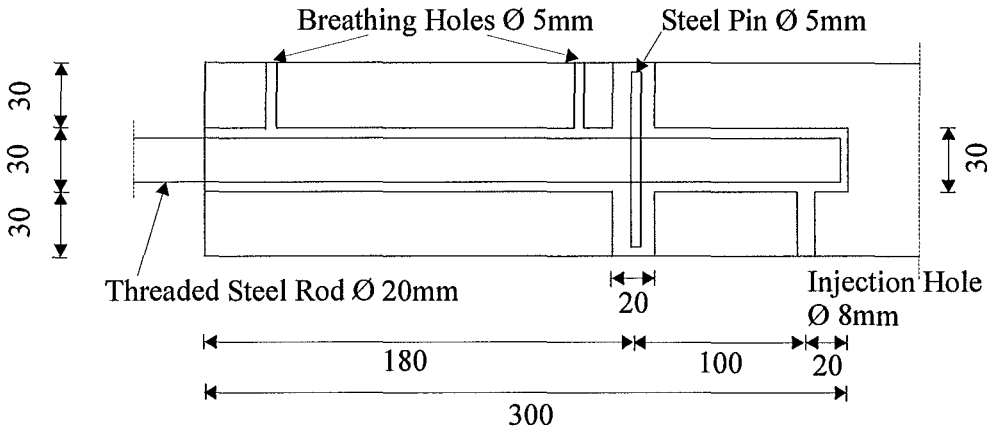

Figure 5.6 Design of Experiment No.5

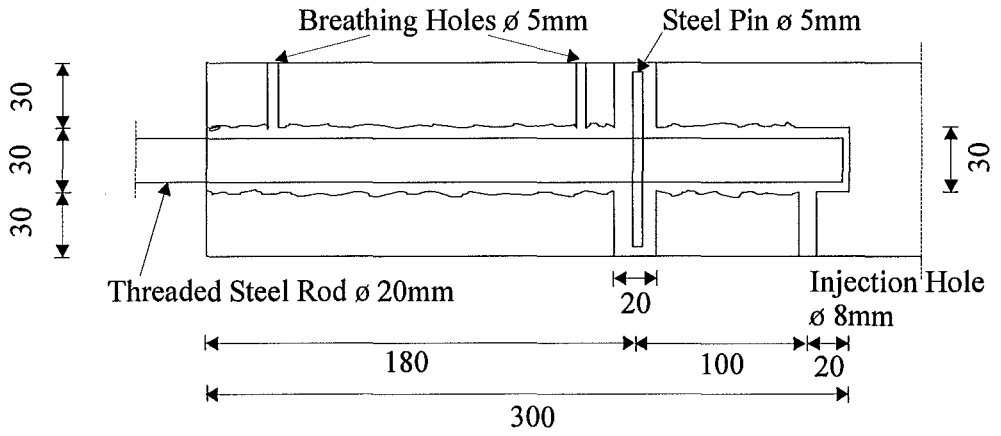

Figure 5.7 Design of Experiment No.6

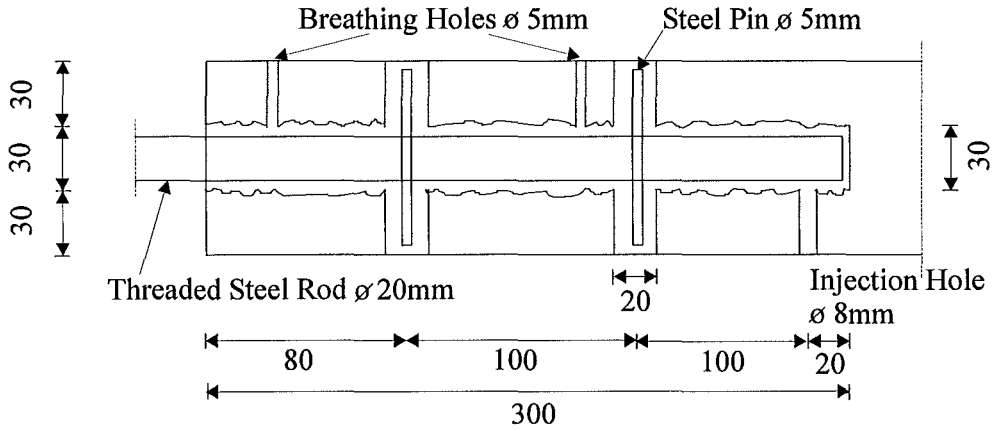

Figure 5.8 Design of Experiment No.7

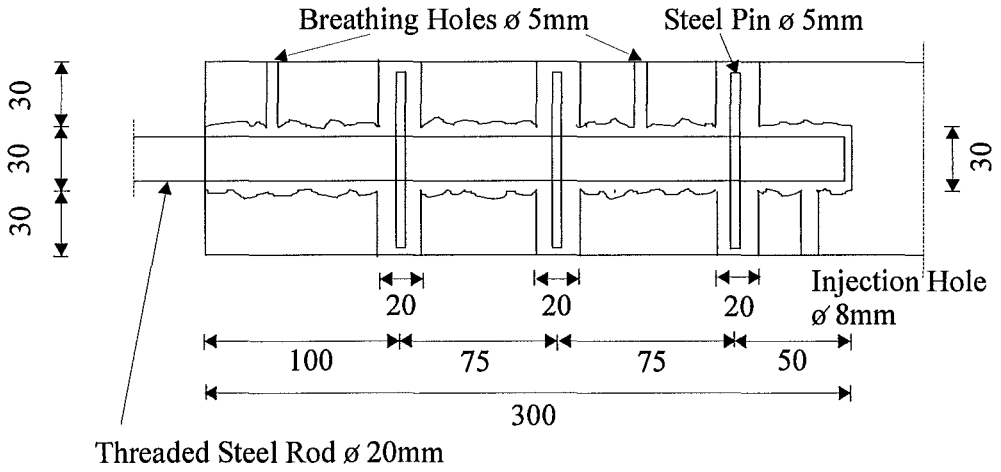

Figure 5.9 Design of Experiment No.8

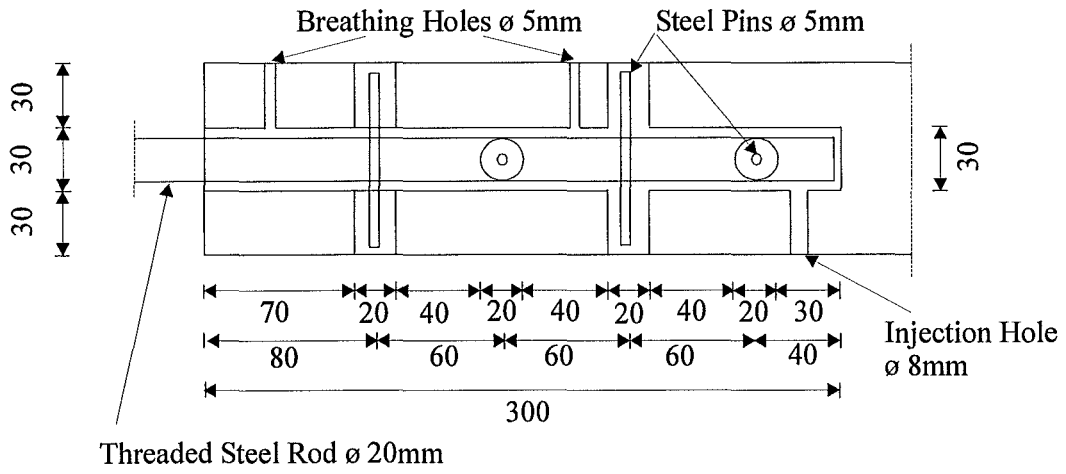

Figure 5.10 Design of Experiment No.9

Table 5.6 Design parameters of Experiments No.5 to No.9

Number of Specimens (each Experiment)	Threaded Rod Dim. [mm]		Embedment Length [mm]
	Length	Diameter	
3	400	20	300
Injecting Method (see 5.4.4)	Steel Pin Length x Diameter [mm]		Embedment Hole Diameter [mm]
1	85 x 5		30

5.2.5 Design of Experiments No.10 and No.11

In order to prevent wood splitting around the connection at the test end, specimens with screws were designed. The screws also acted as a cement reinforcement. In Experiment No.10, eight screws were used as can be seen in Figure 5.11. They were distributed evenly and layed out in one direction through the specimen. A cross section is shown in Figure 5.39. In Experiment No.11, sixteen screws were used; eight in one direction and eight perpendicular to them as shown in Figure 5.12. To keep the screws straight, small guiding holes were drilled with a battery drill. Care had to be taken when twisting in the screws because if they were too near the centre, the threaded rod could not fit in the gap. Two different types of screws were used. Type 1 and Type 2 screws are described in chapter four (paragraph 4.4). For these experiments, type 1 screws were used in two out of three tests and type 2 screws in the third test. The design parameters are listed in Table 5.7.

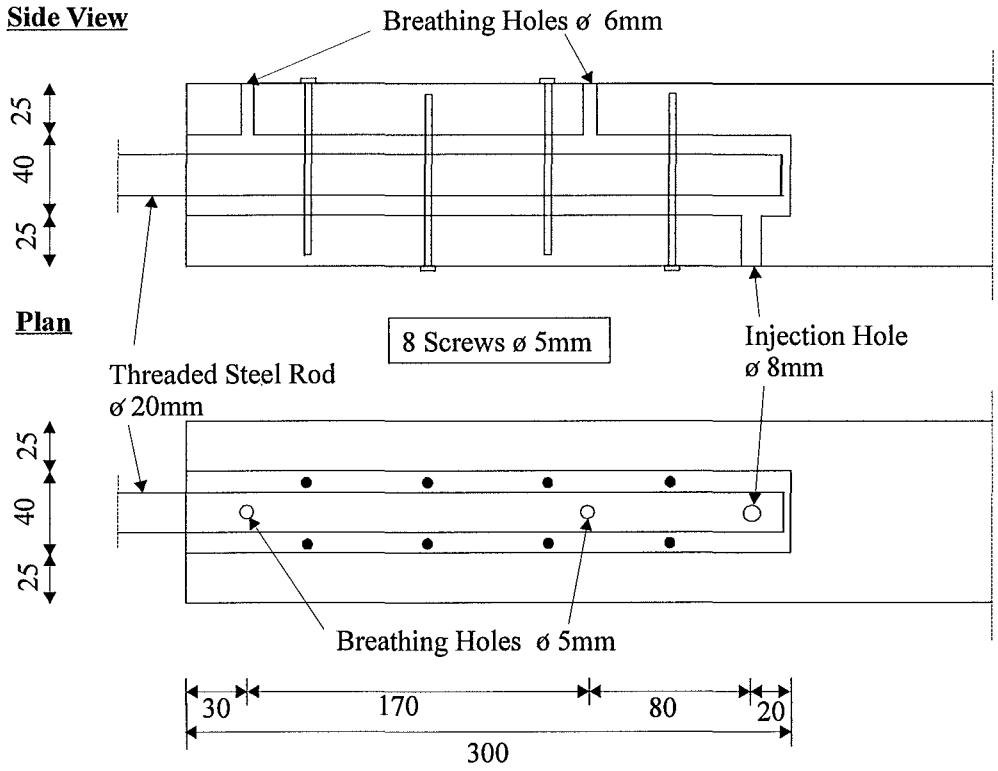

Figure 5.11 Design of Experiment No.10

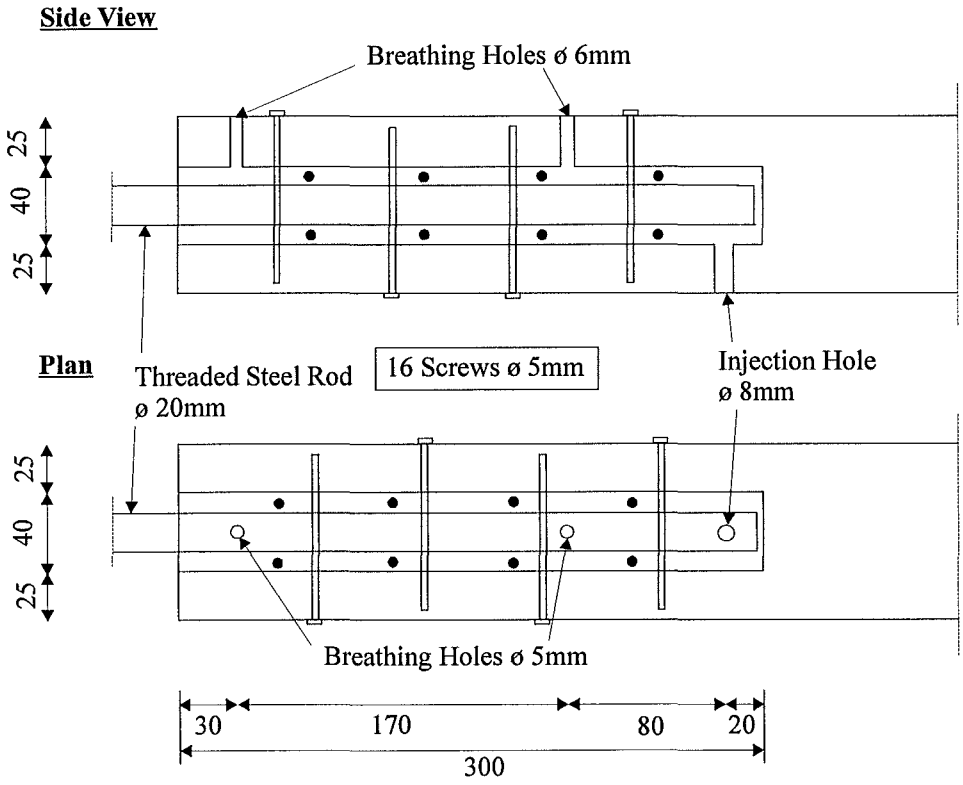

Figure 5.12 Design of Experiment No.11

Table 5.7 Design parameters of Experiment No.10 and No.11

Number of Specimens (each Experiment)	Threaded Rod Dim. [mm]		Embedment Length [mm]
	Length	Diameter	
3	400	20	300
Injecting Method (see 5.4.4)	**Number of Screws**		**Embedment Hole Diameter [mm]**
	Exp. No.10	Exp. No.11	
1	8	16	38

5.3 TEST METHOD AND MATERIALS

Testing was carried out on threaded steel rods bonded by cement grout into predrilled holes. The timber used was radiata pine. These connections were tested under tension load parallel to the wood grain using an Instron Universal testing machine with 250 kN capacity.

5.3.1 Test Design

The specimens were constructed by using timber of 90 x 90 x 800mm. At the test end, a threaded steel rod was placed into the hole. At the other end, a steel bracket was used facilitating an easy to set-up connection to the test machine. The test set-up can be seen in Figure 5.13, with Figure 5.14 showing details of the steel bracket. 20mm diameter bolts were used to fix the bracket to the specimen. This connection was calculated to be stronger than the glued in steel rod to ensure the failure occurring at the test end. Another benefit of this bracket was saving time and material as it was reused for all the tests.

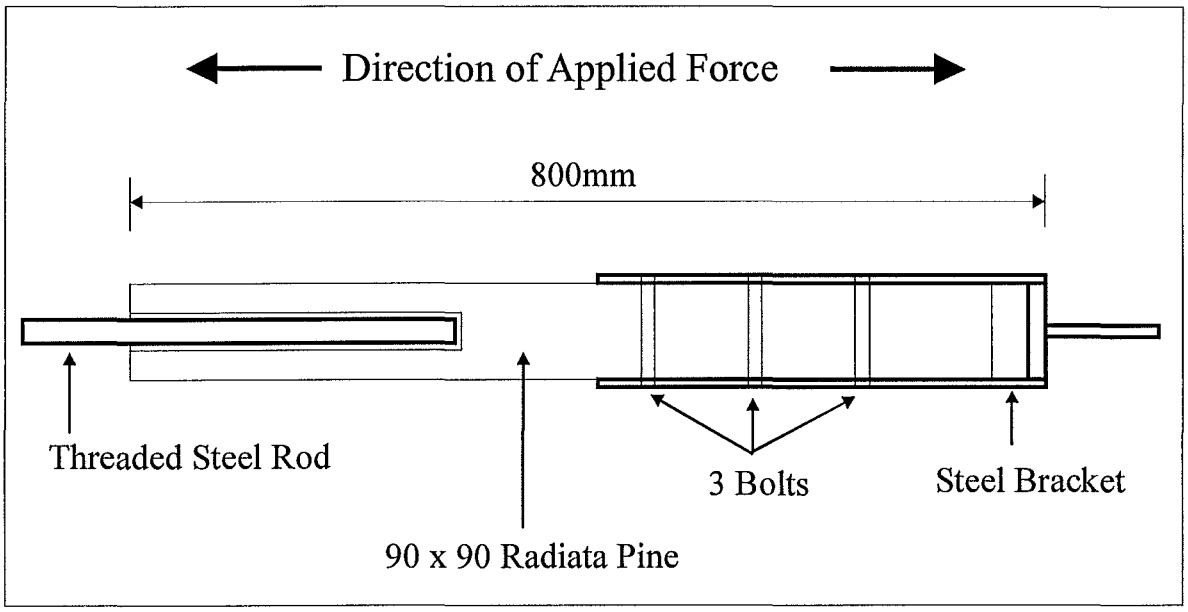

Figure 5.13 Test specimen for tension test

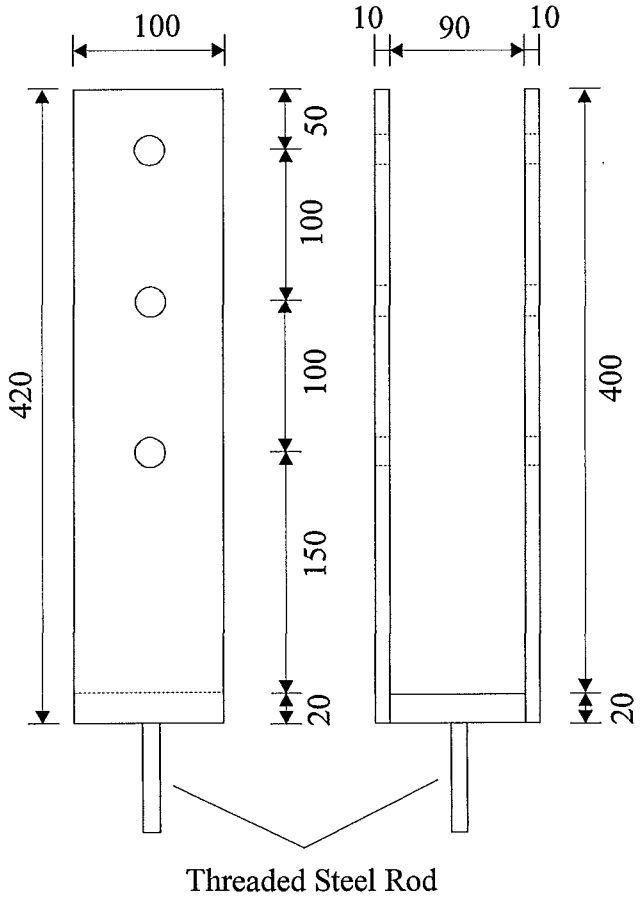

Figure 5.14 Steel bracket

5.3.2 Timber

Pinus Radiata glue laminated timber from Hunter Laminates Ltd. was used for Experiment No.1. The glulam timber, treated with CCA preservative, was fabricated in 1984 as beams for the roof of an indoor ice skating rink in Christchurch. The beams were salvaged from the building damaged by snow in 1992. Since then the timber has been kept in a store. For all the other experiments, Pinus Radiata glue laminated timber from Auckland was used.

Two methods were used to measure the moisture content. The electric moisture meter Protimeter 'Timbermaster' Model D184T measured the moisture content readings just before the testing. After testing, small samples were cut of the specimens and placed in an oven to dry. The moisture content was obtained by comparing the wet and dry weight of the samples. Results are shown in Table 5.8.

5.3.3 Cutting Scheme of Timber

All timber was selected to minimise the number of visible knots and pith. For Experiment No.1, beams 85 x 85mm were cut down to 800mm long specimens. For all other experiments, large cross-sectioned beams were cut to sizes approximately 90 x 90 x 750mm. The length was reduced for a better fit in the test machine. A hand saw and a bench saw was used to cut the timber.

5.3.4 Steel Rods

High strength steel rods were used to ensure the failure occurs within the connection and not by the steel yielding. Due to the better results for threaded bars than for deformed bars by Deng (1997), high strength threaded steel rods 20mm diameter were used. The specific tensile strength of the steel was 850 MPa and the yield strength was 680 MPa.

5.3.5 Cement Grout

Different types of cementitious materials, admixtures and aggregates used are described below.

Cementitious Materials:
Portland cement was used as the main binding agent in the mixes. Portland cement is readily available, relatively inexpensive and commonly used in concrete construction.

Admixtures:
An expansive admixture has been used to reduce plastic volume change as the surrounding dry wood rapidly adsorbs excess water within the grout. The type of expansive admixture used for the experiments is called CAVEX, manufactured by the SIKA Corporation. The main reactive constituent of the admixture is a fine aluminum powder, which reacts with the alkaline cement paste forming tiny bubbles of hydrogen gas, thus offsetting total volume reduction due to water loss. The majority of the expansion occurs between 15 and 60 minutes following mixing (Atkinson and Schuller, 1992).

To be consistent, the same cementitious mixture was used to construct all the test specimens for the testing program.

The ingredients for cement grout used were Portland cement, water and expansive admixture. The water/cement-ratio was 0.68. The amount of expansive admixture used was 0.0533% by weight of cement. This mix had been used before for prestressed concrete beams and was found being a strong cement grout suitable for injection purposes. Test specimens were made to test the compression strength of the grout (see Chapter Four). The average compression strength was 38.43MPa.

5.4 SPECIMEN PREPARATION

5.4.1 Wetting of Holes

Due to the fact that dry wood will suck out water resulting in low strength grout, it is necessary to wet the wood surface inside the hole before pouring in the cement mix. It is important not to leave the water for longer than 40min in the hole to prevent too much shrinkage and swelling of the wood. Sometimes small cracks parallel to the grain occurred after wetting the wood. After excess water was driven out by air pressure, cement grout was filled into the holes.

5.4.2 Drilling and Geometry of Holes

Holes were drilled into the specimens using a drill press. When using a hand drill, care must be taken to ensure that the holes for the long embedment length are drilled correctly. Difficulties may arise due to sloping grain in timber making it difficult to keep the long drill-bit parallel to the edges of the timber and causing the drilled holes to be slightly off-centred. After drilling, holes were cleared of dust and wood-chips using air-pressure. For experiments using air-pressure to inject the cement grout, two breathing holes and one injection hole were drilled perpendicular to each embedment hole, as can be seen on Figure 5.15.

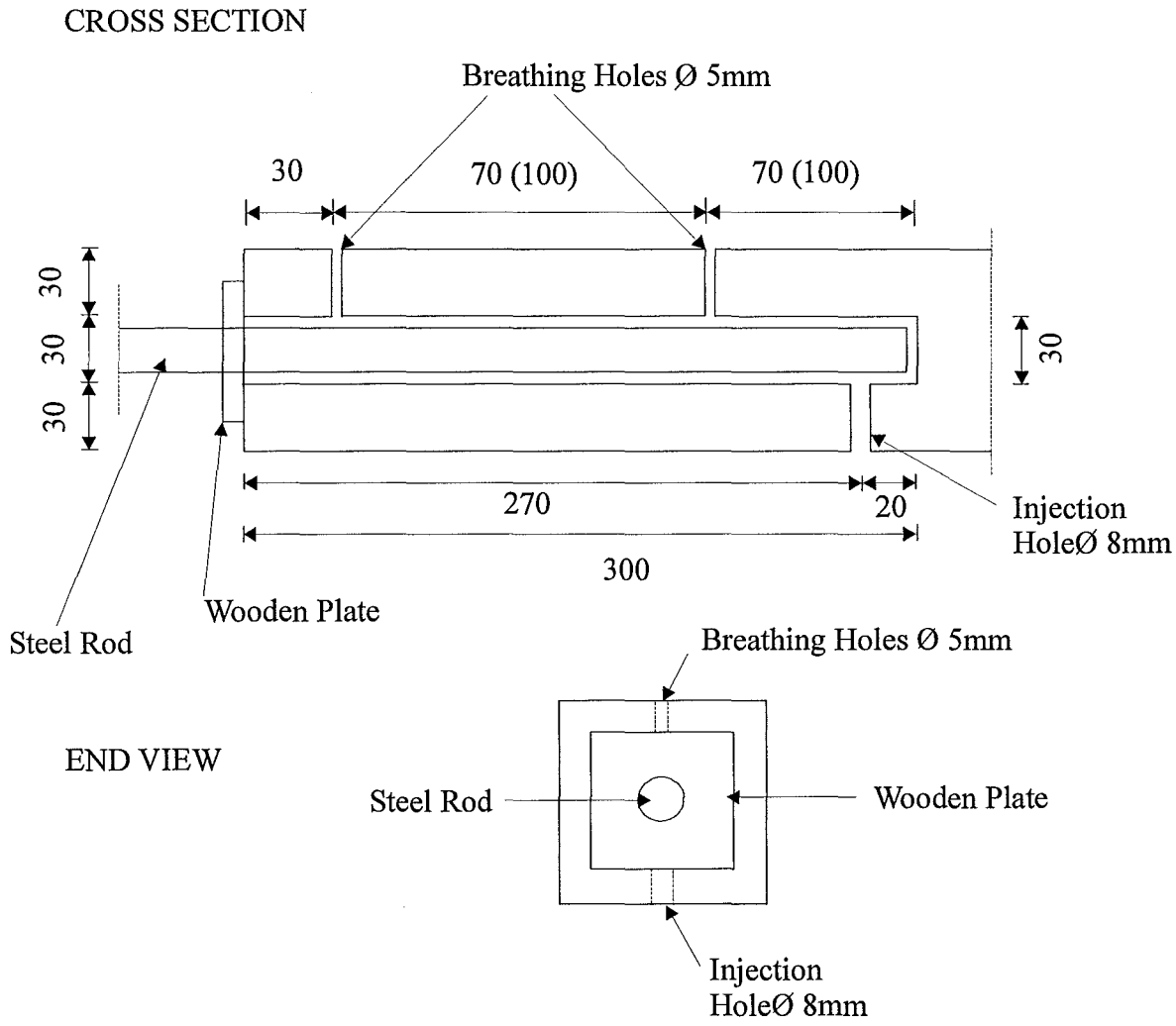

Figure 5.15 Schematic diagram of the specimen

5.4.3 Steel Rod Placement

The threaded steel rods were cut to the required length of 100mm longer than the embedment length. To keep the rod centrally within the hole, a 10mm wooden plate was screwed on to the rod. Then the plate was screwed to the face of the specimen as can be seen in Figure 5.14. The wooden plate was also used to seal the end of the hole and stop the cement grout running out as it was injected. In addition, the interfaces were sealed with silicone to prevent water leaking out.

5.4.4 Mixing and Injecting Cement Grout

All ingredients of the cement mix were weighed on a digital electronic scale. First, water was poured into a bucket, then cement was added gradually while stirring the mixture with a wooden stirrer to avoid lumps. Then the grout was mixed for approximately 5 minutes with an electric stirrer until no lumps were visible. After the addition of admixtures (eg, expansive admixture), the grout was stirred for another 3-4 minutes.

Two different ways of injecting the cement grout were used:

Method 1: The specimens had two breathing holes on the top and one injection hole on the bottom. The steel rod was placed in the hole and a wooden plate was screwed to the end hole (Figure 5.15). The cement grout was injected by air pressure through a hose of 8mm diameter while the specimen was in a horizontal position. As soon as the cement grout ran out of the first breathing hole, it was blocked by a wooden wedge. When the grout came out of the second hole, this hole was blocked as well. All the excess water in the hole was driven out by the cement. This injection procedure is similar to the way it would have to be done in practice.

Method 2: The specimens were standing upright. The cement mix was poured into the hole nearly filling it in order to ensure all the cavities are filled with cement. The wooden plate was screwed on to the steel rod and placed centrally into the filled hole.

Figure 5.16 Injection Procedure

5.5 TEST PROCEDURE

5.5.1 Testing Equipment

The loading system used for the tension tests was an Instron Universal Testing Machine with a 25,000 kg capacity. A 250m kN load cell measured the tensile load. The test specimens were set up as shown in Figure 5.17. The software used for these experiments is called DEFLOAD. It was programmed in such a manner that the signal would be triggered by whichever came first: either the tensile load increasing by 0.5kN or 0.1mm displacement occurring. The tensile load and the displacement were recorded during the experiment and saved by the computer.

The displacement was measured by a linear potentiometer. It was fixed to the machine measuring the movement of the crosshead.

5.5.2 Experimental Procedure

The steel bracket was fastened to the specimen by three bolts. Then the specimen was fixed into the Instron Universal Testing Machine by the loading bracket and the base plate using threaded bolts (Figure 5.18).

The loading rate was set to 0.1mm/min. Once the test machine was started, the computer program ran recording the load and the deflection. The data were saved on the computer and displayed on the screen. Each specimen was loaded until either timber failure or large pull-out deflection occurred.

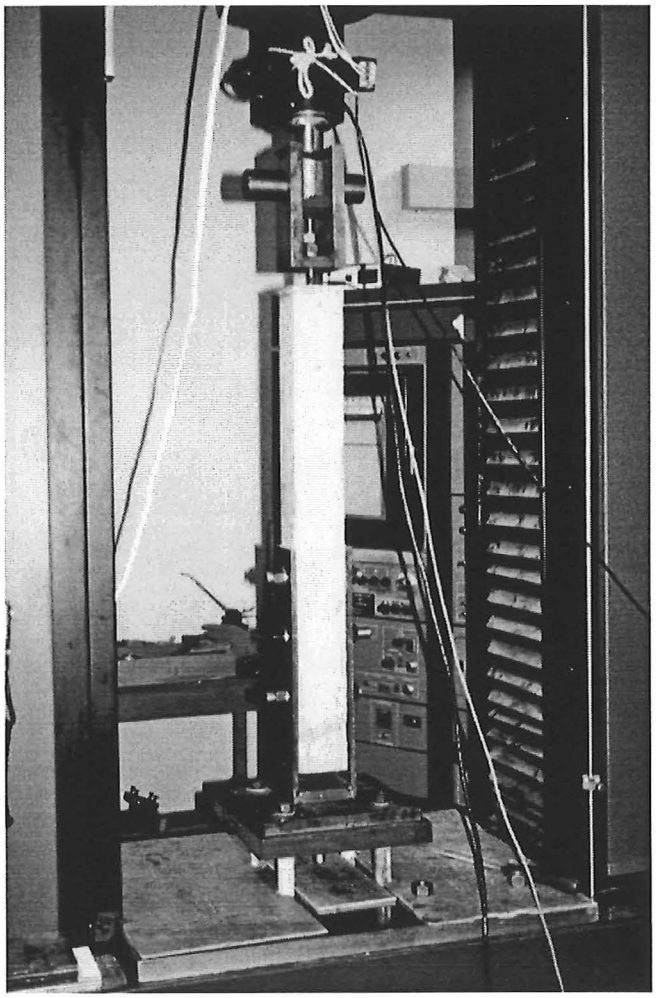

Figure 5.17 General view of the tension tests

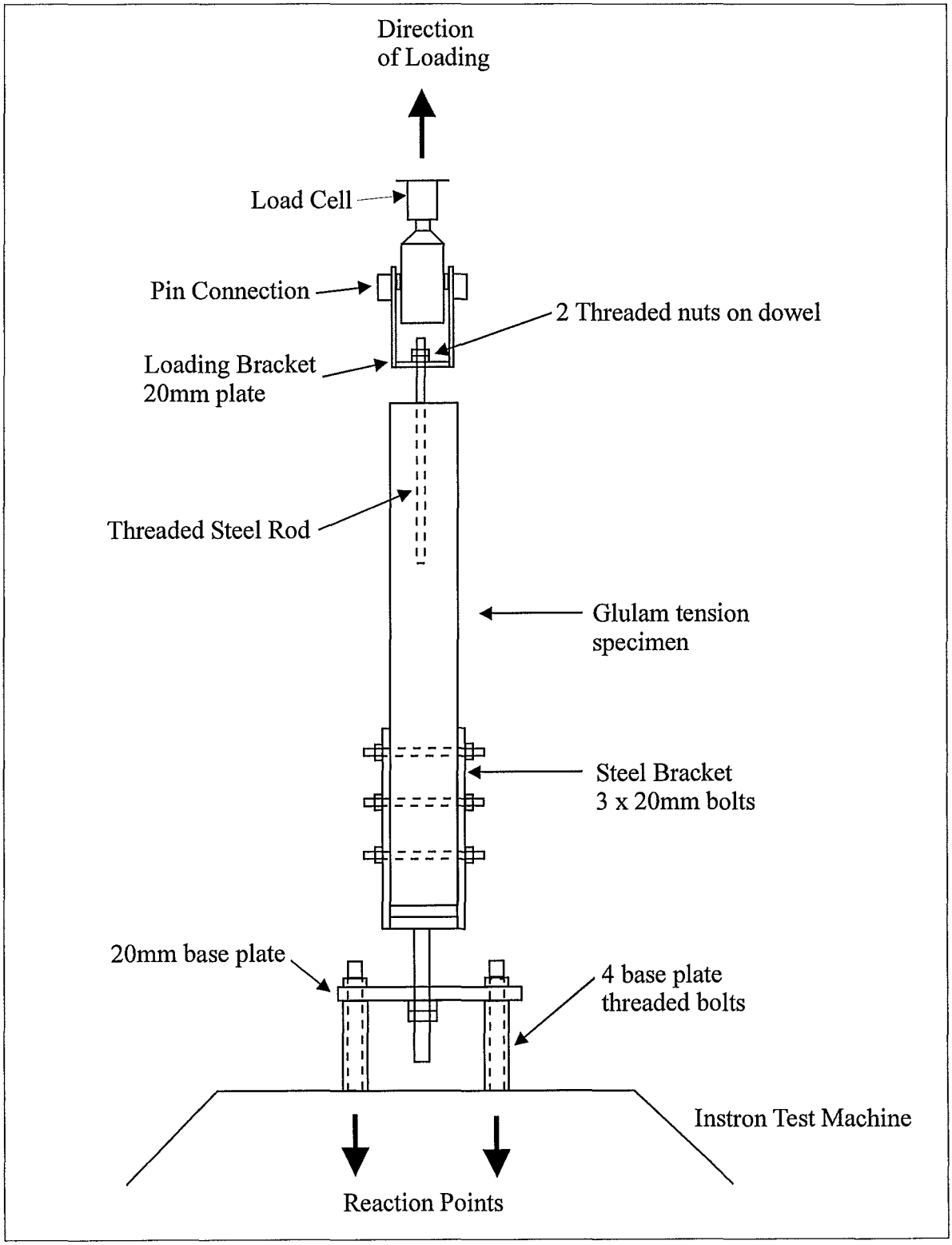

Figure 5.18 Test set-up for tension tests

5.6 TEST RESULTS

5.6.1 Load Deflection Curves and Test Results

In Experiment No.1, straight holes with roughed up surface were tested. The results are plotted together in Figure 5.19. The load deflection curves show a large deflection and a relatively slow increase of the load at the beginning. An initial slipping of the bolts and the bracket might have caused some of the deflection. When the maximum load was reached, the bar is pulling out further and the load was decreasing slowly. The failure was very slow and ductile.

Though the roughed up surface inside the hole cannot be defined exactly, the load deflection curves show a consistency in the performance and the maximum load. The capacity can be increased by increasing the embedment length.

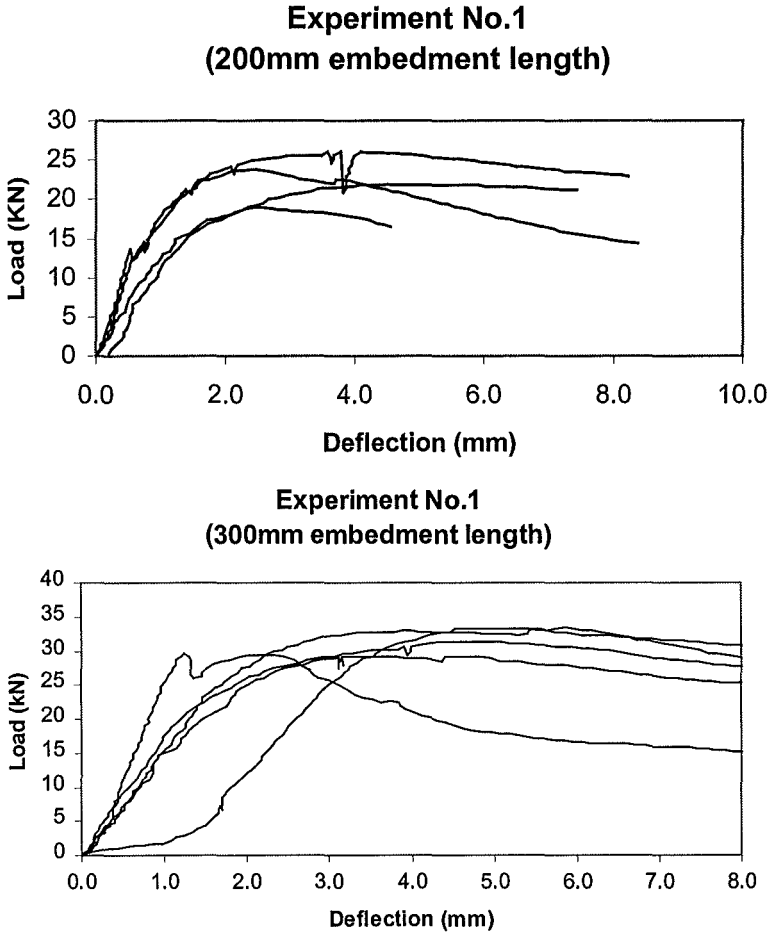

Figure 5.19 Load deflection curves of Experiment No.1

Experiments No.2 to No.4 show scatter in the results as can be seen in Figure 5.20. The slow increase of loads at the beginning of the tests is either staying at a plateau or decreasing slowly after reaching a maximum.

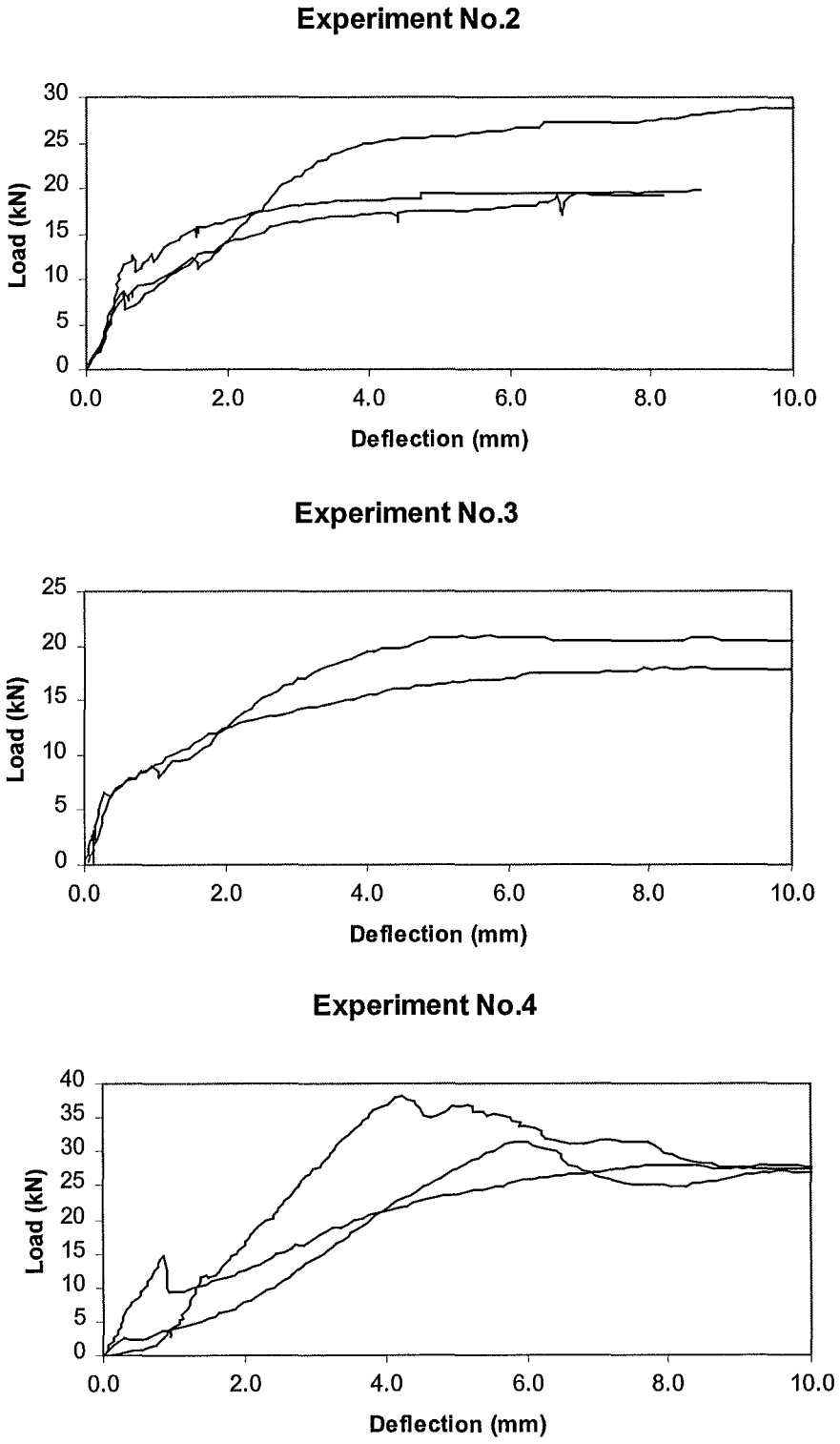

Figure 5.20 Load deflection curves of Experiments No.2 to No.4

The load deflection curves of the tests using bolts show a very good consistency in load and deflection. Figure 5.21 shows the results of Experiments No.5 and No.6 using one bolt. After a steep increase, the load stays on a plateau or decreases very slowly.

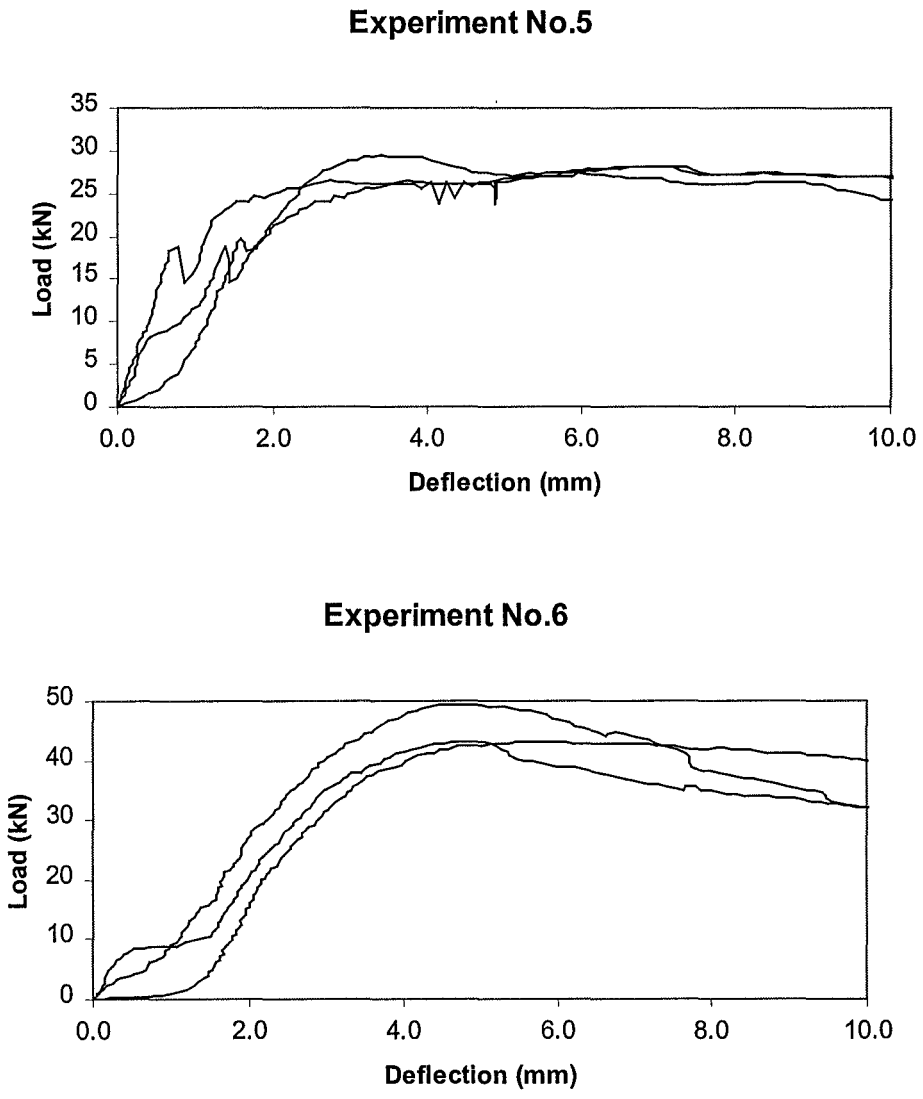

Figure. 5.21 Load deflection curves of Experiment No.5 and No.6

Figure 5.22 shows load deflection curves of Experiments No.7, No.8 and No.9 with two, three and four bolts, respectively. It can be seen that maximum load is reached at a pullout deflection of approximately 6mm regardless of number of bolts. Some curves show a steep, fast decrease of the load after reaching a high. This was caused by cracks that occurred just after wetting the wood, which were getting larger when the load was increased. The specimens split and the bar pulled out fast.

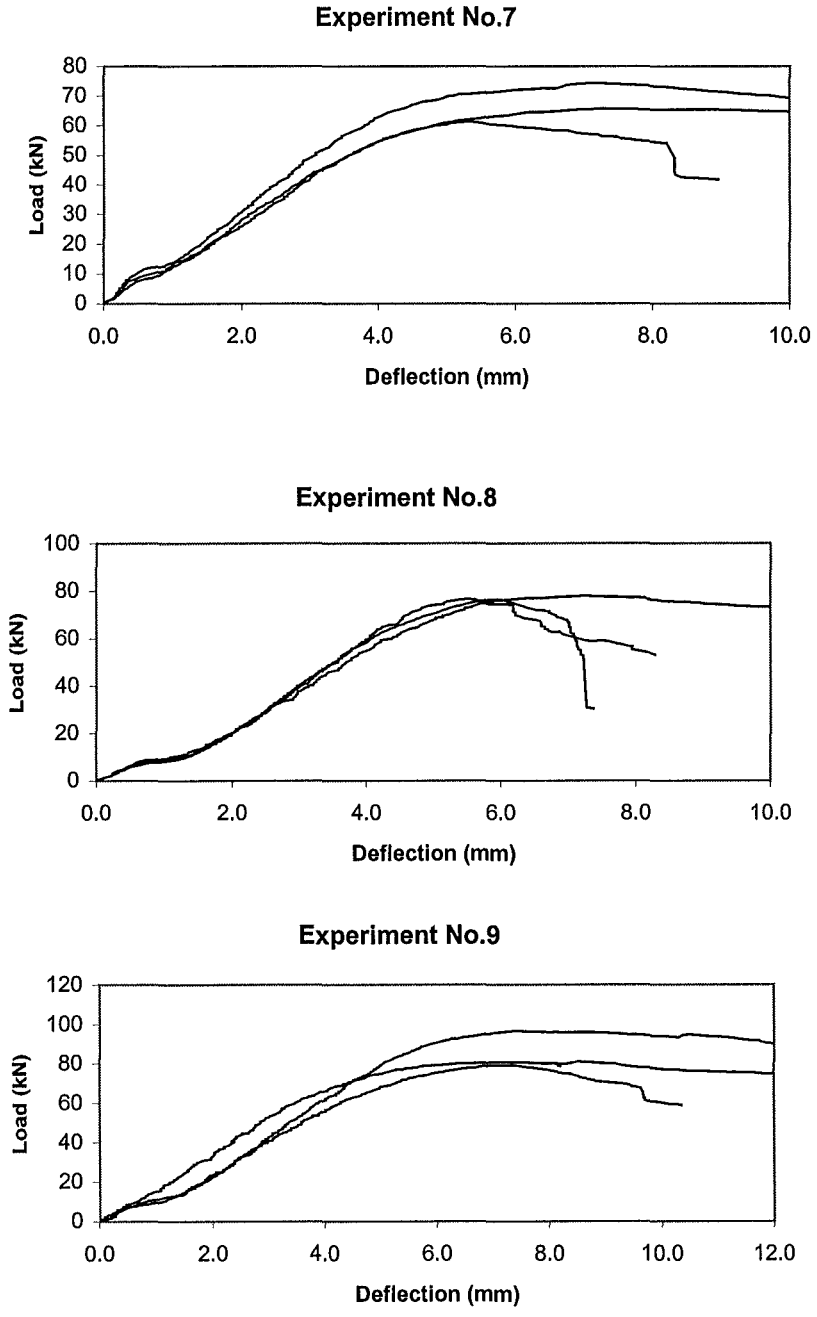

Figure 5.22 Load deflection curves of Experiments No.7, No.8 and No.9

The results of the tests using screws are shown in Figure 5.23. The load deflection curves show that the specimens of Experiment No.10 are holding the load after reaching the ultimate load, as did the connections using bolts. But it appears in Experiment No.11 that ductility drops off as the strength of the connection increases.

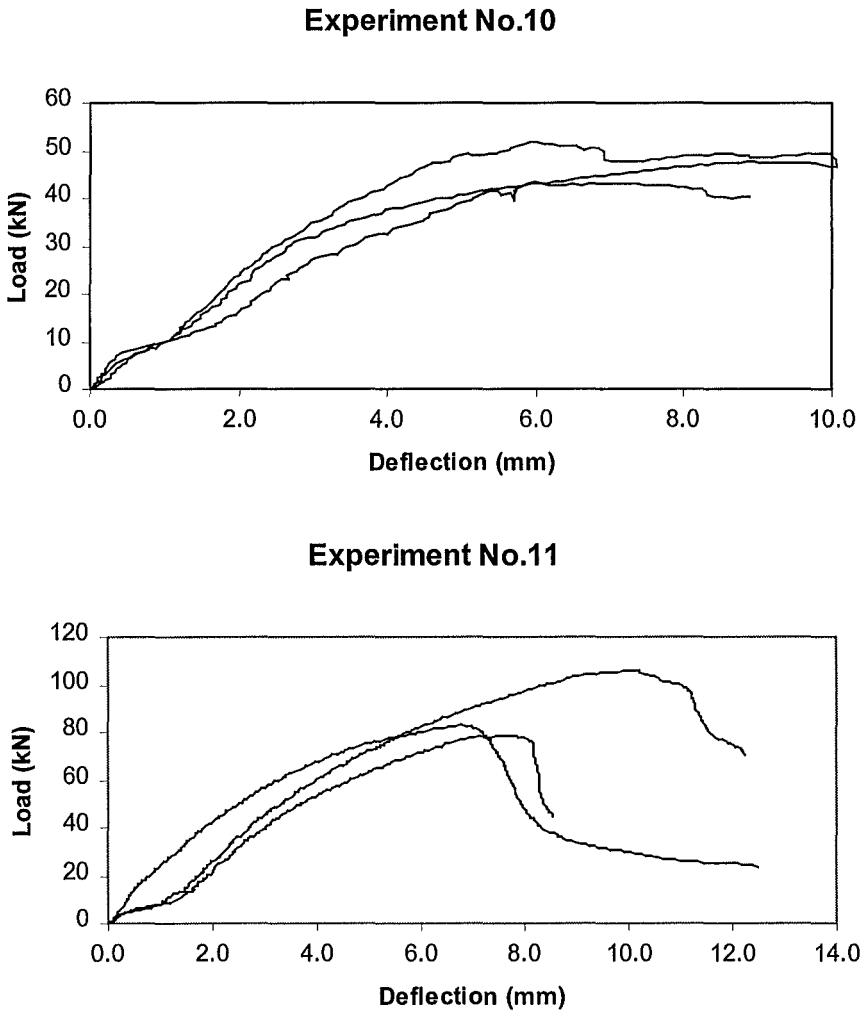

Figure 5.23 Load deflection curves of Experiments No.10 and No.11

The test results of all tension tests are listed in Table 5.8. The first column in the table shows the specimen number. Column four in the table shows the results of the two different methods of measuring the moisture content. The average moisture content measured with the moisture meter just before testing was 13.4%. In comparison to this, the moisture content measured by drying small specimen in an oven was insignificantly less with 12.3%.

The fifth column records the ultimate load, which was determined to be either the maximum tensile load of the load deflection curves, or the load where a plateau was reached. Slight increases of the load following the plateau were neglected.

Table 5.8 Results of tension tests

Specimen Number	Embedment Length (mm)	Oven-dry Density (Kg/m^3)	Moisture Content (%)		Ultimate Load (kN)
			Moisture Meter	Oven drying	
1003	300	496	14.5	14.0	31.4
1013	300	508	13.9	13.8	29.2
1023	300	544	13.2	12.6	33.5
1033	300	522	13.0	11.3	29.6
1043	300	499	13.8	11.9	33.1
1052	200	481	13.8	13.3	26.0
1062	200	469	13.3	11.9	23.7
1072	200	466	13.8	13.0	19.1
1082	200	533	12.8	12.2	21.8
1092	200	463	13.4	13.1	20.4
2013	300	508	12.1	10.3	19.8
2023	300	495	12.6	12.0	29.2
2033	300	555	12.5	10.4	19.33
3013	300	514	13.8	10.5	18.0
3023	300	524	12.2	10.5	25.4
3033	300	494	12.5	10.3	20.9
4013	300	452	11.9	11.8	38.3
4023	300	557	13.0	12.0	31.3
4033	300	511	14.6	13.0	28.1
5013	300	529	12.8	12.4	29.4
5023	300	513	12.0	12.0	26.3
5033	300	500	12.7	12.1	25.0

Specimen Number	Embedment Length (mm)	Oven-dry Density (Kg/m^3)	Moisture Content (%)		Ultimate Load (kN)
			Moisture Meter	Oven drying	
6013	300	517	14.5	12.5	43.2
6023	300	494	14.4	12.2	43.1
6033	300	478	16.5	12.7	49.2
7013	300	557	15.2	13.3	74.3
7023	300	481	14.1	13.1	61.2
7033	300	547	13.8	13.5	65.7
8013	300	552	14.6	13.2	76.6
8023	300	532	13.2	13.6	76.3
8033	300	545	13.2	13.1	78.0
9013	300	519	14.4	13.4	80.6
9023	300	520	13.8	13.4	79.1
9033	300	506	14.2	13.2	96.5
10013	300	559	12.4	11.0	51.9
10023	300	437	12.4	11.3	43.3
10033	300	493	12.7	10.9	47.9
11013	300	474	13.4	10.3	82.8
11023	300	521	11.2	12.1	105.6
11033	300	505	12.8	10.7	78.7

5.6.2 Failure Modes

The failure mode of the connections was dependent on the design of the hole geometry as described below. All the specimens were cut open after the experiment to observe the internal damage and deformation. Some crushing of the cement grout might have been caused by the relatively rough method of taking the specimens apart by means of a chisel and a hammer. For that reason, it was not always clear if crushing happened during the test procedure, or when the specimens were taken apart.

Experiment No.1:

As load increases the cement grout is pulled out of the timber. This is a slow bond failure occurring in the wood-cement interface. The bond between steel and cement is intact. Little pieces of timber are sticking to the cement grout, withdrawn from the rough surface inside the hole. The failure mode is shown in Figure 5.24.

Experiments No.2, No.3:

Timber crushed around the load bearing area of the distinct key, followed by the withdrawal of the cement grout. The bond between steel and cement is intact. The failure mode is shown in Figure 5.25.

Experiment No.4:

Initially as the load was increased, the key area started to bear against the wood causing local crushing. As the load further increased, a 45^{o} tension failure of the grout occurred. This tension failure propagated along the steel rod as a shear failure as the rod pulled out further. The bond between steel and cement remains intact. The failure mode is shown in Figure 5.26.

Experiments No.5, No.6, No.7, No.8, No.9 (bolted connections):

The specimens failed through bending failure of the bolts. As the threaded steel rod started to pull out, the bolts locally crushed the grout. Occasionally the crushing

propagated along the steel rod. The failure mode is shown in Figure 5.27 and Figure5.28.

Experiments No.10 and No.11 (screwed connections):

As the loading was increased, the screws carried the load through bending. Once the screws yielded, there was some local crushing of the timber. The threaded steel rod then started to pull out with increased load causing the screws to bend. On some occasions it was observed that there was a shear failure between the grout and the threaded rod, when the grout was restrained by the screws. The failure mode is shown in Figure 5.29 and Figure 5.30.

Figure 5.24 Failure mode of Experiment No.1

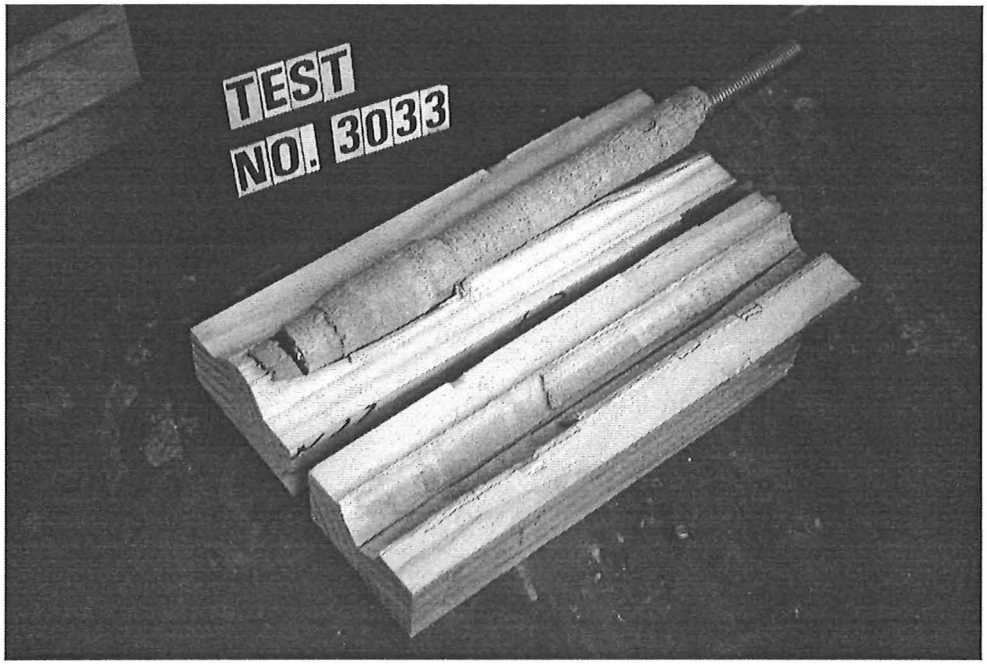

Figure 5.25 Failure mode of Experiment No.2 and No.3

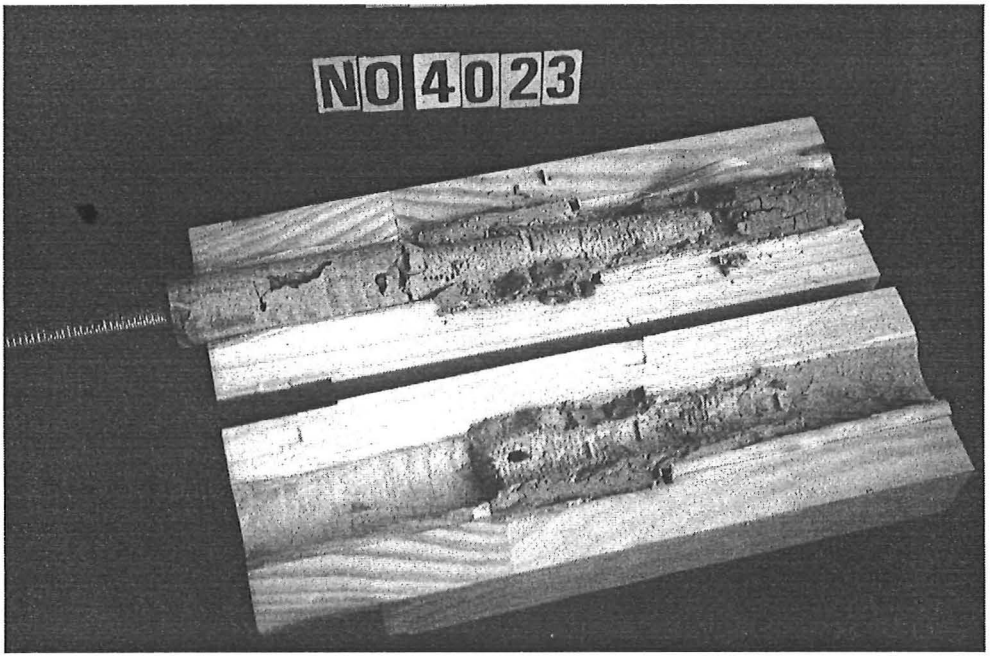

Figure 5.26 Failure mode of Experiment No.4

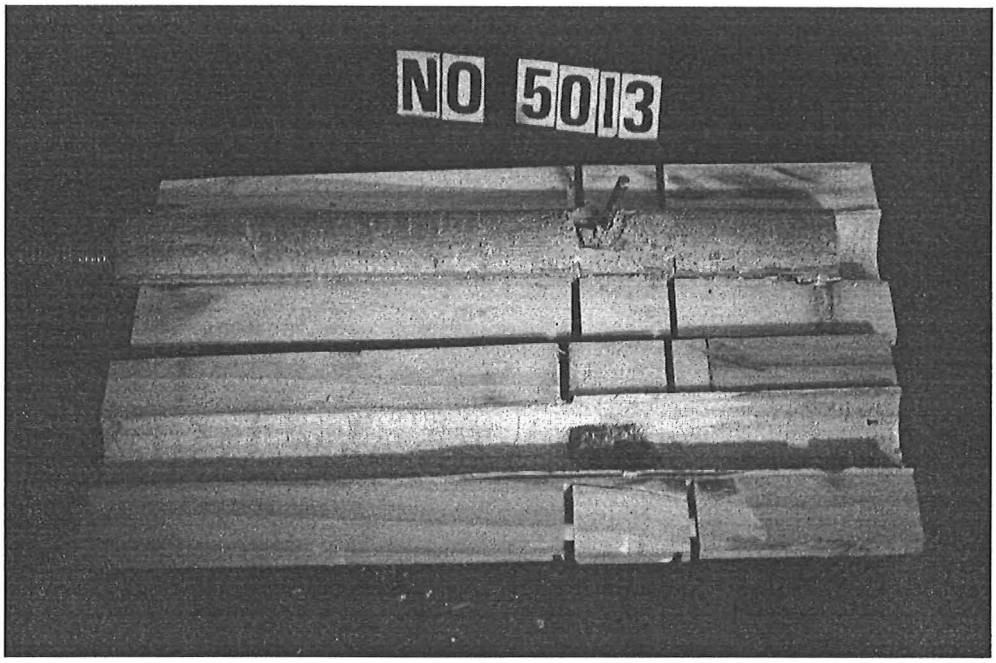

Figure 5.27 Failure mode of Experiment No.5

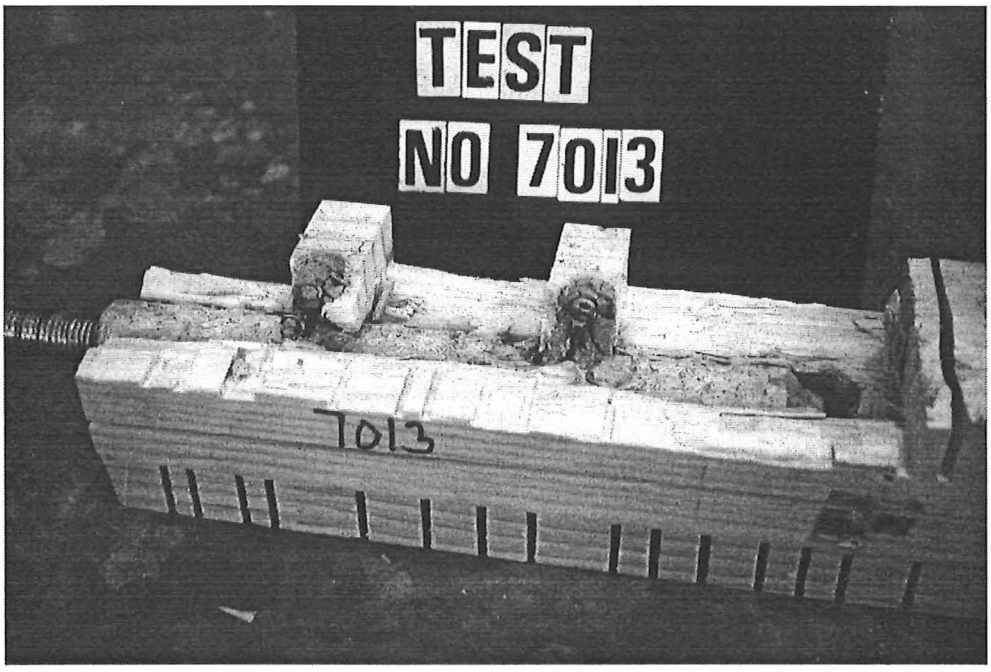

Figure 5.28 Failure mode of Experiment No.7

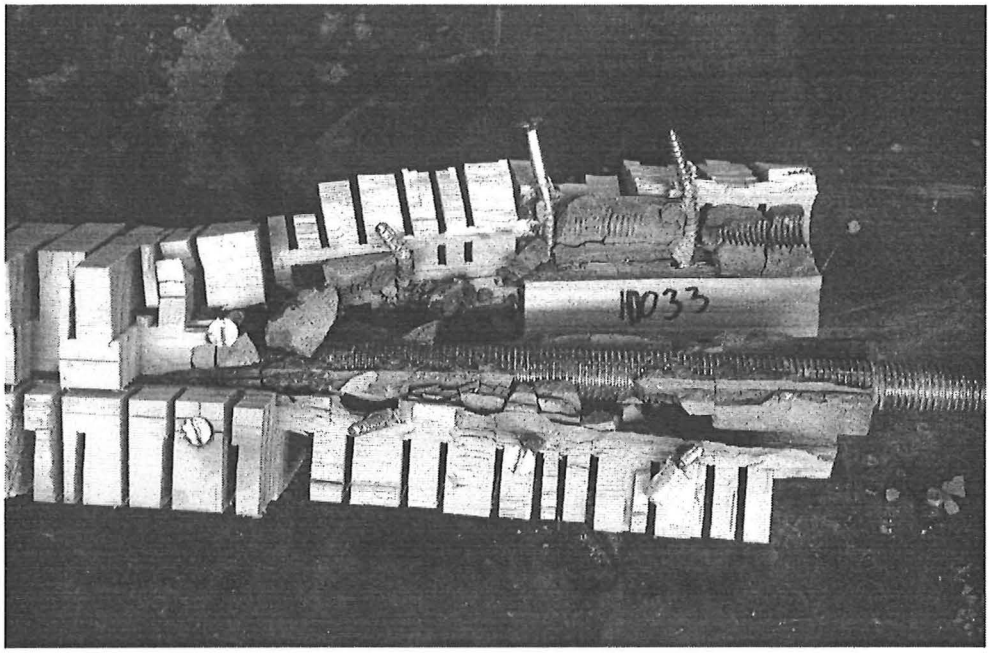

Figure 5.29 Failure mode of Experiment No.11

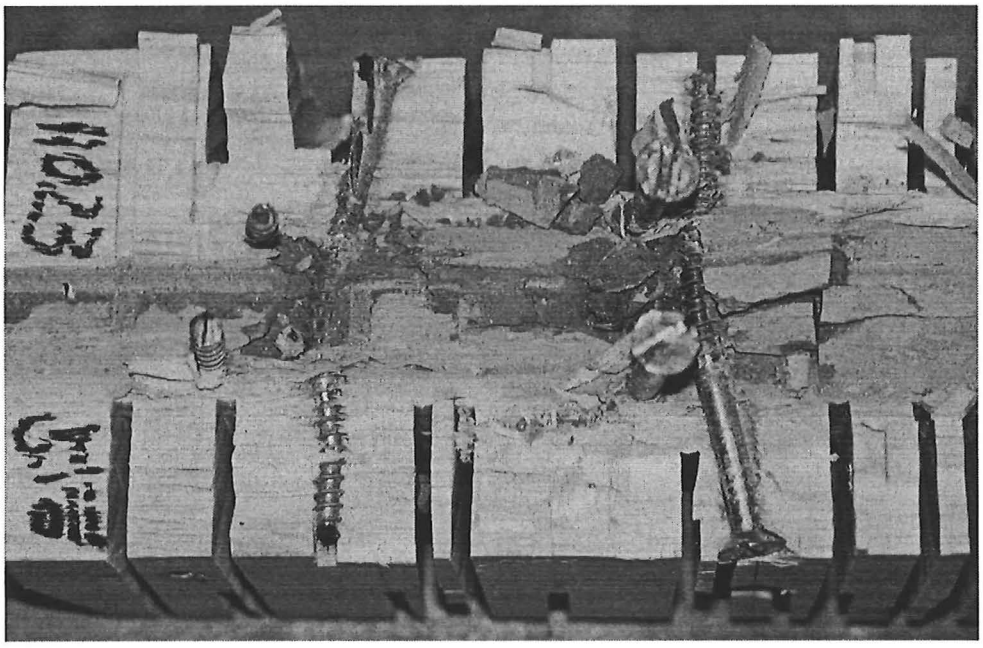

Figure 5.30 Bending of screws in Experiment No.11

CHAPTER SIX: DESIGN EQUATIONS

6.1 CONNECTIONS WITH DISTINCT KEY

Based on the results of the tension tests the following equation can be formed for predicting the strength of these connections:

$$F = f_{h1d}\frac{\pi\left(D^2 - d^2\right)}{4} + \sigma_{friction}\,\pi\,d\,l$$

where
- f_{h1d} = characteristic timber strength [MPa]
- d = hole diameter [mm]
- x = key size [mm]
- D = d + 2x [mm]
- $\sigma_{friction}$ = friction shear strength 0.15 [MPa] for a smooth hole surface, 0.50 [MPa] for a rough hole surface
- l = embedment length of steel rod [mm]

For this equation, a timber compression strength of 45 MPa was chosen. This was approximately the compression strength obtained by testing small clear specimens in compression according to the British Standard 373. The friction shear strength was obtained by comparing test results of Experiment No.5 with one bolt and smooth hole surface and test results of Experiment No.6 with one bolt and rough hole surface.

Figure 6.1 shows a comparison of the measured strength and the calculated strength, using the following equation of Experiments No.2, No.3 and No.4. The straight diagonal line represents the ideal result of measured strength equal to calculated strength. In the graph, the points above the ideal line have a lower measured strength than calculated. The results show scatter between the specimens. This can be explained by the fact of a varying key size inside the hole due to the inability of visually controlling the actual key size while drilling on the lathe. When increasing the key size, an increasing deviation from the calculated strength can be observed.

This means that not only the crushing strength of the timber and the friction influence the strength of the connection, but also unknown factors.

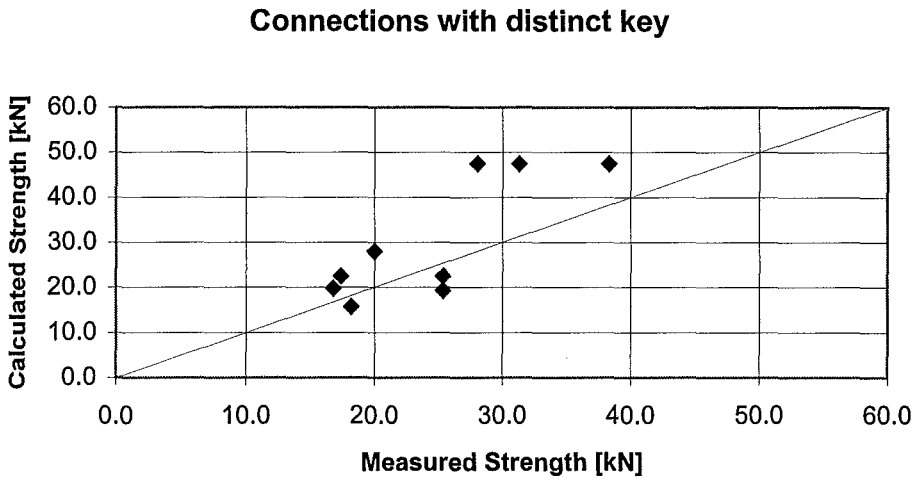

Figure 6.1 Estimation of the predicted values for connections with a distinct key

6.2 CONNECTION WITH BOLTS

The equation used, to calculate the strength of the connection is based on Johansen's equation for steel-to-timber joints (Timber Engineering STEP1, 1995). In deriving this equation it is assumed that both the fastener and the timber are ideal rigid-plastic materials, eg, the load-embedment characteristic for timber is as shown in Figure 6.2 (Timber Engineering STEP1, 1995). This approximation can make little difference to the result but simplifies the analysis. Figure 6.3 shows the failure mode for Johansen's equation.

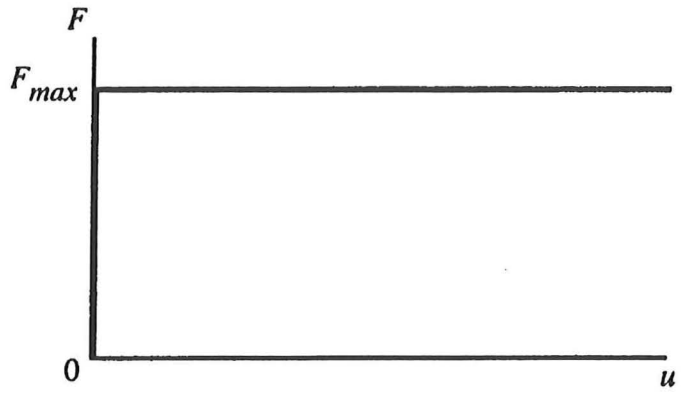

Figure 6.2 Simplified load-embedment characteristic

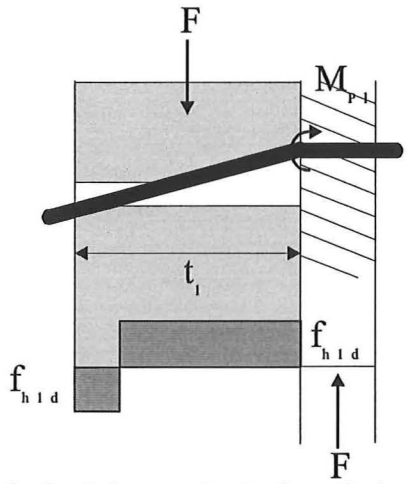

Figure 6.3 Failure mode for Johansen's steel-to-timber equation

Johansen's equation was used, assuming that the bolt forms a plastic hinge at the face of the main bar, and the bolt surrounded by grout acts as a dowel-type fastener bearing against the wood.

In addition to Johansen's formula, friction shear stress along the cement-wood interface and a reduced number of bolt, when using more than one bolt, is taken into account in the following equation:

$$F = f_{h1d}\, d_b\, t_1 \left[\sqrt{2 + \frac{4\, M_{pl}}{f_{h1d}\, d_b\, t_1^{\,2}}} - 1 \right] 2\, n_{ef} + \sigma_{friction}\, \pi\, d\, l$$

where F = pull-out strength [N]

f_{h1d} = characteristic timber strength [MPa]

d_b = diameter of cement block around bolt [mm]

d_{rod} = diameter of steel rod [mm]

t_1 = $(l_b - d_{rod})/2$ [mm]

l_b = length of bolt [mm]

M_{pl} = 31,500 [Nmm] Plastic moment of steel bolt

$\sigma_{friction}$ = friction shear strength 0.15 [MPa] for a smooth hole surface, 0.50 [MPa] for a rough hole surface

d = main hole diameter [mm]

l = embedment length of steel rod [mm]

n = number of bolts

n_{ef} = $1+(n-1)x2/3$

Figure 6.4 shows a cross section of a connection with bolts. The plastic moment of the bolts M_{pl} was obtained by bending tests described in Chapter Four. It was observed that, when increasing the timber strength in the equation, the difference between the calculated and the measured strength is increasing as well. For this reason, and to obtain the best results, the timber strength of 50 MPa was chosen. This was approximately the average between the two results for compression strength of timber, as described in Chapter Four.

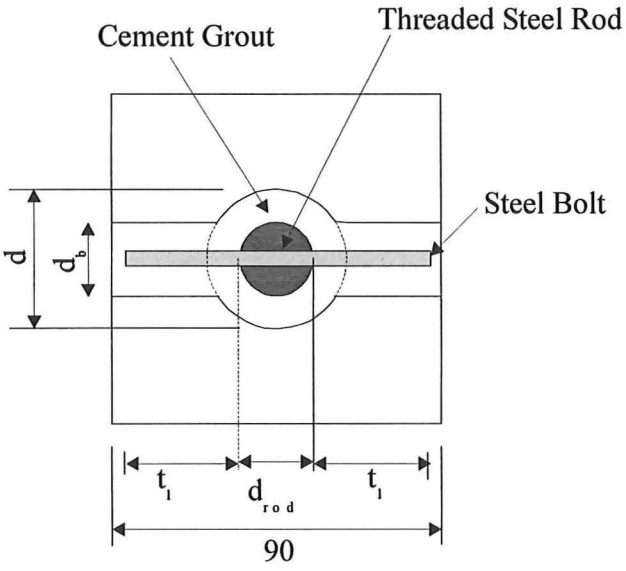

Figure 6.4 Cross section of connection with bolts

In the equation an effective number of bolts n_{ef} was used, adopted from Schneider Bautabellen fuer Ingenieure (1994) to give better prediction of the tests, shown in Figure 6.5. Still, it is unknown whether the effective number of bolts can be used for an increasing number of bolts. More tests would have to be carried out.

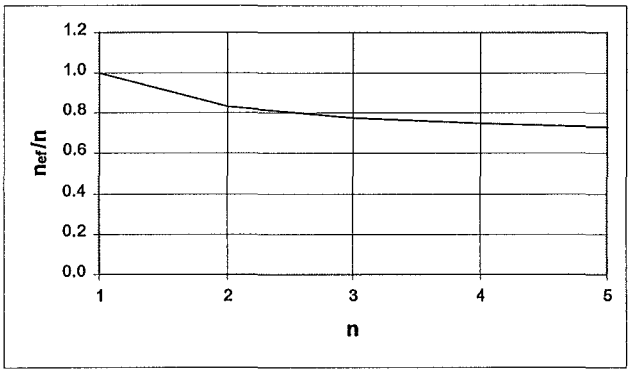

Figure 6.5 Effective number of bolts

Figure 6.6 shows a comparison of the measured strength and the calculated strength of the Experiments No.5 to No.9. The straight line depicts the ideal result, when measured strength is equal to the calculated strength. The scatter in the results increases a little, with an increasing number of bolts, but the trend of the strength increase is obvious.

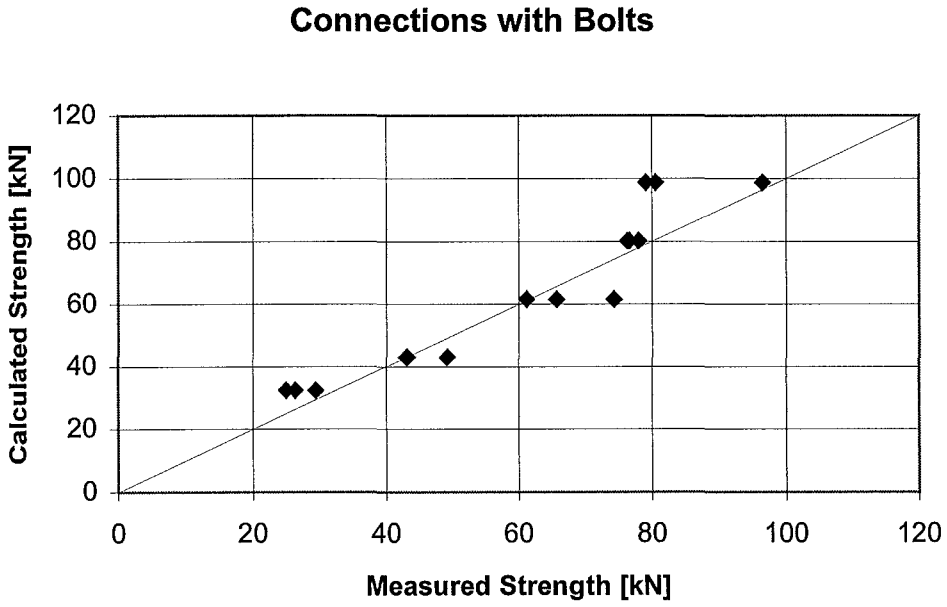

Figure 6.6 Estimation of the predicted values for connections with bolts

6.3 CONNECTIONS WITH SCREWS

Due to the fact that two types of screws were used with different yield strength and bending behaviour, the failure mode of each type had to be analysed separately. The failure modes, as can be seen in Figure 6.7 (Figure 8 and Figure 10, Timber Engineering STEP1, 1995), were investigated. On the basis of Johansen's equations (Timber Engineering STEP1, 1995), formulas were formed to predict the strength of the connections for each type of screw. In using the failure modes 2(a) and 3, it is assumed that the material 1 is the wood and the material 2 is the cement grout.

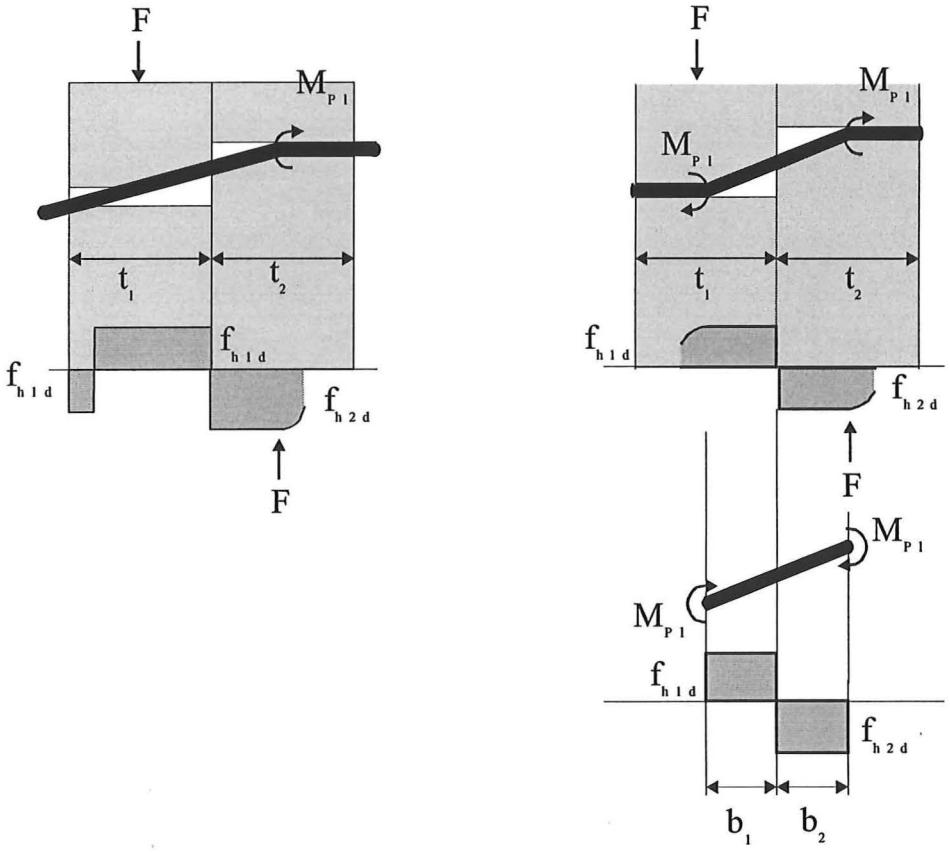

Failure Mode 2(a) Failure Mode 3

Figure 6.7 Failure mode 2(a) and 3 for Johansen's equation for fasteners in single shear

• Type 1 Screw

Two different curvatures of type 1 screws were found in the tension tested connections, as can be seen in Figure 6.8. Therefore, failure mode 2(a) and failure mode 3 were investigated, giving lower values for failure mode 3 (Figure 6.7). This means that failure mode 3 would occur first. This was expected, due to the ductile behaviour of the screws (see Chapter Four) and Johansen's equation, belonging to this failure mode, has been used for further calculations.

The equation used for calculating the strength of connections using type 1 screws is as follows:

$$F = \sqrt{\frac{2\beta}{1+\beta}}\sqrt{2\,M_{pl} f_{h1d} d_s}\;2\,n + \sigma_{frict}\pi\,d\,l$$

where

F	=	pull-out force [N]
f_{h1d}	=	Characteristic strength of timber [MPa]
f_{h2d}	=	Characteristic strength of cement [MPa]
β	=	f_{h2d}/f_{h1d}
M_{pl}	=	9,860 [Nmm], Plastic moment of type 1 screw
d_s	=	4.65 [mm], screw diameter + ½ thread
n	=	number of screws
$\sigma_{friction}$	=	friction shear strength 0.15 [MPa] for a smooth hole surface, 0.50 [MPa] for a rough hole surface
d	=	main hole diameter [mm]
l	=	embedment length of steel rod [mm]

Figure 6.8 Curvature modes of screws of the tension tested connections

Although the wood and cement grout have been tested separately, it is not clear which strength values should be used in the design equation. For this reason, several alternative values have been used in an attempt to get a good prediction of test results. Figure 6.9 depicts the influence of the value of β on the calculated strength of connections using 8 or 16 screws. The numbers in the legend are the fraction of timber strength and cement strength. The β-value is below 1.0, when using numbers for timber and cement strength obtained by the material tests in Chapter Four. The strength values for those are always below the measured strength. The calculated strength of β-values above 1.5, with a high value for cement strength, show better agreement with the test results.

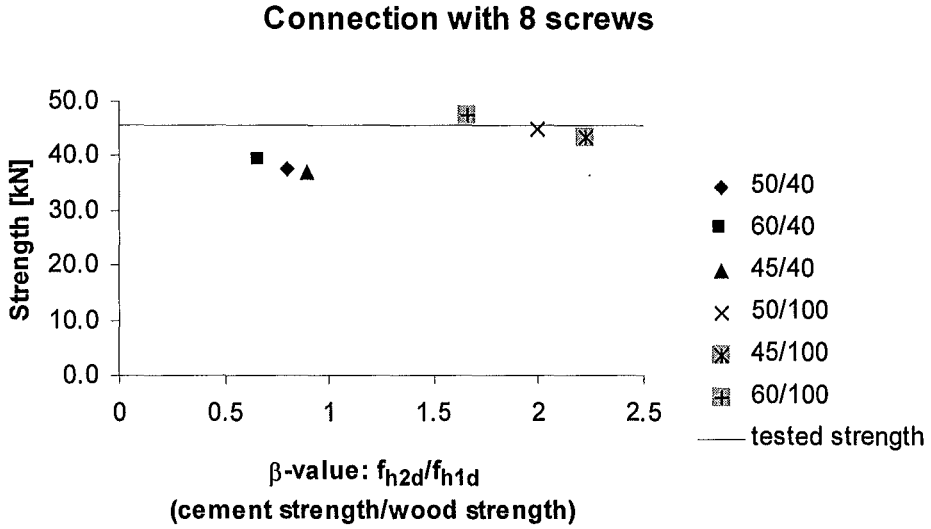

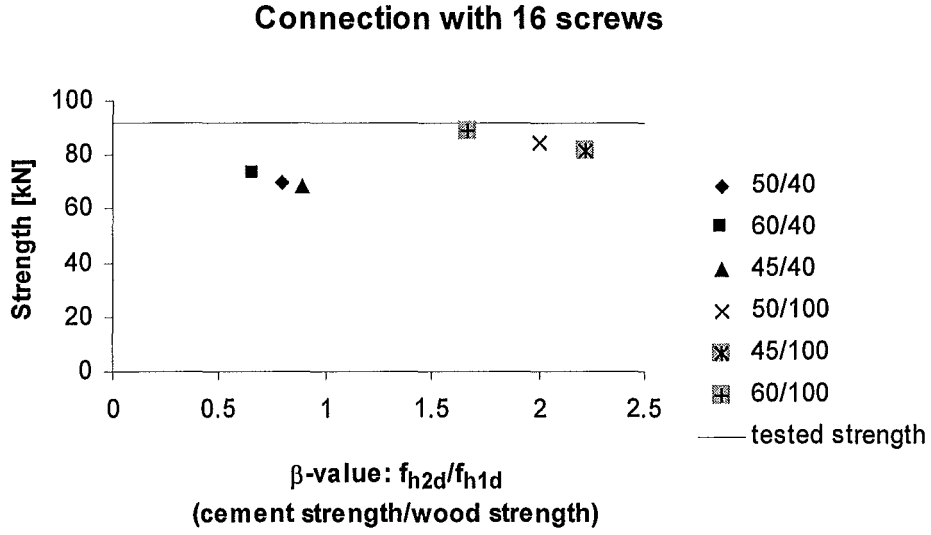

Figure 6.9 Influence of timber and cement strength on the equation for type 1 screw connections

• Type 2 Screw

When comparing failure mode 2(a) and failure mode 3 for type 2 screws, failure mode 2(a) was found to give lower values, and thus being the decisive failure mode for further calculations. This can be explained by the more brittle behaviour of these screws (see Chapter Four). The following equation, based on Johansen's equation for fasteners in single shear of failure mode 2(a), was developed:

$$F = \frac{f_{h1d}\, d_s\, t_1}{2+\beta}\left[\sqrt{2\,\beta\,(1+\beta)+\frac{4\,\beta\,(2+\beta)\,Mpl}{f_{h1d}\, d_s\, t_1}} - \beta\right] 2\,n + \sigma_{frict}\,\pi\, d\, l$$

where

F = pull-out force [N]

f_{h1d} = Characteristic strength of timber [MPa]

f_{h2d} = Characteristic strength of cement [MPa]

β = f_{h2d}/f_{h1d}

t_l = length of screw in timber [mm], see Figure 6.10

M_{pl} = 25 650 [Nmm], Plastic moment of type 2 screw

d_s = 5.4 [mm], screw diameter + ½ thread

n = number of screws

$\sigma_{friction}$ = friction shear strength 0.15 [MPa] for a smooth hole surface, 0.50 [MPa] for a rough hole surface

d = threaded steel rod diameter [mm]

l = embedment length of steel rod[mm]

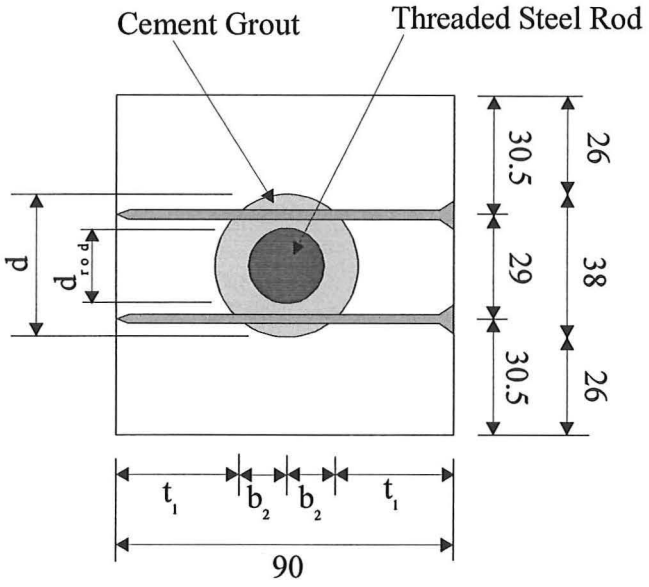

Figure 6.10 Cross section of connection with screws

Figure 6.11 depicts the influence of various β-values on the calculated strength of connections with 8 and 16 type 2 screws. For 8 screws, the values are all slightly above the tested strength. In the graph for connections with 16 screws the calculated values are significantly higher than the test results. The conclusion from this analysis is that even though the type 2 screws have a plastic moment more than twice that of the type 1 screws, the full benefit of this strength cannot be achieved because brittle failure of the screws occurs before full strength is reached.

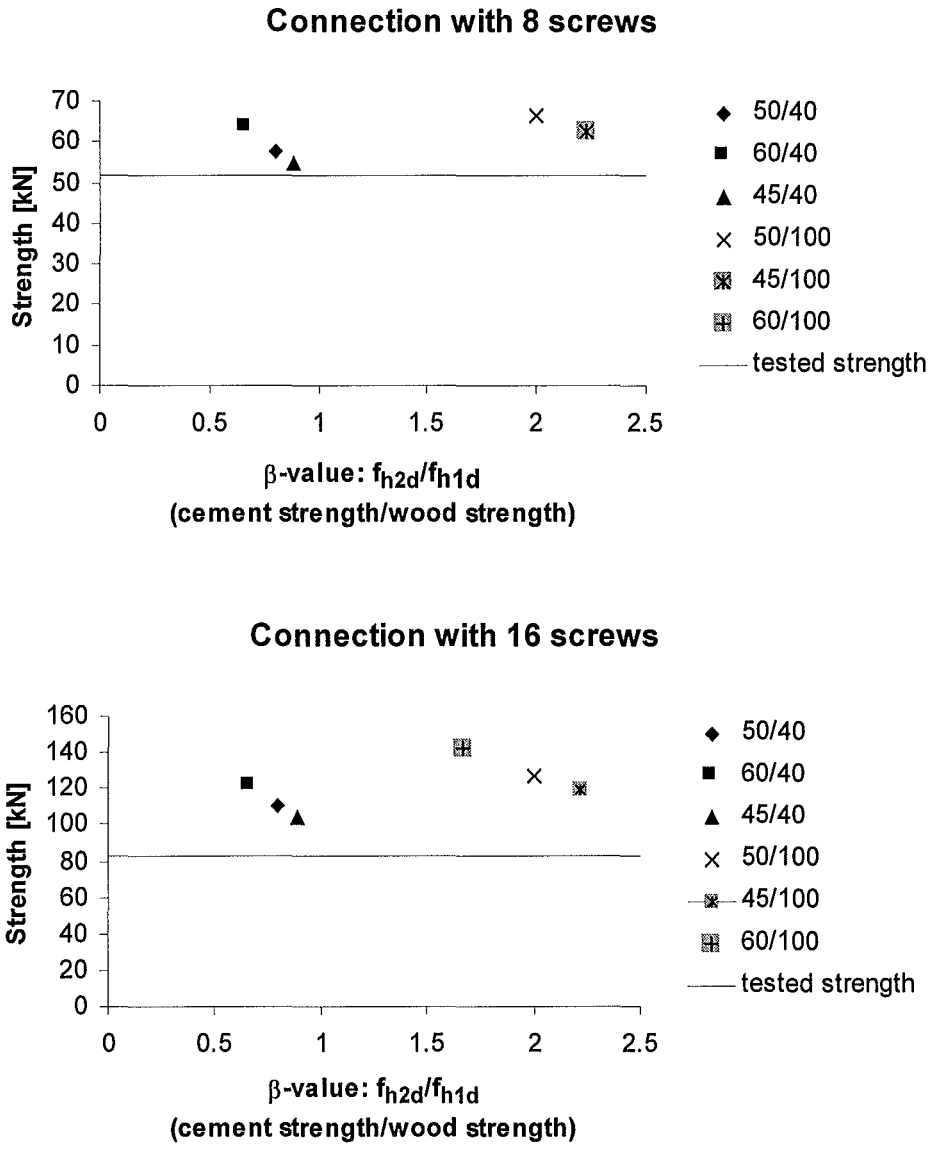

Figure 6.11 Influence of timber and cement strength on the equation for type 2 screw connections

CHAPTER SEVEN: SUMMARY AND CONCLUSION

7.1 SUMMARY

Epoxy bonded steel connections, as a method to construct moment resisting joints, gain increasing application in timber construction. Glulam timber is known for its low charring rate and thus good fire resistance, but previous research showed that this type of connection using epoxy has a low fire resistance. This is due to the fact that above a temperature of approximately 50°C the strength of epoxy decreases rapidly, causing the connection to fail.

An experimental study was carried out to investigate steel connections in glue laminated timber bonded by cement. Cement, as an alternative to epoxy, was chosen because cement has good fire resistance and is available at an economical price.

The experimental programme consisted of two parts: material property tests and tension tests of cement bonded steel connections. Compression and shear strength of the timber, compression strength of the cement grout and yield strength of screws and bolts were tested. These tests were carried out to obtain strength values of the materials for further calculations. Ten various designs of cement bonded steel connections were tested. After testing specimens with straight embedment holes, it became clear that the major problem would be to provide a mechanical bond between the timber and the cement grout. Therefore, three methods of mechanically bonding cement to timber were tested. The first one was by means of a distinct key inside the main hole and the second by using small diameter bolts drilled through the threaded steel rod and surrounded by cement. The third one was by means of screws through the timber and the cement, preventing the timber from splitting and the cement from pulling out.

The failure modes were investigated and equations were developed to predict the strength of the cement bonded steel connections with various designs.

6.2 CONCLUSIONS

1. Straight holes are not giving enough bond between timber and cement, even if they are roughened up. A mechanical bond has to be provided.

2. A minor increase in connection strength can be achieved by a distinct key inside the embedment hole.

3. Strong connections can be made using bolts or screws. The strength of these connections can be increased by an increasing number of bolts or screws, but there is not a linear relationship between the number of bolts or screws and the strength of the connection.

4. There is not a proportional relationship between increased screw strength and connection strength because high strength screws are less ductile.

5. Failure of all the cement bonded steel connections is by ductile pull-out of the cement-steel block. No wood failure occurred.

6. Initial splits along the specimens, due to wetting the hole before grouting, have no effect on the ultimate tensile strength of the connection. When the bar is pulling out further the splits become larger.

6.3 FURTHER RESEARCH

1. Tests at elevated temperatures should be carried out to investigate the fire resistance of cement bonded steel connections.

2. More tension tests using bolts and screws should be carried out to expand the present work and to confirm test results obtained in this research.

3. The influence on strength of an increasing diameter of the main hole, when screws are employed, could be investigated.

4. Various cement mixtures and the influence of a higher cement compression strength could be investigated.

5. Other alternatives to cement and epoxy, such as high temperature epoxy could be investigated for strength and heat resistance.

REFERENCES

Aarnio, M. (1979). Glulam timber construction and the fire resistance of the joints [in Finnish]. Helsinki school of technology, Division of building engineering, Diploma work, Otnas

Aarnio, M. and Kallioniemi, P. (1983). Fire safety in joints of load bearing timber construction [in Finnish]. VTT research report No.233. Technical research centre of Finnland

Alawady, M., Avent, R.R. and Mukai, D. (1998). Repair of Timber Poles by Injection Grouting. Proceedings of the fifth World Conference on Timber Engineering, Montreux, Schwitzerland, pp 610 – 617

Atkinson, R.H. and Schuller, M. (1993). Evaluation of injectable cementitious grouts for repair and retrofit of masonry. ASTM Special Technical Publication, Proceedings of the Symposium of Masonry, No 1180. Publ by ASTM Philadelphia PA USA, pp 355 - 368

Barber, D.J. (1994). Fire Resistance of Epoxied Steel Rods in Glulam Timber. Research Report 94/1, Department of Civil Engineering, University of Canterbury, Christchurch

Batchelar, M.L. and McIntosh, K.A. (1998). Structural Joints in Glulam Timber. Proceedings of the fifth World Conference on Timber Engineering, Montreux, Switzerland, pp 289 – 296

Bazant, Z.P. and Kaplan, M.F. (1996). Concrete at high temperatures: Material properties and mathematical models. Concrete design & construction series, United Kingdom

British Standard 373 (1957). Methods of testing small clear specimens of timber. London, UK

Buchanan, A.H. (1999). Structural design for fire. University of Canterbury, Christchurch, New Zealand

Buchanan, A.H. and King, A.B. (1991). Fire performance of gusset connections in glue-laminated timber. Fire and materials, Vol15, pp 137-143

Carling, O. (1989). Fire resistance of joint details in load bearing timber construction – a literature survey [translated from Swedish]. BRANZ Study report SR 18. Building research association of New Zealand

Czernin, W. (1962). Cement Chemistry and Physics for Civil Engineers. Crosby Lockwood & Son LTD, England

Deng, J.X. (1997). Strength of Epoxy Bonded Steel Connections in Glue Laminated Timber. Research Report 97/4, Department of Civil Engineering, University of Canterbury, Christchurch

Faiweather, R.H. (1992). Beam Column Connections for Multi-Storey Timber Buildings. Research Report 92-5, Department of Civil Engineering, University of Canterbury, Christchurch

Gaunt, D.J. (1998). Joints in Glulam Using Groups of Epoxy Grouted Steel Bars plus an Alternative to Epoxy Bonding. Proceedings of the Fifth World Conference on Timber Engineering, Montreux, Switzerland, pp 281 – 288

Guan, Z.W. (1998). Structural Behaviour of Glued Bolt Joints Using FRP. Proceedings of the Fifth World Conference on Timber Engineering, Montreux, Switzerland, pp 265 – 272

Haller, P. (1998). Progress in Timber Joint Development and Modelling. Proceedings of the Fifth World Conference on Timber Engineering, Montreux, Switzerland, pp 337 – 344

Hansson, P. (1996). Filtration Stability of cementitious injection grouts with low w/c ratio. Concrete in the Service of Mankind, Proceedings of the International Conference at the University of Dundee, Scottland, UK

Leitjen, A. (1998). The development of pre-stressed timber joints using a densified veneer wood an expanded tube fasteners. Proceedings of the final COST C1 Conference, Liege, Belgium

Neville, A.M. and Brooks, J.J. (1990). Concrete Technology. Longman Scientific & Technical, England

Riberholt, H. (1986). Glued bolts in glulam. Serie R No.210. Departement of Structural Engineering, Technical University of Denmark

van Rickstal, F. and van Gemert, D. (1996). Evaluation of cement grout and brick masonry for injection purposes. Concrete in the Service of Mankind, Proceedings of the International Conference at the University of Dundee, Scottland, UK

Rodd, P. and Pope, D. (1994). Resin injected dowels in moment transmitting joints. Proceedings of the Pacific Timber Engineering Conference, Gold Coast, Australia

Schneider Bautabellen fuer Ingenieure mit europaeischen und nationalen Vorschriften (1994). Werner-Verlag, 11. Auflage, Germany

Timber Engineering STEP1 (1995). First Edition, Centrum Hout, The Netherlands

Townsend, P.K. (1990). Steel Dowels Epoxy Bonded in Glue Laminated Timber. Research Report 90/11, Department of Civil Engineering, University of Canterbury, Christchurch

APPENDICES

APPENDIX 1: Load Deflection Curves for Grout Testing

Grout Test No.1

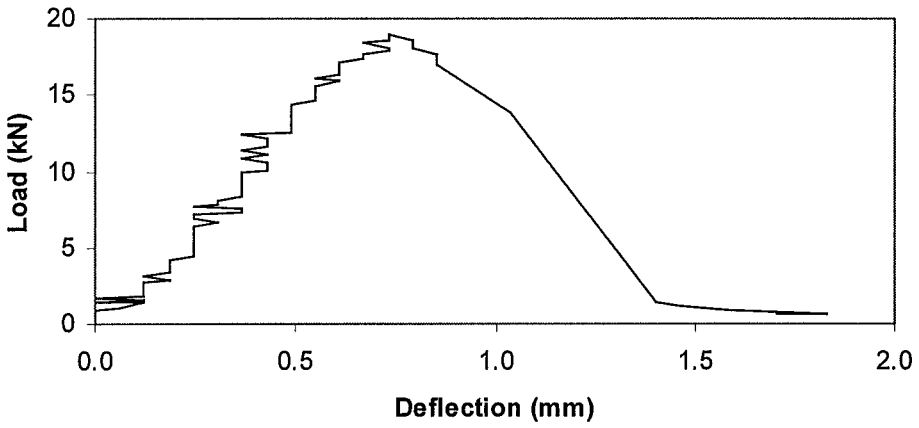

Grout Test No.2

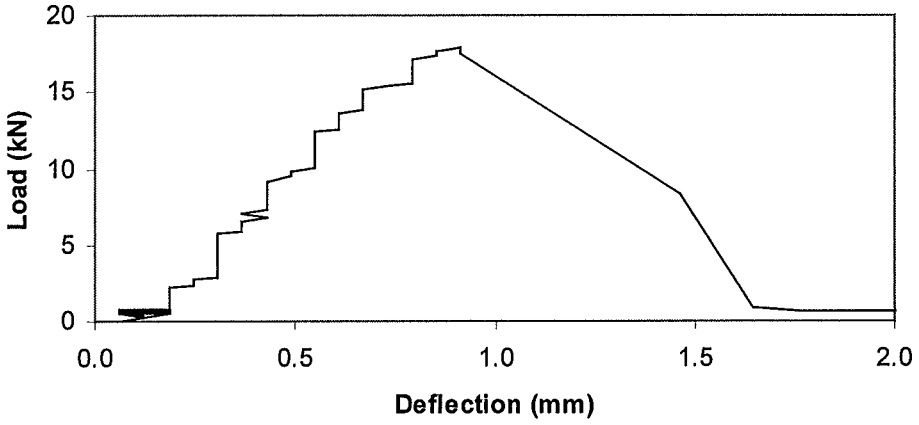

Grout Test No.3

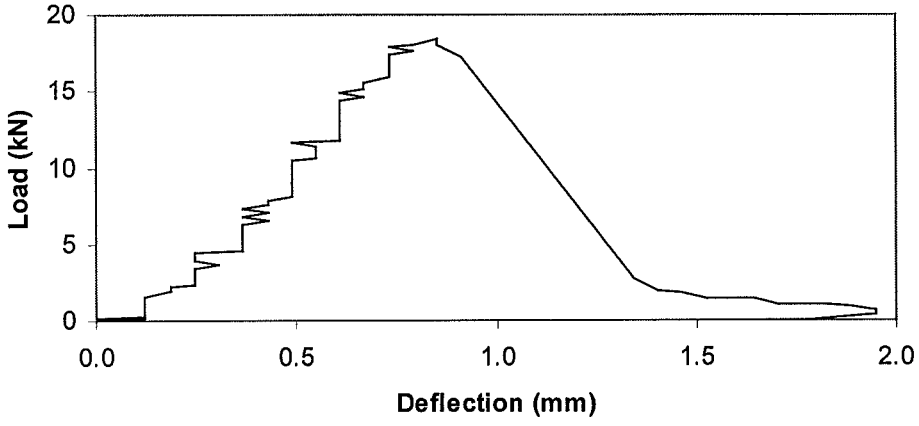

Grout Test No.4

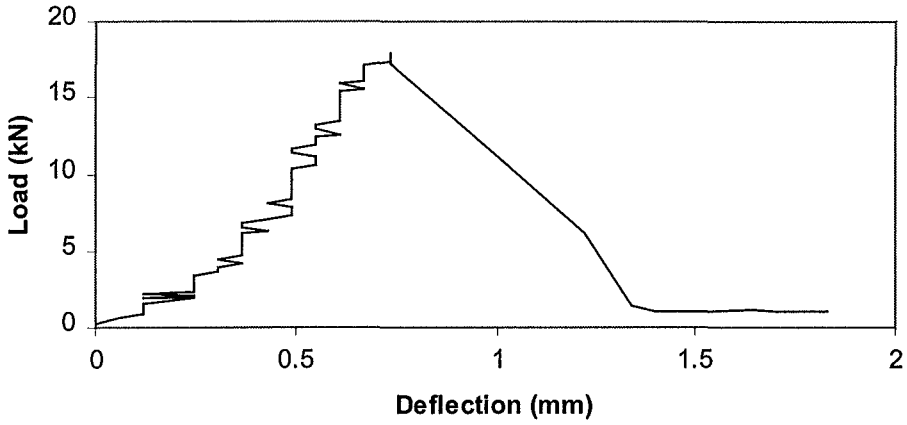

Grout Test No.5

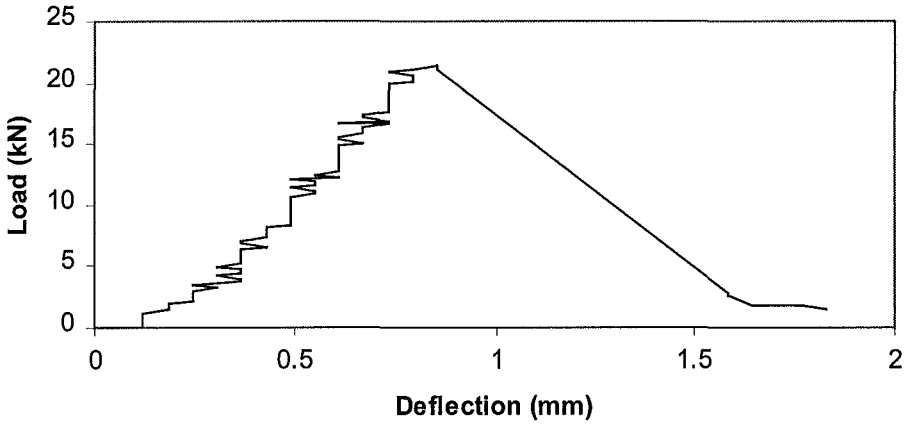

Grout Test No.6

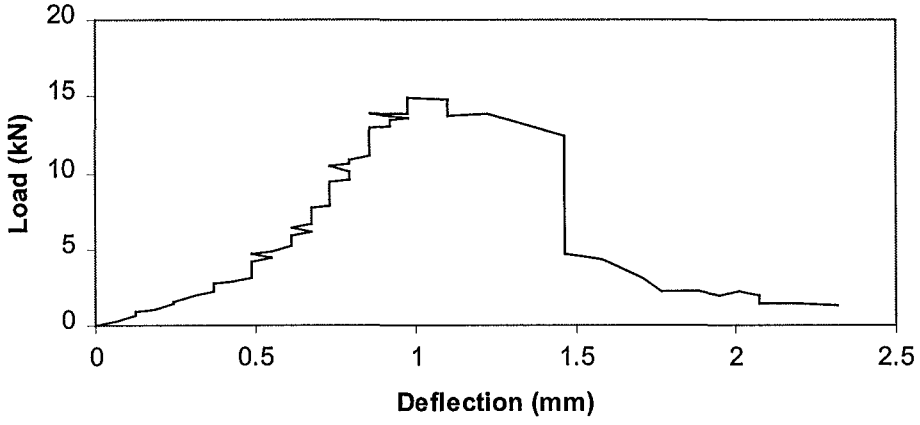

Grout Test No.7

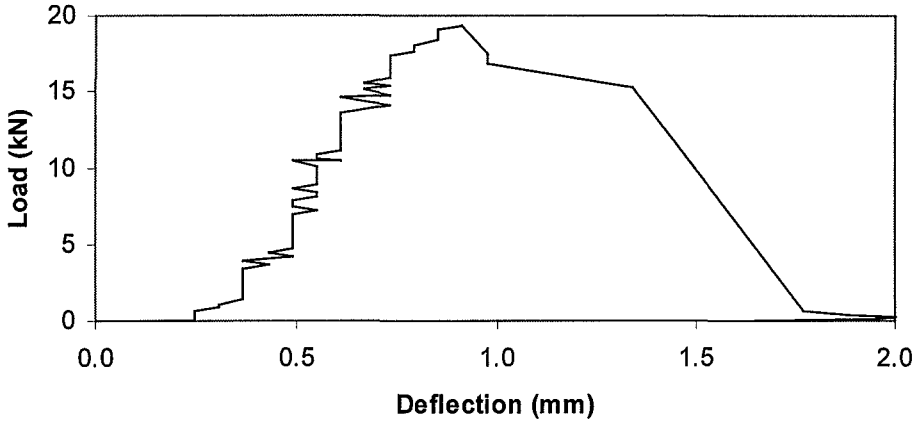

Grout Test No.8

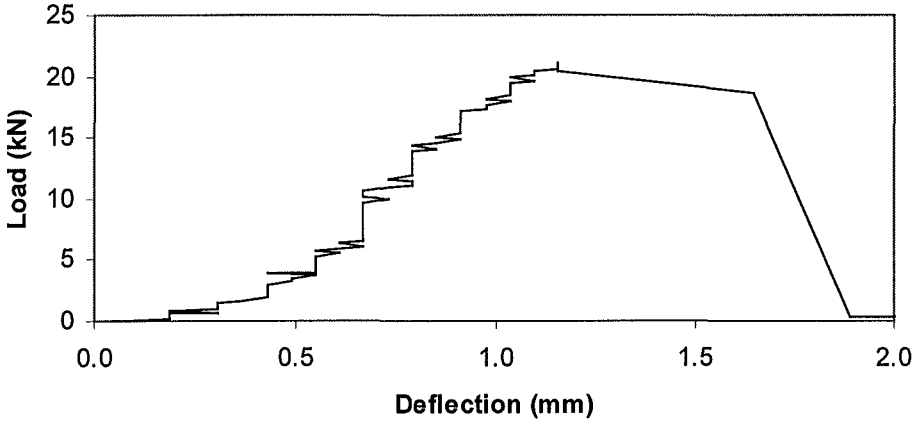

Grout Test No.9

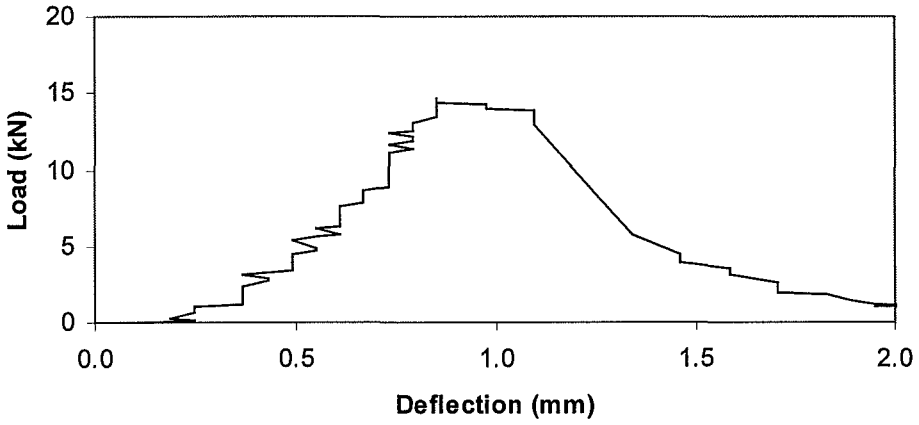

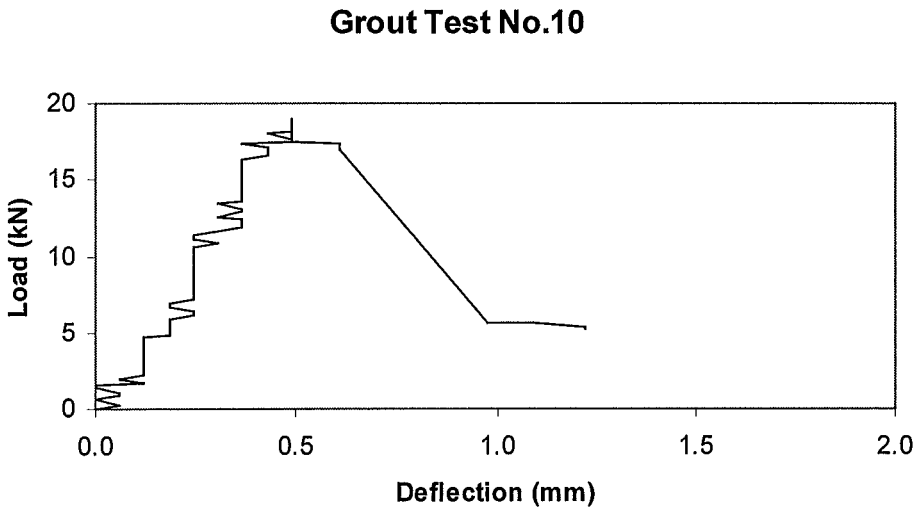
Grout Test No.10
Load (kN)
20
15
10
5
0
0.0
0.5
1.0
1.5
2.0
Deflection (mm)

APPENDIX 2: Load Deflection Curves for Bending Tests

Bolt 1

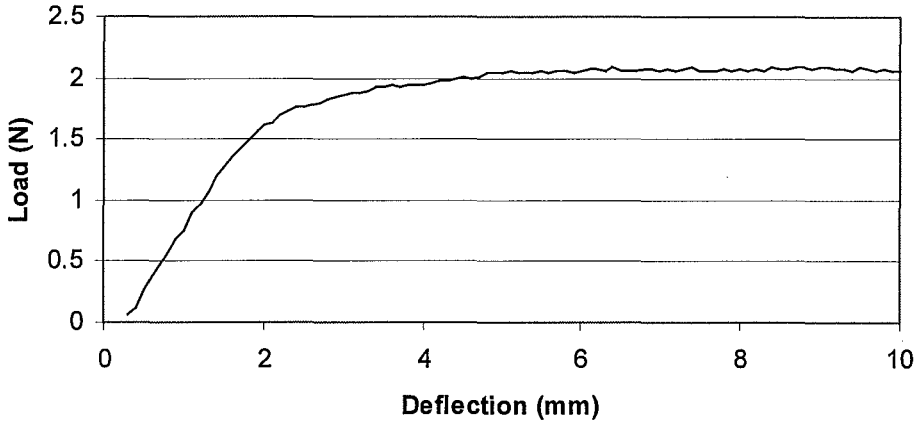

Bolt No.2

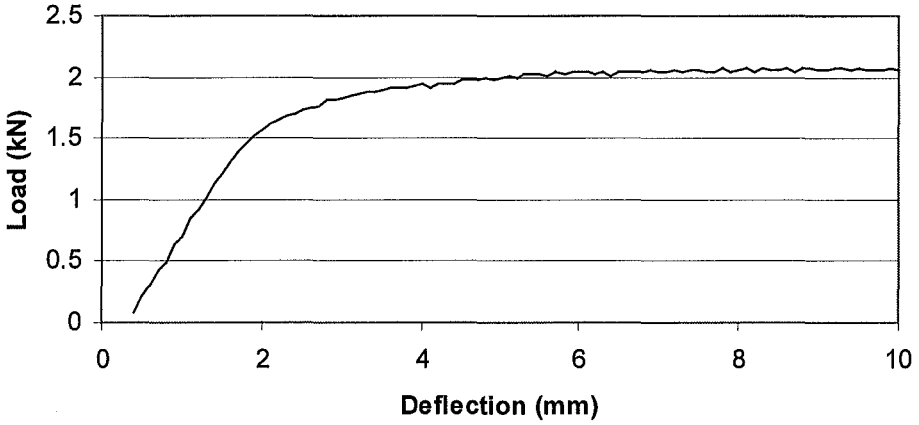

Bolt No.3

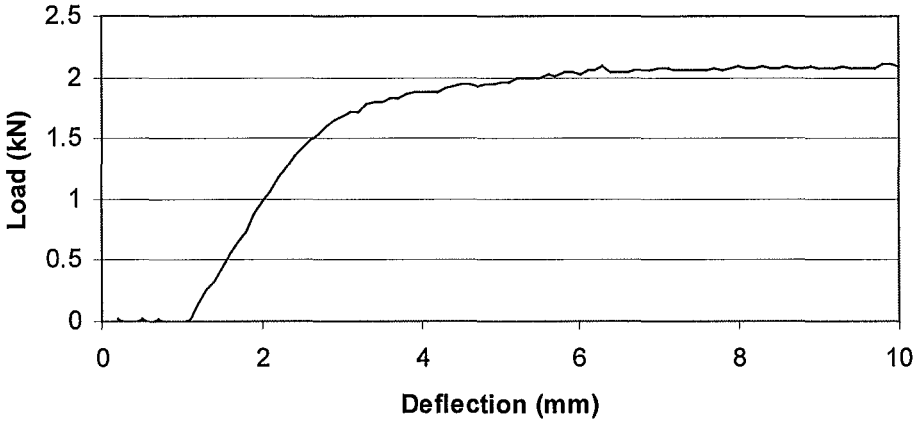

Bolt No.4

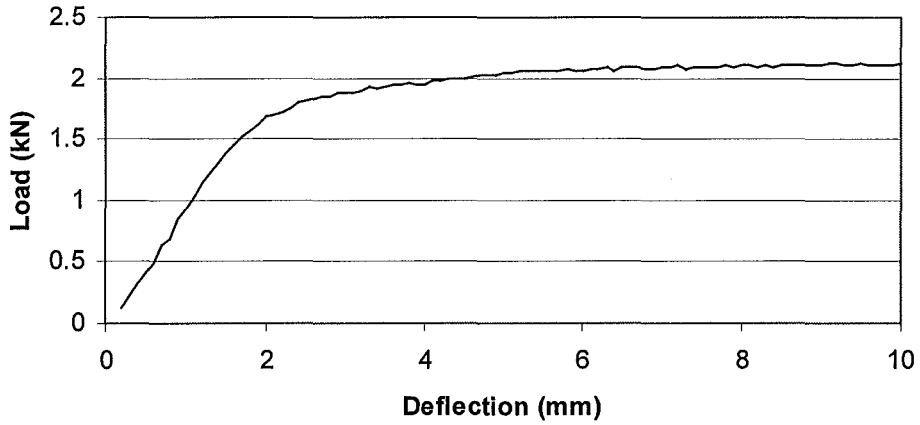

Bolt No.5

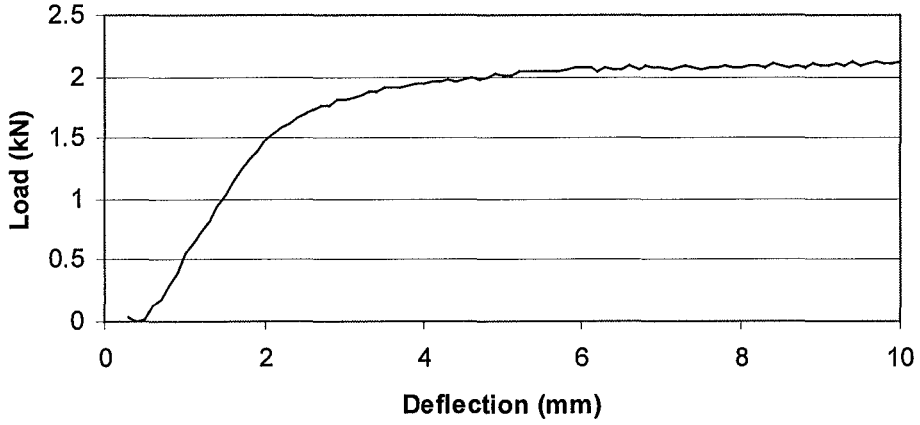

Screw Type 1, No.1

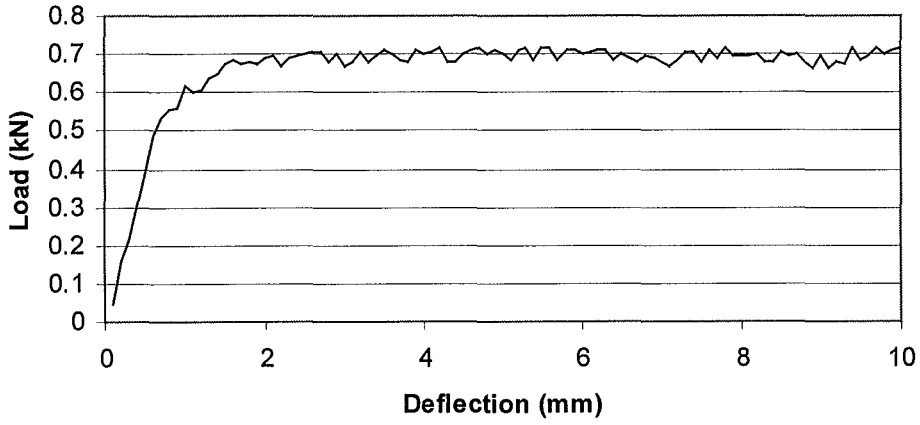

Screw Type 1, No.2

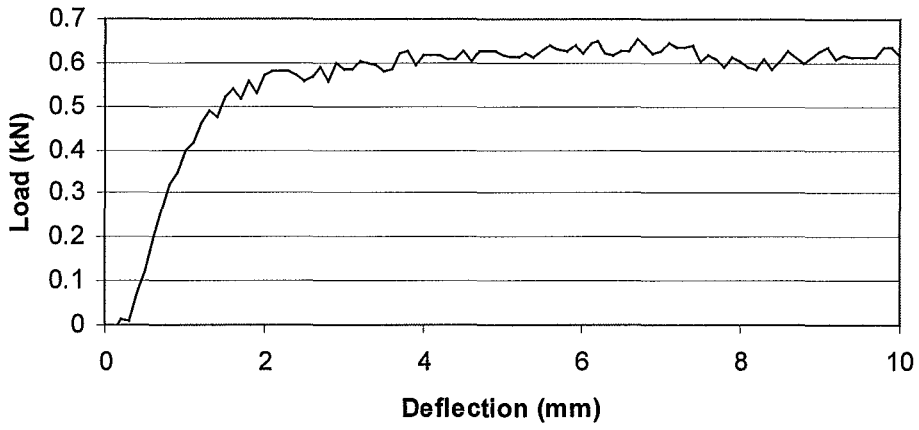

Screw Type 1, No.3

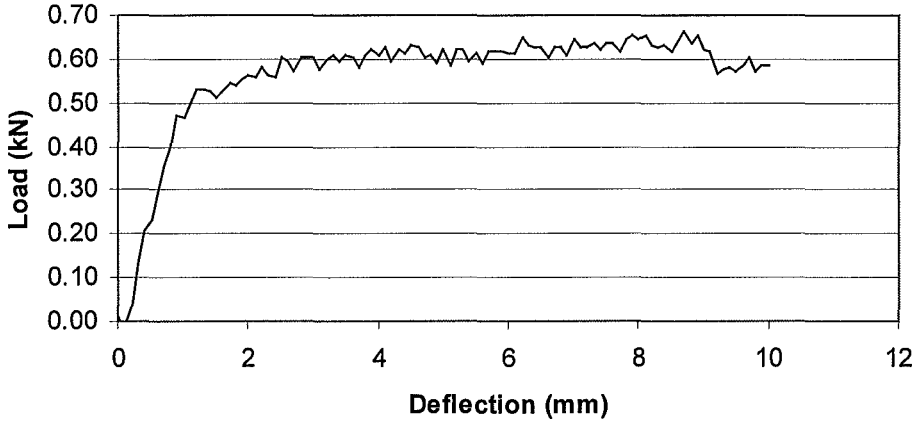

Screw Type 1, No.4

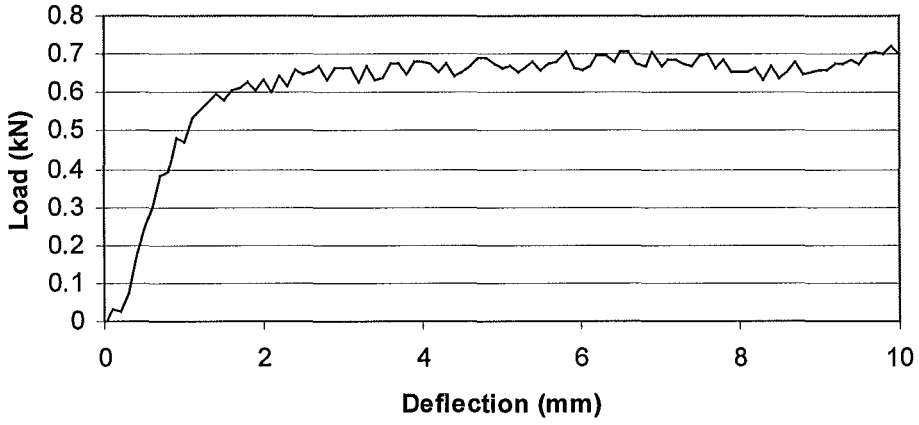

Screw Type 1, No.5

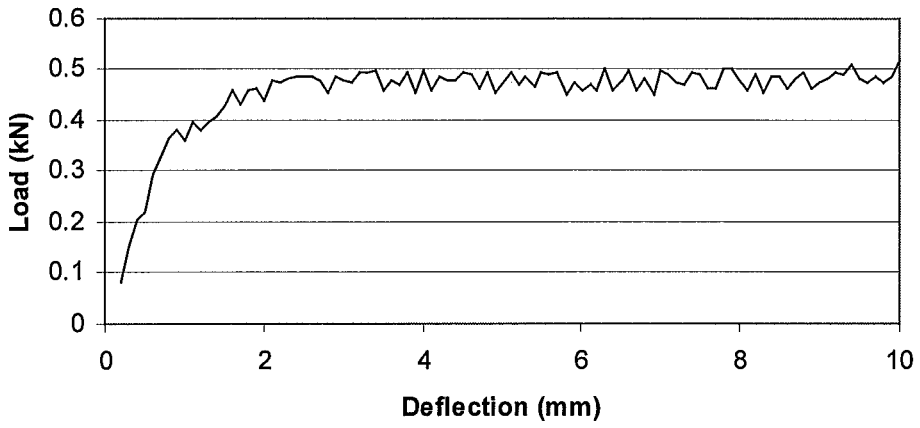

Screw Type 2, No.1

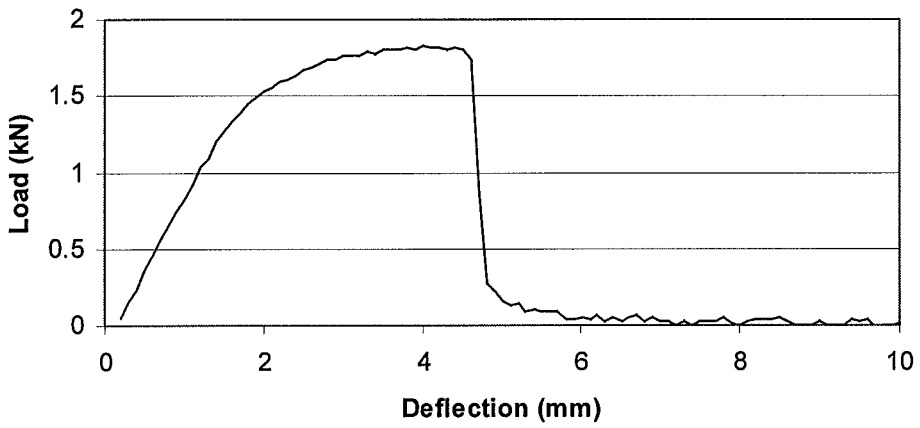

Screw Type 2, No.2

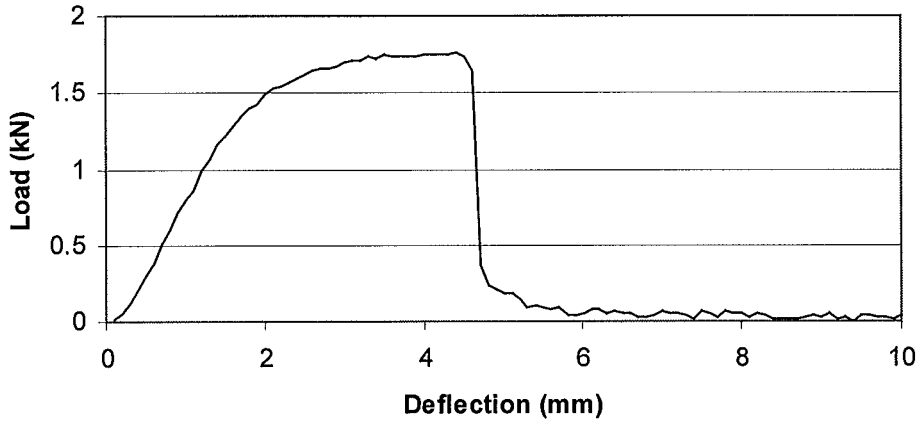

Screw Type 2, No.3

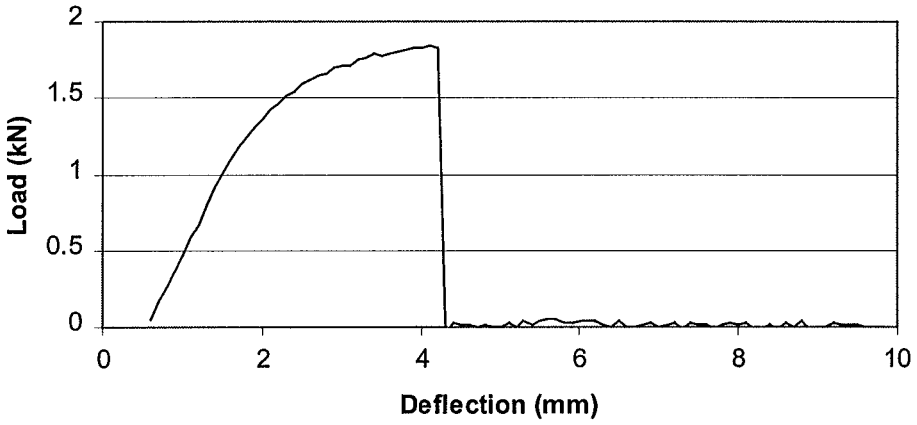

Screw Type 2, No.4

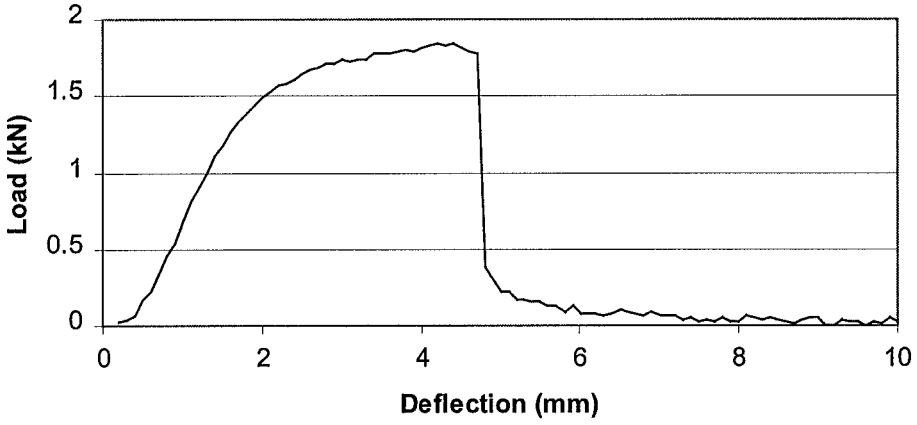

Screw Type 2, No.5